

The Bakerian Lecture, 1990: New Microcrystalline Catalysts

J. M. Thomas

Phil. Trans. R. Soc. Lond. A 1990 **333**, 173-207

doi: 10.1098/rsta.1990.0158

Email alerting service

Receive free email alerts when new articles cite this article - sign up in the box at the top right-hand corner of the article or click [here](#)

To subscribe to *Phil. Trans. R. Soc. Lond. A* go to: <http://rsta.royalsocietypublishing.org/subscriptions>

THE BAKERIAN LECTURE, 1990

New microcrystalline catalysts

BY J. M. THOMAS

*Davy Faraday Research Laboratory, The Royal Institution, 21 Albemarle Street,
London W1X 4BS, U.K.*

[Plates 1–8]

Contents

1. Introduction	174
2. The study of catalysts in action	176
3. Why crystalline catalysts?	177
4. Monophasic uniform heterogeneous catalysts	180
5. Solid acids: families of uniform heterogeneous catalysts	182
5.1. <i>Clays and pillared variants</i>	183
5.2. <i>Heteropolyacid (Keggin ion) catalysts</i>	185
5.3. <i>Metal phosphonates</i>	185
5.4. <i>Microporous, three-dimensionally uniform catalysts</i>	187
6. Zeolites unlimited: new types of uniform heterogeneous catalyst	192
7. Metal-ion-exchanged zeolites as uniform heterogeneous catalysts	193
7.1. <i>Catalysis of the cyclotrimerization of acetylene by nickel-ion-exchange zeolite Y: an in situ study</i>	194
8. Catalysis by zeolites and the role of computational chemistry	196
9. Solid oxides: pyrochlores and perovskites	198
10. New vistas	201
References	203

Owing to recent developments there is now a prodigality of crystalline inorganic solids capable of catalysing the chemical conversions of numerous gaseous molecules, especially hydrocarbons. Very many of these new catalysts are microporous and microcrystalline, and have their accessible active sites distributed uniformly throughout their bulk. They are, therefore, amenable to investigation by essentially all of the premier experimental and computational tools of solid-state physics and solid-state chemistry. The deployment of these tools has yielded fresh insights into the mechanisms of catalytic action and also suggested new strategies, some of which have already been tested, for the design of specially tailored selective catalysts.

The benefits of multi-pronged approaches to the investigation of the reactivity of catalysts, made possible by the combined use of intense X-ray sources (both laboratory-based and synchrotron radiation) and supercomputers, are illustrated by specific reference to zeolitic solids that contain cages and channels of molecular dimension. Such crystalline solids, either in their highly acidic or metal-ion-exchanged forms, are of great practical value on an industrial scale. They are also ideally suited for *in situ* exploration of the subtle structural changes that accompany,

Phil. Trans. R. Soc. Lond. A (1990) **333**, 173–207

Printed in Great Britain

8

Vol. 333. A (15 October 1990)

or are responsible for, the activation and deactivation of catalysts. Ways of optimizing the performance of catalysts, including the possible construction of 'tea-bag' analogues, and of coping computationally with their properties and performance so as to deepen our understanding of their mode of operation are outlined with reference to both the zeolites and the ever-widening range of solid oxides crystallizing with pyrochlore and perovskite structures.

1. Introduction

When Michael Faraday came to the Royal Society to give his Bakerian Lecture in 1829, he journeyed from the Royal Institution in Albemarle Street on three separate occasions; for so comprehensive was his account of 'The manufacture of glass for optical purposes', that it was delivered in part on November 19th, in part on December 3rd and finally on December 10th. This particular reference to Faraday at the outset of my talk is not to be construed, Mr President, as a disguised plea for extra time this evening. It is mentioned merely so that I may recall that Faraday made several contributions to heterogeneous catalysts, as he did to so many fields. It was Faraday who first clearly recognized that the products of a catalysed reaction may sometimes poison or inhibit the ensuing catalysis. And it was Faraday's contemporary William Grove who, during the course of his Bakerian Lecture on 'Voltaic Ignition and Decomposition' in 1847, first demonstrated that a catalyst for the forward reaction is also a catalyst for the reverse reaction. He did this by showing how heated platinum facilitated both the formation of water from H_2 and O_2 and its decomposition into its components, thereby leading to a state of equilibrium.

When I commenced my studies of gas–solid interaction as a research student in the pre-laser era, the preferred method of analysing small quantities of H_2 or CO in the gas phase entailed its catalytic combustion over a heated filament of platinum and measuring the resulting drop in pressure. Since that time the detection limit for analysing small reactive molecules has improved more than a billion fold. Our understanding of heterogeneous catalysis has not. Nevertheless there has been substantial progress, which I shall adumbrate this evening.

As a student I began to ruminate over the phenomenon of catalysis and its seemingly bewildering variety of manifestations. I was soon to learn of its ancient lineage: the existence of the phenomenon was certainly known to Aristotle. As a student I also learned that whereas thermodynamics and quantum mechanics, and the laws they embrace, had a permanence and inexpugnable finality, theories of catalysis possessed a fragile, evanescent character. In the years that have elapsed since my student days – when, as Faraday put it in another context 'My fear was greater than my confidence, and both far greater than my knowledge' – many theories of catalysis along with certain concepts and guidelines that at one time held dominant sway, have since passed into dark oblivion. The so-called geometric principle, so much in vogue thirty years ago, when coupled with an almost intoxicating absence of concrete evidence was used to prove almost any theory of catalysis that one chose. Just as these days, the concept of the so-called electronic principle, now coupled with an embarrassing wealth of experimental evidence, can also be used to substantiate a favoured theory.

Heterogeneous catalysis is, as I hope to demonstrate, perennially relevant and endlessly fascinating; but it remains rather enigmatic. Plausible mechanisms of

catalysed conversions abound, some commended by their immediacy, very few by their demonstrated veracity. Nevertheless, as I perceive things, heterogeneous catalysis is now passing through a phase of passionate prodigality. There is an intricate, almost infinite, variety of profusion of crystalline solids that display catalytic behaviour.

But if theoretical progress, to the extent that it renders feasible the precise design and fabrication of new heterogeneous catalysts, has been uneven and inadequate, it has been more than compensated by a sequence of major successes at the practical level. I would be the last person – dyed in the wool academic that I am, and fearful of being accused of being the money-lender in the temple – to justify my choice of research in catalysis in terms of the magnitude of its importance in the market-place. I turned to catalysis because I was fascinated by it; and I continue to be captivated by it because it is also an ideal testing ground for exploring new techniques which, as a physical chemist, I am engaged in devising. Nevertheless, it would be perverse to ignore the central role that catalysis plays in the economy of nations. Each year, world-wide, goods worth many trillions of pounds sterling are produced using catalysts. Catalysts themselves, though they should in theory remain unchanged, are consumed during use, chiefly because of mechanical attrition. And, world-wide, it is estimated that by A.D. 2000 more than six billion pounds worth of catalysts will be consumed per annum, more than half of it for the auto-exhaust catalyst market. Last year, more than fifty million emission control units were fitted to vehicles in the western world.

Catalysts will play a major role in the evolution of new processes that are inherently clean. They will also be used in the rethinking of existing processes that currently generate hazardous or intractable products but which, in future, will be made benign and readily disposable or fashioned into desirable stepping stones to other products. Catalysts will be centre-pieces in fundamentally new processes for dealing with the legacy of past pollution. They will also be used in the evolution of new technologies, which circumvent the use of dangerous intermediates.

There are openings for a range of new catalysts in fuel cells for energy production. Fuel cells, invented by William Grove in 1839, constitute a much more efficient method of generating electricity than the conventional method based on direct combustion of fossil fuels. The first commercially available fuel cell units are currently under construction in the U.S.A. and Japan in sizes ranging from 50 kW to 11 MW. Such units can run on a variety of fuels including natural gas, methanol, liquefied petroleum gas, and even waste gases from landfill sites. Their especial attraction is that they are compact, silent and clean. These qualities make them prime candidates to replace old urban power stations. They are also far cleaner than other means of generating electricity, and may be constructed on a timescale that is a mere fraction of that required for a conventional power station. When one examines the emissions (see figure 1) associated with the various ways of generating electricity, the advantages of fuel cells are seen to be compelling. Perhaps it is timely to return to the prospect entertained by the great German chemist Ostwald who, at the opening of the first meeting of the German Physical Chemistry Society over ninety years ago, predicted that the fuel cell would be man's preferred method of generating power for fuel, and transport in the twentieth century.

All these are general considerations with societal as well as scientific consequences. It is inappropriate that I should dwell further on them here. I now wish to enter, and stay broadly within, the arena of fundamental studies.

Phil. Trans. R. Soc. Lond. A (1990)

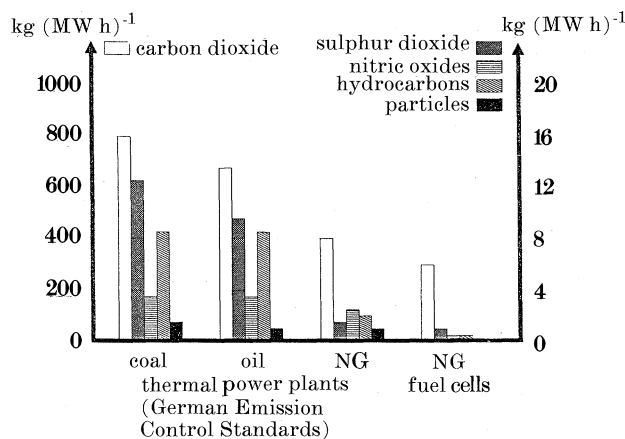


Figure 1. Emissions associated with various modes of generating electrical power from coal, oil and natural gas (NG). (By kind permission of Dr Ulf Bossel, ETH, Zurich.)

2. The study of catalysts in action

Homogeneous catalysts which, in general, have the active agent dissolved in an appropriate solvent, are much easier to investigate than heterogeneous ones, where there are two or more phases because, in the former, all the myriad modern spectroscopic and kinetic tools of the chemist may be used to good effect under actual reaction conditions. By contrast, it is no mean task to probe heterogeneous catalysts under operating conditions when pressures may be tens of bars and temperatures approaching 1000 K. All electron-based techniques, for example, of which there are many, are demonstrably inapplicable because of the minuteness of the mean free path of the electrons under these conditions.

It is not, therefore, surprising that our understanding of the mode of operation of homogeneous catalysts far exceeds that of heterogeneous ones. The well-known Rh triphenyl phosphine chloride (Wilkinson) catalyst for the hydrogenation of alkenes to alkanes by H₂ under mild conditions is a case in point. Morokuma and co-workers (Koga & Morokuma 1989), by means of *ab initio*, restricted Hartree–Fock quantum mechanical calculations, have traced the precise geometry and energetics associated with the various steps in the Halpern mechanism of this catalytic process (see figures 2 and 3). (The dynamics of this catalytic process were illustrated in video form at the lecture.)

In view of the complexity (discussed later) of heterogeneous catalysts, it is, as yet, not possible in principle to undertake computations as ambitious and comprehensive as these for heterogeneously catalysed reactions. One apparent exception turns out to be the conversion of SO₂ and O₂ to SO₃ over a silica-supported mixture of V₂O₅ and K₂S₂O₇. It is now known that the V₂O₅ and K₂S₂O₇ form a molten film, of some 100 to 1000 Å† thickness, on the high-area SiO₂ support. And, in effect, this catalyst consists of a homogeneous liquid, amenable to spectroscopic investigation (by multinuclear ¹⁷O and ⁵¹V NMR for example). The mechanism of this catalytic process has recently been elucidated by Zamaraev *et al.* (1989).

Until the last five years or so, almost all heterogeneous catalysts used commercially

† 1 Å = 10⁻¹⁰ m = 10⁻¹ nm.

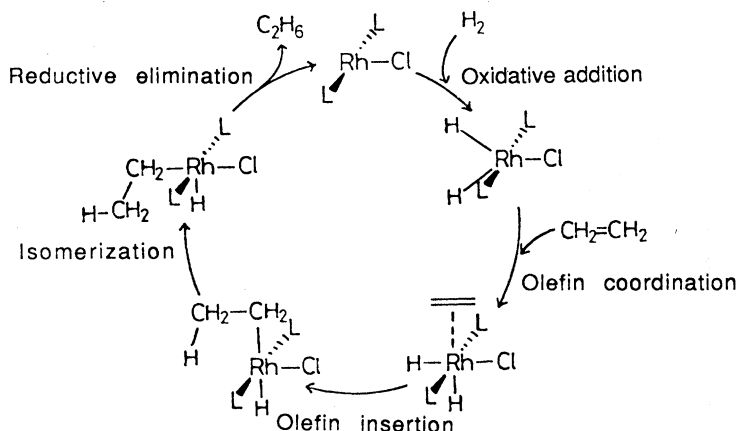


Figure 2. Scheme summarizing salient steps associated with catalysed hydrogenation of alkenes to alkanes by a homogeneous Rh triphenylphosphine chloride (Wilkinson) catalyst. L = PH_3 .

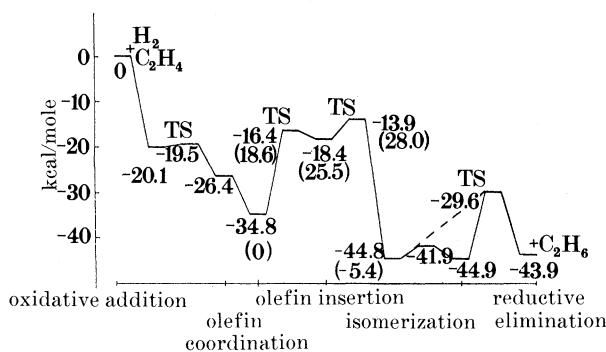


Figure 3. Potential energy profile, computed by Koga & Morokuma (1989) using restricted Hartree-Fock procedures, of the entire catalytic cycle outlined in figure 2. (By kind permission of the American Chemical Society.)

were discovered by accident. This state of affairs offers little comfort; a major industry should not be so vulnerable to the operation of chance. It is my conviction that studies of crystalline catalysts will transform this situation.

3. Why crystalline catalysts?

There are two reasons why one is attracted by the study of crystalline catalysts. First, a crystalline catalyst, provided that its surface area is maximized, will tend to have a greater concentration of active sites than one that is amorphous; the latter lacks translational symmetry, and therefore the active sites are not repeated so efficiently in the solid or its surface. Secondly, a crystal may, under ideal circumstances, be made to yield its structure by X-ray diffraction or some other powerful technique. And the structure of the crystal naturally contains within it the structure of the active site. But let us note the crucially important point that it is the precise disposition of atoms – the local structure of the active site – *under reaction conditions* that holds the key to our understanding of the mode of operation of the heterogeneous catalyst. I shall return to this point later.

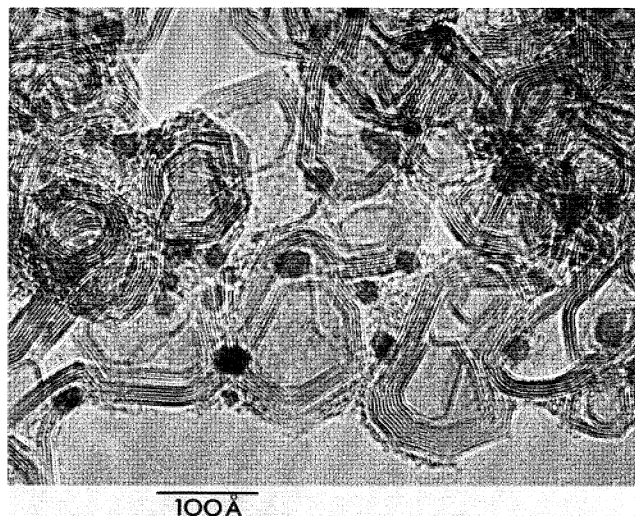


Figure 4. Electron micrograph showing the multiphasic, multicomponent nature of a powerful new catalyst for the synthesis of NH_3 . The small black patches are microcrystallites of Ru distributed on a graphitic carbon (interplanar spacings *ca.* 0.34 nm) support. A veneer of a calcium-rich phase (*ca.* 0.1 nm thick) covers the catalyst.

We need only recall how much our knowledge of enzymes – their mode of action, their inhibition, their design by site-selective mutagenesis and other means – has been transformed since their crystal structures were first elucidated less than a quarter of a century ago. Knowledge of structure illuminates our understanding of biochemical phenomena; and this understanding continues to deepen, for it is possible frequently to perform biochemical conversions inside crystals of an enzyme (Phillips 1967) and of RNA crystals (Brown *et al.* 1983) and thereby observe precisely which bonds are ruptured in the catalytic act.

But the crystals that concern us here are those that are inorganic and capable of functioning as heterogeneous catalysts. They fall into two large categories: those that are (a) multicomponent and multiphasic, or (b) monophasic and spatially uniform.

Typical of those in the first category is the one shown in figure 4. This consists of minute crystallites of Ru on graphitic carbon. Invisible in this electron micrograph, but apparent by X-ray emission microanalysis from this very region, there is a veneer of a caesium-containing compound, which has so far eluded complete identification. This is a powerful new catalyst for the synthesis of NH_3 from H_2 and N_2 ; it is much more active than the traditional Fe-based catalyst for the well-known Haber process.

Table 1 contains a list of some of the more important multiphasic, multicomponent heterogeneous catalysts now in massive use. It is a reflection of our state of comparative ignorance that no single unifying theory of heterogeneous catalysis, refined to the degree that it has real predictive value, unites these various examples; and that the nature of the active sites in these catalysts is still a contentious issue. For the methanol synthesis (ICI) catalyst, the consensus of opinion is that each exposed atom of metallic Cu functions as the seat of conversion of CO and H_2 , via probably a formate intermediate. But precisely what the details of the mechanism

Table 1. *Examples of multicomponent, multiphase heterogeneous catalysts extensively used in industrial production*

composition of catalyst	catalysed reaction
cobalt and other transition metals on a variety of supports (Fischer-Tropsch reaction)	$\text{CO} + \text{H}_2 \begin{matrix} \longrightarrow \text{C}_n\text{H}_{2n+2} \\ \longrightarrow \text{C}_n\text{H}_2 \\ \longrightarrow \text{C}_n\text{H}_{2n+1}\text{OH} \end{matrix}$
copper on $\text{ZnO}/\text{Al}_2\text{O}_3$ (‘ICI’ methanol synthesis reaction)	$\text{CO} + \text{H}_2 \rightleftharpoons \text{CH}_3\text{OH}$
nickel on alumina (methanation reaction)	$\text{CO} + \text{H}_2 \rightleftharpoons \text{CH}_4$
iron with traces of K, Si, Al (Haber synthesis)	$\text{N}_2 + \text{H}_2 \rightleftharpoons \text{NH}_3$
rhodium, platinum and palladium on CeO_2 , Al_2O_3 and cordierite (auto-exhaust catalyst)	$\text{CO} + \text{NO} \rightleftharpoons \text{CO}_2 + \text{N}_2$ $\text{CO} + \text{O}_2 \rightleftharpoons \text{CO}_2$ $\text{C}_x\text{H}_y\text{O}_2 \rightleftharpoons \text{CO}_2 + \text{H}_2\text{O}$

are is enigmatic; contrast the Rh-based homogeneous, hydrogenation catalyst discussed above.

The situation is thought (Somorjai 1990; Boudart & Djega-Mariadassou 1984; Sinfelt 1983) to be different for other metal-based catalysts, such as those enumerated in table 1. For certain face-centred-cubic metal crystallites, huge differences in catalytic activity and selectivity are known to exist between some of the high-symmetry faces, {111}, {110} and {100}. But in some instances there are indications that the most catalytically significant atoms in a crystallite are those in the penultimate surface layers. There are yet further examples where it is thought (Sachtler 1981; Cusumano 1990) that ensembles of six or more surface atoms, separated by adsorbed atoms of sulphur or carbon constitute the active sites.

In a few special recent cases it has proved possible to design selectively modified supported-metal catalysts. An example is the Ni-based steam reforming catalyst which converts natural gas (CH_4) with steam to a desired ratio of H_2 and CO (synthesis gas). Here, formation of deleterious carbon at the surface is prevented by ‘ensemble control’ via selective modification of the surface by pre-absorbed sulphur (Alstrup & Anderson 1987). In general, however, it has to be recognized that, for multiphase, multicomponent heterogeneous catalysts, we are still at a rather primitive stage of understanding so far as fully identifying the active sites, and hence of designing, *de novo*, new catalysts of this kind is concerned.

The impressive panoply of modern tools, encompassing photoelectron and Auger electron spectroscopy, low-energy electron diffraction, electron energy loss spectroscopy, ion- and particle-scattering studies and dynamic mass spectroscopy, admirable as they are in revealing the intricacies of model systems and in retrieving the structures of adsorbed layers, are inadequate – where they are not inappropriate – for identifying the active sites of multiphase, multicomponent inorganic catalysts. The prospects are not altogether bleak, as others (Cusumano 1990; Joyner 1990; Somorjai 1990) have indicated; but there is still a good deal to be done before tailored catalysts of this kind may be routinely fabricated.

The prospects for the controlled designs of the other large category of heterogeneous catalyst – those that are monophasic and spatially uniform – are altogether different. But before we proceed to discuss them, it is noteworthy to recall that accumulated experience has served us well in formulating a number of robust

Table 2. A selection of reactions catalysed by the uniform heterogeneous catalyst H ZSM-5

(H ZSM-5 stands for the protonated form of a highly siliceous (composition close to SiO_2) molecular sieve in which some of the Si atoms have been isomorphously replaced by Al. Si:Al ratios may vary from *ca.* 20:1 to 1000:1 (see Haag *et al.* 1984) and H^+ concentrations, determined by ^1H MASNMR and other methods (Makarova *et al.* 1990; Williams *et al.* 1990) are typically $3 \times 10^{20} \text{ g}^{-1}$. The all-silica variant of ZSM-5 is known as silicate I. Ti and many other elements may also be incorporated into the framework yielding other powerful uniform catalysts (Notari 1987; Van Bekkum *et al.* 1989). (See also figure 26.)

alkylation of benzene by ethylene or propylene
 isomerization of xylenes
 conversion of toluene to benzene and xylene
 synthesis of petrol from methanol
 thermal cracking of *n*-alkanes

and effective multicomponent, multiphase catalysts. The triumphant successes in developing three-way auto-exhaust catalysts for conversion of CO, NO and hydrocarbons to benign products testify to this fact.

4. Monophasic uniform heterogeneous catalysts

The most effective way of conveying the essence of a uniform heterogeneous catalyst is to describe a specific example, the so-called pentasil molecular sieve known as ZSM-5. This catalyst, which has an idealized stoichiometry $\text{H}_n \cdot \text{Si}_m \text{O}_{2m} \cdot \text{Al}_n \text{O}_{2n}$ ($m/n = 20\text{--}20,000$, $m > 60$) as well as compositional (but still monophasic) variants of it, is used commercially to effect a number of commercially important conversions (see table 2). It is microcrystalline in the sense that the individual particles, which are generally coffin-shaped, are in the size range 0.1–50 μm . A typical high-resolution electron micrograph is shown in figure 5. Each of the white circular patches denotes a 5.5 Å diameter aperture running in a direction perpendicular to the plane of the micrograph (along [010]). Depending upon the particle size, some 95% or more of the accessible surface area, usually 400–500 $\text{m}^2 \text{ g}^{-1}$, of the catalyst is internal. In other words, around 95% of all surface sites are also internal, bulk sites. There is a spatially uniform distribution of active sites, the nature of which is to be described shortly, inside the microcrystals and these sites are accessible to all molecules capable of diffusing through the extensive three-dimensional network of pores.

For catalysts of this kind, bulk techniques of analysis – be they skeletal, atomic structure-determining techniques like X-ray diffraction, or those spectroscopic ones designed to probe the electronic and dynamic properties of the reactants and products – are synonymous with surface techniques. The entire gamut of methods of the solid-state physicist and solid-state chemist are, therefore, at our disposal for the study of these uniform catalysts. Moreover, a high proportion of these techniques may be adapted to investigate the microcrystalline catalysts *in situ*. Thus:

(a) X-ray diffraction, if initial photon fluxes are adequate, may often be adapted to this end;

(b) neutron scattering studies are almost-invariably applicable since even stainless steel containers may be penetrated by neutrons;

(c) multinuclear, high-resolution, solid-state NMR (employing magic-angle-spin-

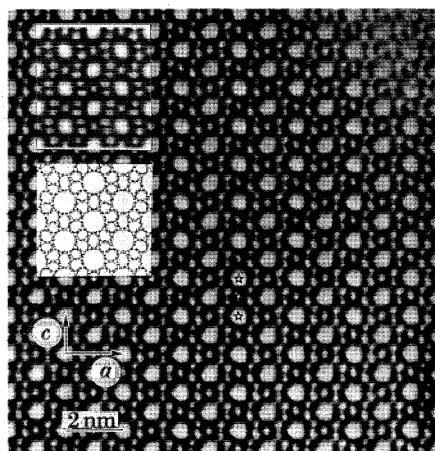
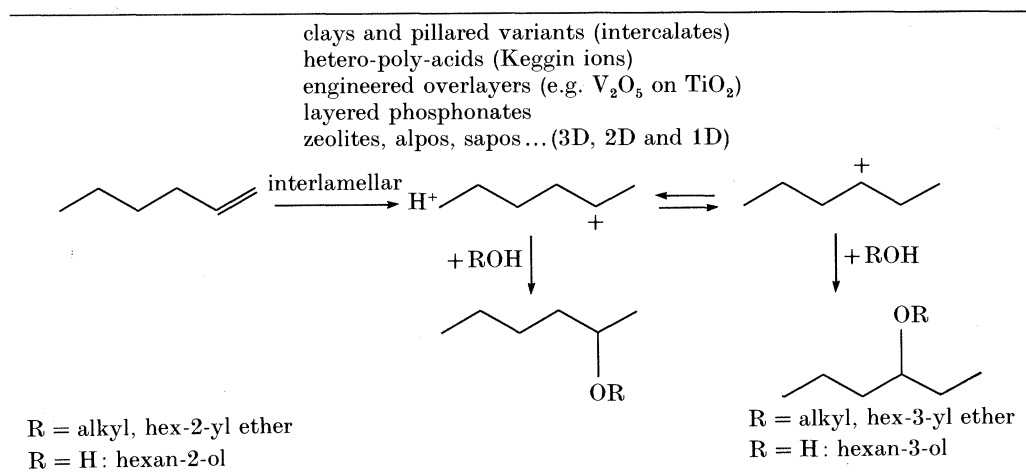


Figure 5. High-resolution electron micrograph of a ZSM-5 (molecular sieve) uniform heterogeneous catalyst. The regular white patches denote apertures of 5.5 Å diameter. (At the top left (inset) is shown the computed electron-optical image and, centre left, a projection drawing of the structure. The asterisks denote local centres of symmetry.)

Table 3. Solid acid catalysts and an illustration of a proton-catalysed addition of water (or alkanol) to an alkene



ning and/or multiple-pulse procedures) may occasionally be used to probe catalysts under operating conditions; and

(d) X-ray absorption, using synchrotron sources that permit near-edge and extended-edge fine structures and 'white line' intensities to be explored under reaction conditions.

My colleagues and I have already spent a good deal of our time developing and deploying such techniques for the study of uniform heterogeneous catalysts (Thomas 1989*a, b*; Wright *et al.* 1982, 1985; Thomas 1988; Couves *et al.* 1990*a, b*; Dooryhee *et al.* 1990).

The vast majority of the monophasic uniform heterogeneous catalysts described in table 3 (and subsequently in this lecture) are polycrystalline. The crystalline sizes are simply too small to be amenable to conventional four-circle X-ray crystallographic

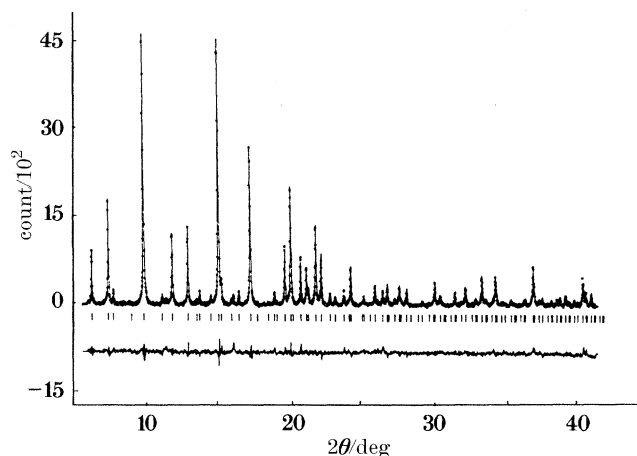


Figure 6. A typical diffractogram taken using synchrotron radiation ($\lambda = 1.0033 \text{ \AA}$) of a zeolitic catalyst (Ni^{2+} - and Li^{+} -exchanged zeolite Y) under operating conditions (acetylene vapour at $50 \text{ }^\circ\text{C}$). The diffractogram has been subjected to Rietveld analysis to yield precise bond lengths and angles, and the positions of the Ni^{2+} ions, see figure 25. The difference plot, along with vertical lines showing peak positions are also shown.

methods of structural elucidation. Instead, the highest grade of powder diffractometry has to be used to reveal the structural secrets of the catalysts. So, likewise, must ultra-high-resolution electron microscopy be deployed to its fullest, so as to image (*ex situ*) the projected structures of these microcrystals in real space. The details of the experimental procedures, as well as the necessary background theory, have been outlined elsewhere (Thomas & Vaughan 1989; Thomas 1982*a, b*, 1984, 1989*a, b*; Cheetham *et al.* 1989).

And so, begotten by opportunity out of intellectual necessity, some years ago we embarked on a programme of research which, on the one hand, involves ever more commitment to synchrotron radiation and neutron sources, and, on the other, relies heavily on high-resolution electron microscopy (HREM) to uncover from microcrystalline catalysts those structural characteristics not otherwise retrievable by X-rays. Figure 5 typifies the kind of result we obtain by HREM (see Terasaki *et al.* (1989) and Thomas (1989*a*) for further details), whereas figure 6 illustrates the kind of information obtained using synchrotron radiation for recording the diffractogram of an active catalyst under operating conditions. By Rietveld analysis (Rietveld 1969; Cheetham *et al.* 1989; Dooryhee *et al.* 1989, 1990) of such data, we obtain the structure of the active sites in the catalyst at atomic resolution.

An added bonus of synchrotron radiation for such studies is that X-ray absorption, notably extended fine-structure (EXAFS), may also be acquired simultaneously, and in a time-resolved fashion (Couves *et al.* 1990), with diffraction data provided an appropriate *in situ* cell – such as the one built at the Davy Faraday Research Laboratory (see Maddox *et al.* 1988; Pickering 1990) – is employed. EXAFS reveals the local structure of the active site, even if the catalyst lacks crystalline order.

5. Solid acids: families of uniform heterogeneous catalysts

There are many examples of uniform microcrystalline catalysts upon which we shall now focus. The simplest, the most instructive, and arguably the most important, are the solid acids (see table 3).

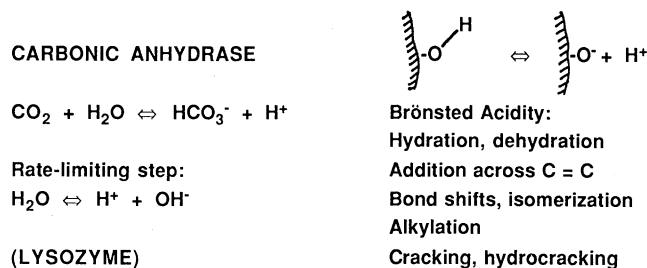
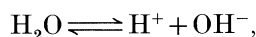


Figure 7. Solid acid catalysts (see table 3 and text) function through their high concentration of available protons, which are the agents responsible for catalysing reactions of hydrocarbons such as those listed on the right with the less demanding reactions at top, more demanding ones at bottom. These solid acids have much in common with many proteolytic and other enzymes such as lysozyme and carbonic anhydrase.

Table 4. *Techniques used for the characterization of the active sites in uniform solid-acid catalysts*

^1H Magic-angle-spinning NMR
Fourier transform infrared spectroscopy
neutron scattering, both elastic and inelastic
multinuclear NMR and other spectroscopic means of monitoring interaction of organic amines or ammonia

They all possess a high concentration of accessible, surface OH groups from which, depending upon the intrinsic Brønsted acidity of the particular system, protons are detachable (see figure 7). It is the production of the quasi-free proton, the agent of catalysis, that holds the key to the catalytic performance in this class of solid. To some degree it is possible to tailor all three – the number per unit area, the degree of accessibility, and the intrinsic strength – of these features associated with acidic OH groups. (The analogy with enzyme catalysts is useful (Eigen 1964; Williams 1982). Carbonic anhydrase, for example, serves to hydrate CO_2 ; and it has been shown that the rate-limiting step in its mode of operation is the dissociation of water:



not the formation of the C–H bond to form HCO_3^- . Two hundred and fifty nine amino acids are ‘required’ to orchestrate this process in carbonic anhydrase.)

Given the range of solids listed in table 3, our aim is to seek ways of optimizing the catalytic performance of the OH to fabricate the required end product. The active centres are the surface OH groups of the requisite acidity. It is therefore essential first to devise reliable experimental methods of detecting and quantitatively characterizing these (acidic) active sites, since the principal facilitating factor in catalysis by solid acids is the detachment and/or the availability of accessible protons. The premier techniques used for this purpose are given in table 4.

5.1. *Clays and pillared variants*

The first family of solid acid catalysts in table 3 is enormous, encompassing montmorillonites (and other smectites such as hectorite, beidellite and saponite), kandites (such as kaolinite and dickite) and the vermiculites, which are structurally more akin to the former than the latter. The interlamellar ions present in naturally

Table 5. *A selection of organic reactions catalysed by acidic clays*

conversion of primary amines or alkanols to secondary ones
isomerization, alkylations, cyclizations
hydration, alkylation and acylation of alkenes to form alkanols, ethers and esters
dehydration of alkanols, with the formation of ethers, alkenes and naphthenes
dimerizations, oligomerizations and polymerizations
decarboxylations of lactonizations
polycondensations (e.g. peptides from amino acids)
cracking and hydrocracking of hydrocarbons

occurring vermiculites and smectite clays, which have negatively charged aluminosilicate sheets, may be readily exchanged for potent acidic ones. These are H_3O^+ (or H_5O_2^+) ions formed by gentle and repeated acid washing or by substitution of highly charged ions such as Al^{3+} which produce quasi-free interlamellar protons by interaction with their hydration shells ($\text{Al}(\text{H}_2\text{O})_6^{3+} \rightarrow (\text{Al}(\text{H}_2\text{O})_5\text{OH})^{2+}$ (see Weisz 1980; Thomas 1974, 1982, 1984; Thomas *et al.* 1976; Ballantine *et al.* 1984; Ballantine 1986; Thomas & Catlow 1987; Thomas & Theocharis 1989; Purnell 1990).

Figure 8, plate 1, represents how Brönsted bases (amines or water, for example) may be protonated in the interlamellar region. It is known from high-resolution neutron powder diffraction work on analogous, acidic layered structures such as hydrogen uranyl phosphate hydrates (Fitch 1981) that H_3O^+ and H_5O_2^+ species may exist as such in interlamellar regions. Both neutral and protonated bases may coexist in close proximity within the clay interlamellar microenvironment which is itself a region of high electrostatic field. These interlamellar regions occur regularly, in a spatially uniform fashion, throughout the clay. And proton-catalysed organic reactions, of the type shown below, where the addition of water or alkanols to intercalated alkenes leads to the production, via the carbocation, of the respective alkanol or ether, occur readily in the interlamellar spaces of clay catalysts (see also table 5).

One catalysed reaction, which my colleagues and I stumbled upon in our early studies, is now of great commercial importance; the addition of methanol to isobutylene (2-methyl propene) to yield methyl tertiary butyl ether (MTBE) an important additive to petrol. MTBE boosts the octane rating of the latter and dispenses with the need to use lead-containing additives. Solid-state NMR may be used to monitor the clay-catalysed formation of MTBE (Thomas 1984).

When used at temperatures above a few hundred degrees Celsius, the layers of a clay catalyst tend to collapse, thereby hampering the entry of reactant species into the interlamellar spaces and nullifying their catalytic properties. If, however, an appropriate bulky cation is inserted into the spaces beforehand, the individual layers are kept apart by their pillaring effect thus conserving access to, and the catalytic capacity of, the interior surfaces of the clay. The multiply charged aluminium oxyhydroxide cation $[\text{Al}_{13}\text{O}_4(\text{OH})_{24}(\text{H}_2\text{O})_{12}]$ functions well as a precursor pillar (Vaughan & Lussier 1980; Tennakoon *et al.* 1986). Pillared clays (see figure 9, plate 1) have far greater thermal stability than ordinary, acidic clays and have found application as catalysts in oil refining (e.g. in durene production by the alkylation of 1,2,4-trimethylbenzene by methanol), conversion of methanol to hydrocarbons and in the esterification of alkanols (Figueras 1988). Subtle changes, via isomorphous

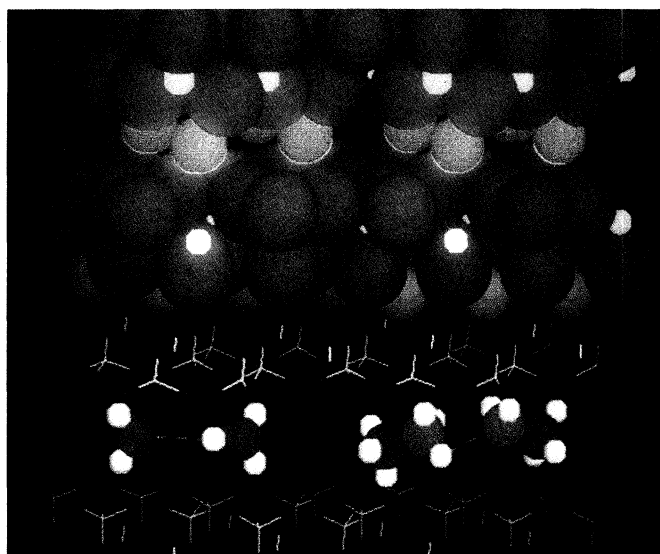


Figure 8. The top half, with ions approximately to scale, shows a Na^+ -exchanged vermiculite; the lower half is a skeletal representation of a vermiculite in which the Brønsted acidites of the interlamellar region is represented by the 'free' hydronium ions (H_3O^+) and by a protonated amine. (Vermiculite itself has the idealized formula $\text{Mg}_3(\text{Si}_3\text{Al})\text{O}_{10}(\text{OH})_2 \cdot \text{Mg}_{0.5}(\text{H}_2\text{O})_4$.) The interlamellar $\text{Mg}_{0.5}(\text{H}_2\text{O})_4$ may be readily replaced by other ions or ions and organic reactants taken up by intercalation. Colour code: oxygen ions, red; Na^+ , light blue; Al^{3+} and Si^{4+} , yellow; hydrogen, white; nitrogen, dark blue.

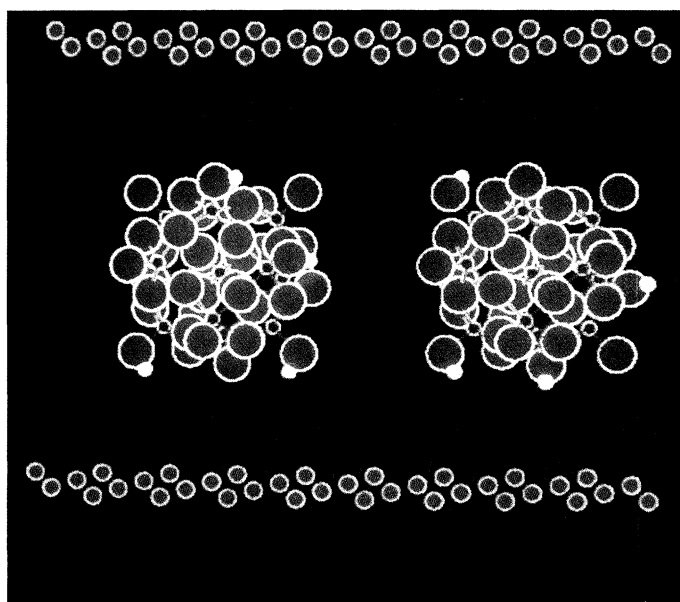


Figure 9. View of clay catalyst in which the interlamellar spaces contain Keggin ions such as $[\text{Al}_{13}\text{O}_4(\text{OH})_{24}(\text{H}_2\text{O})_{12}]^{7+}$ (see figure 10). Each polynuclear cation has a central tetrahedrally coordinated Al, surrounded by twelve octahedrally coordinated ones (Al, O and H atoms shown in green, red and white respectively, and the aluminosilicate sheets are represented skeletally)

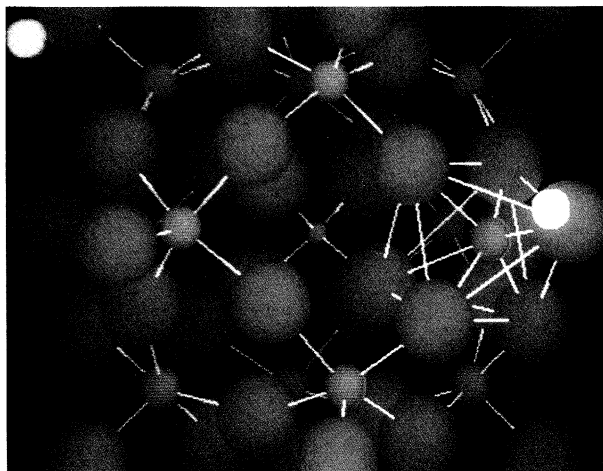


Figure 10. The Keggin anion may have P, As, Si, Ge or B in the central, tetrahedrally coordinated state (small red atom), whereas the twelve surrounding, octahedrally coordinated ones (larger mauve atoms) may be W, Mo, V, Cr, etc. Phosphomolybdic acid is $\text{H}_3\text{PMo}_{12}\text{O}_{40}$. (Small white atoms denote detachable hydrogens.)

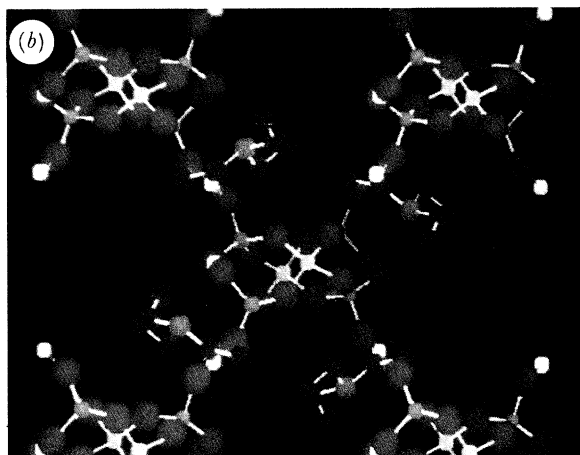
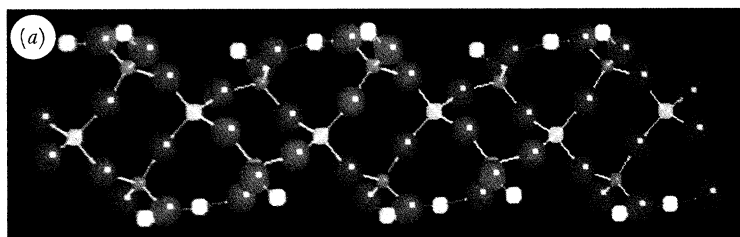


Figure 12. A newly discovered chain structure $(\text{AlH}_2\text{P}_2\text{O}_8)^-$ along the back-bone of which there occurs a recurrence of OH groups attached to phosphorous (after Jones *et al.* 1990). (a) Shows the view perpendicular to the chain axis. The sites of the protonated triethylamine are shown in (b), the view along the chains $(\text{C}_2\text{H}_5)_3\text{NH}^+(\text{AlH}_2\text{P}_2\text{O}_8)$. Aluminium atoms are yellow and phosphorous are purple.

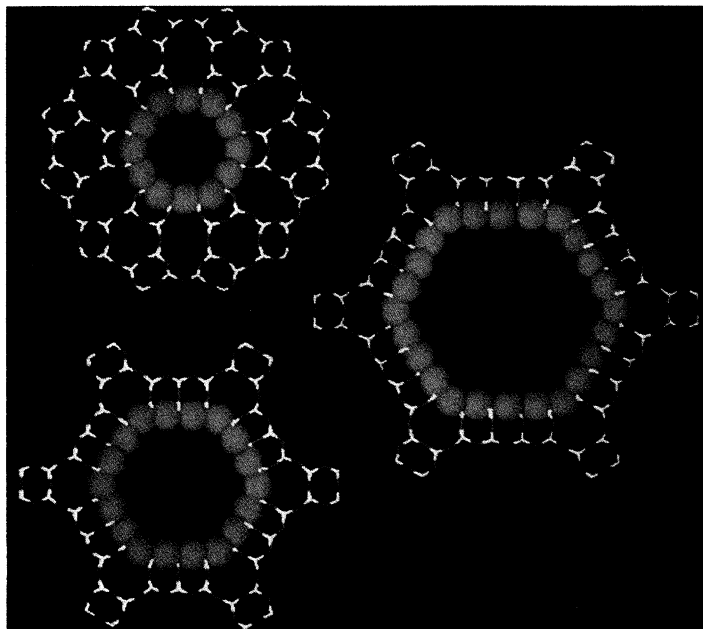


Figure 14. Representations (to scale) of the apertures in zeolite L (top left), where the diameter of the 12-ring of oxygen atoms is *ca.* 7.4 Å, in VPI-5 (bottom left) which has 18-ring openings (*ca.* 12.0 Å), and in the hypothetical (right) 24-ring opening (*ca.* 18 Å) (see text).

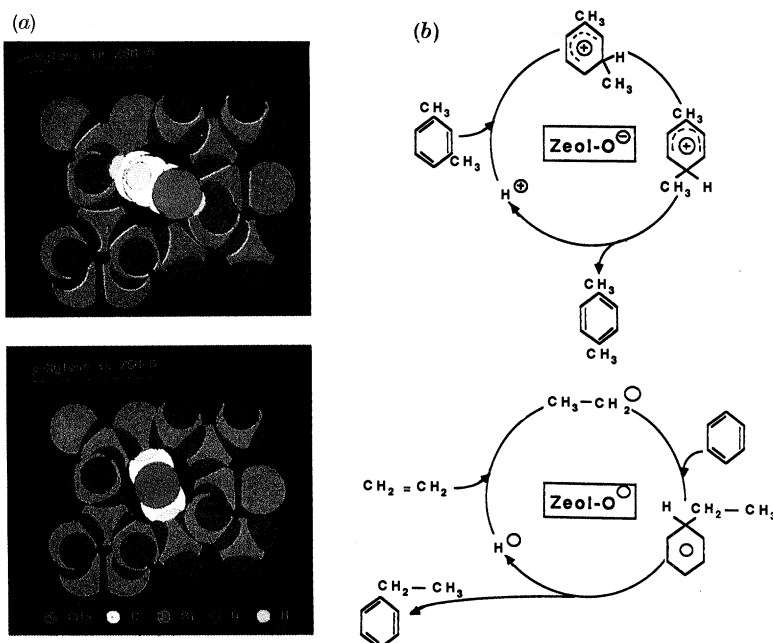


Figure 20. (a) It is easier (bottom) for *para*-xylene, more difficult for *meta*-xylene (top), because of their shape, to diffuse through a H-ZSM-5 catalyst. (b) Examples of proton-catalyzed reactions of hydrocarbons: the isomerization of *meta*- to *para*-xylene (top) and the alkylation of benzene by ethene to yield ethylbenzene (bottom).

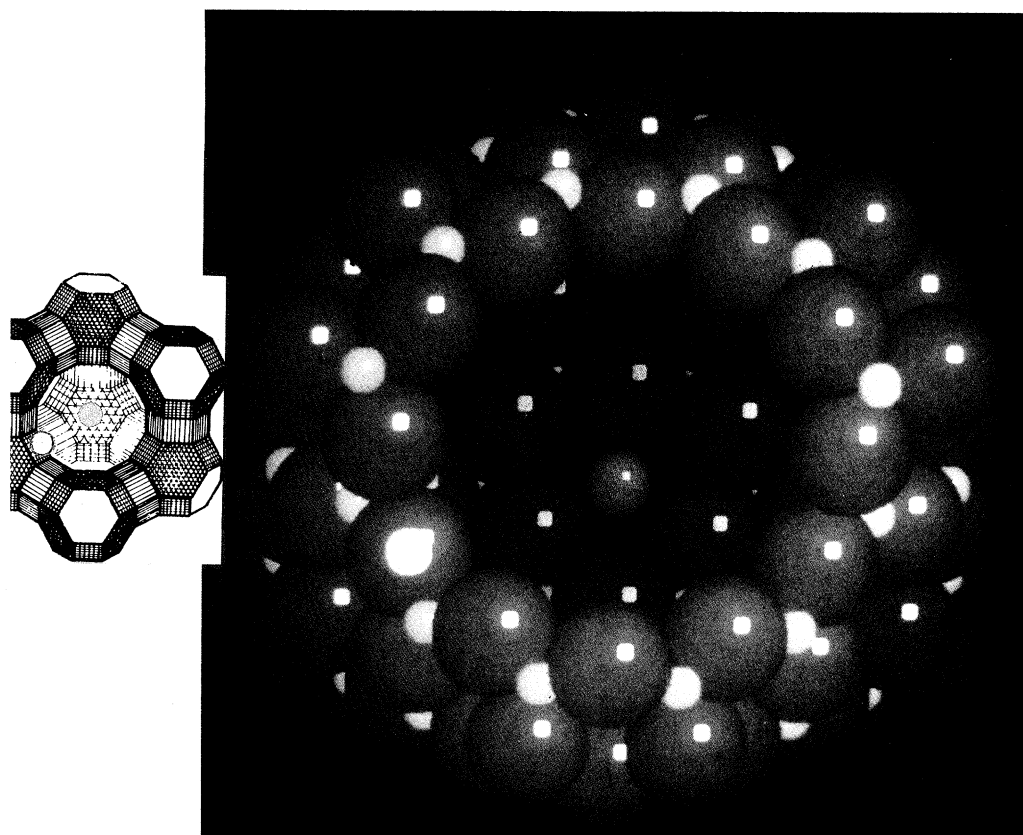


Figure 18. The white spot in the drawing on the left, and the white spot on one of the (red) oxygen atoms in the aperture of La^{3+} -exchanged zeolite Y denote the position of the detachable proton in the catalytically active site. There are six crystallographically equivalent sites for the proton around the periphery of the cage (after Cheetham *et al.* 1983).

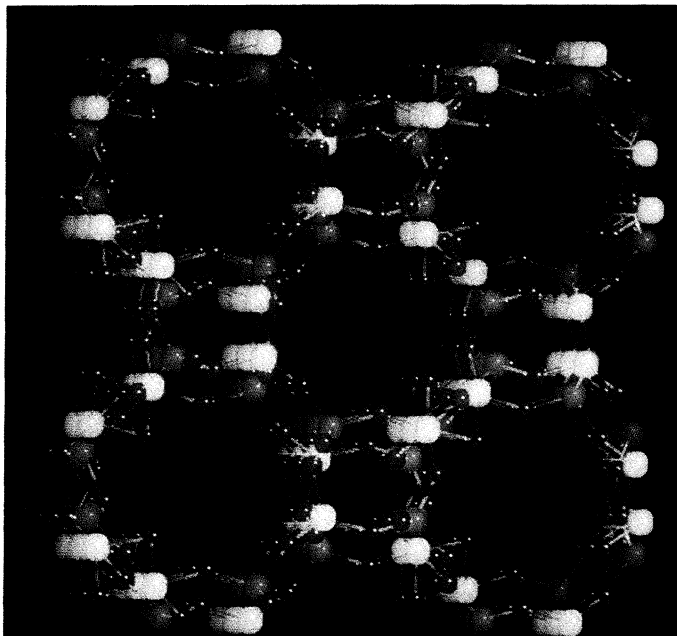


Figure 22. Segment of the structure of a new zeolitic solid discovered by R. Xu and co-workers and designated $\text{AlAsO}_4\text{-I}$.

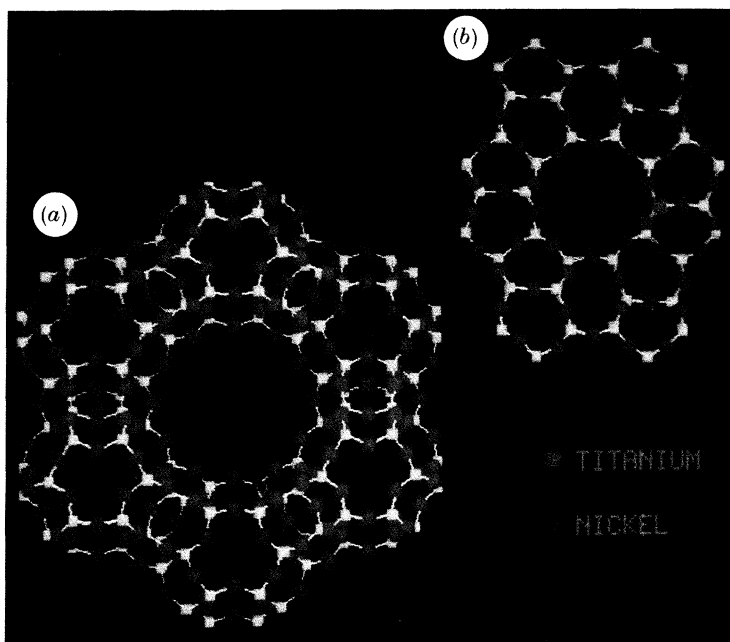


Figure 26. (a) Ni^{2+} ions may occupy extraframework sites (like the S_1 shown here) or framework tetrahedral sites. (b) In titanosilicalite the Ti^{4+} ions are part of the framework lining. Some doubt exists as to whether they occur singly or in associated pairs (see Young *et al.* 1989) (see text).

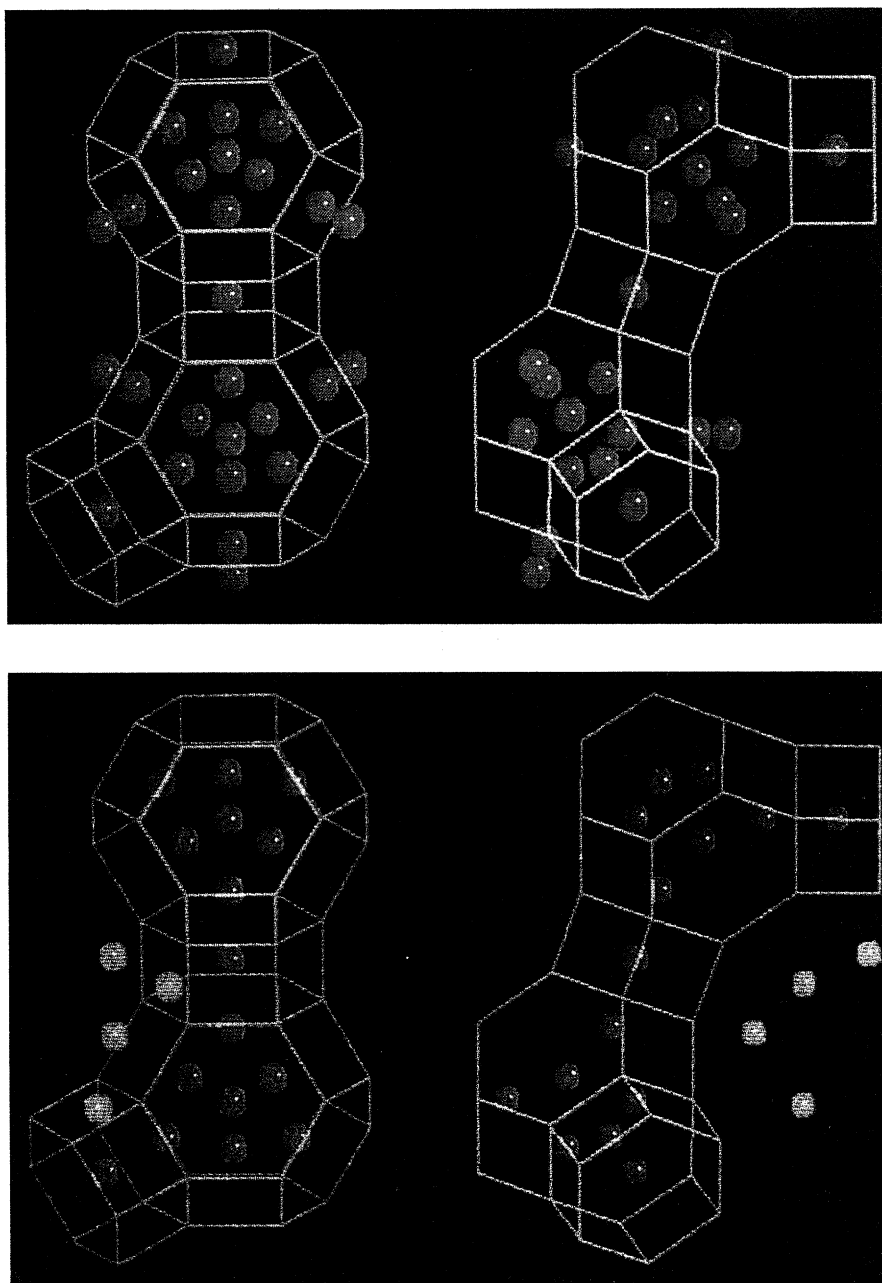


Figure 25. Computer graphic representation showing the marked difference in location of the Ni^{2+} (and Na^+) ions in the dehydrated zeolite before (upper) and after (lower) the onset of catalysis. All the extra framework cations (Ni^{2+} and Na^+) are shown in the same colour in the 'before' state, whereas in the catalytic state those Ni^{2+} that have migrated out of the supercage are shown in green. (Note that the S_1 site is situated in the centre of the double six prisms joining the adjacent sodalite cage.) The framework structure, consisting of corner shared tetrahedra TO_4 ($T = \text{Si}, \text{Al}$) is also shown in green. The two adjacent views in each representation show the pair of sodalite cages rotated by 90° with respect to one another (Couves *et al.* 1990a).

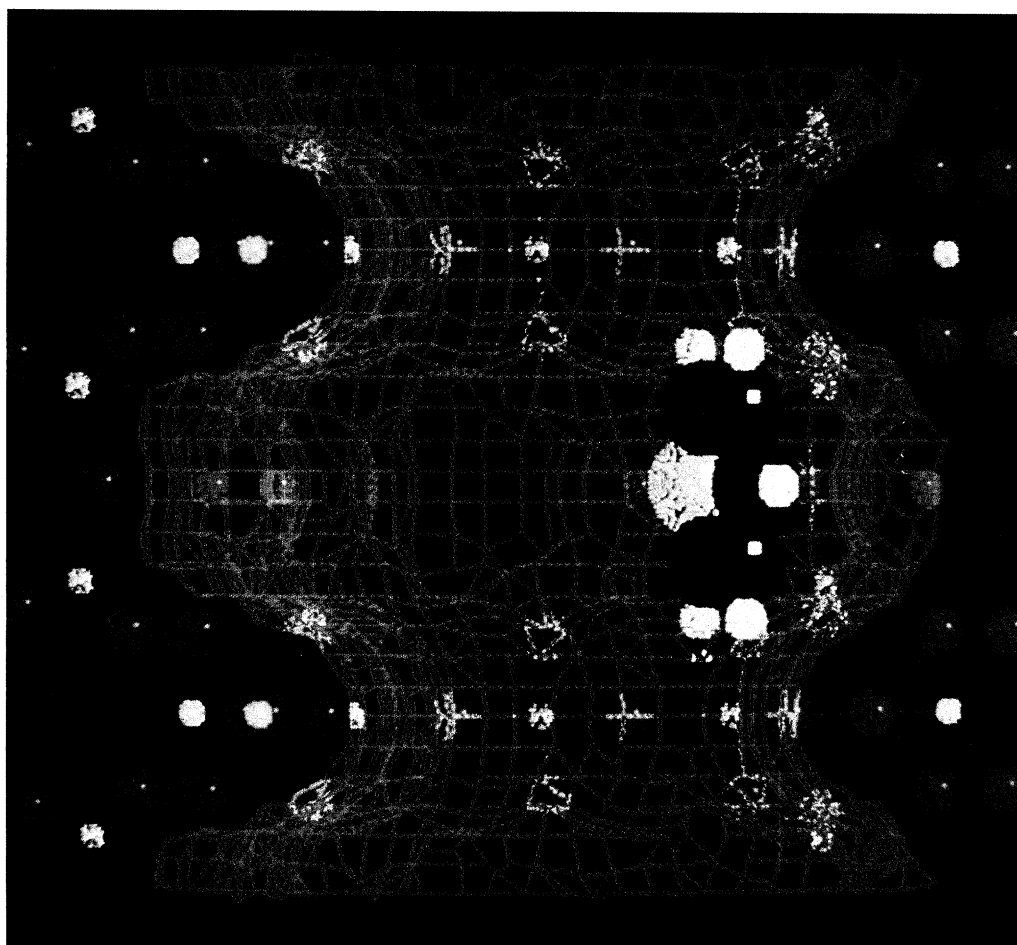


Figure 27. Elevation view of the location of a single deuteropyridine molecule in the channel of zeolite L. The green lines represent the van der Waals limits of the framework atoms shown in small yellow and red spheres. Blue spheres are K; white, H; black, C; large yellow, N. The siting was determined from a Rietveld analysis of the neutron powder diffraction profile (Wright *et al.* 1985).

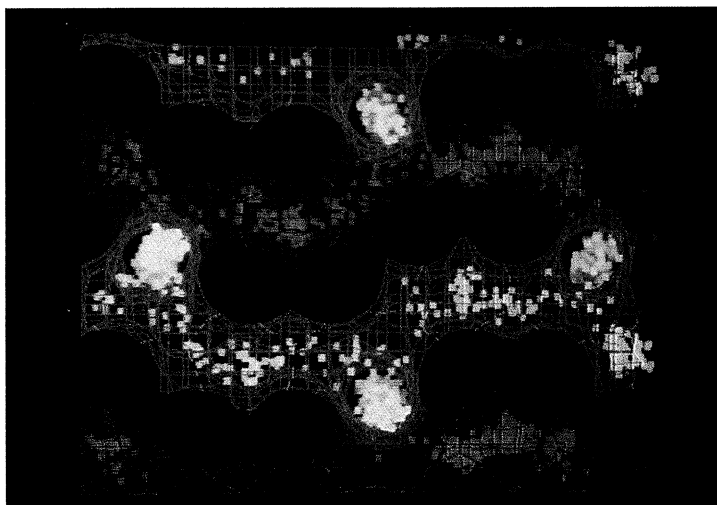


Figure 28. Trajectories of Xe at 298K in the straight and the sinusoidal channels of silicalite, the siliceous end-form of ZSM-5. Xe centre-of-mass positions are shown in yellow, Si-O bonds in red and the internal zeolitic surface is represented by the blue net (Pickett *et al.* 1990).

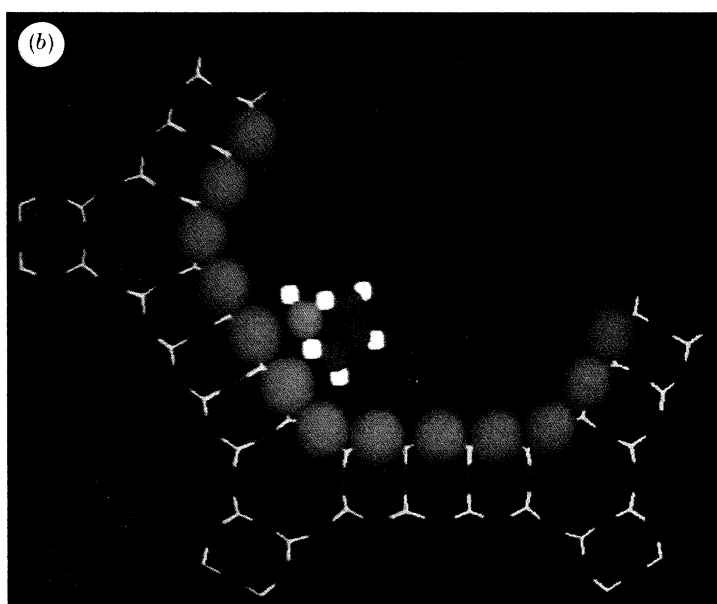
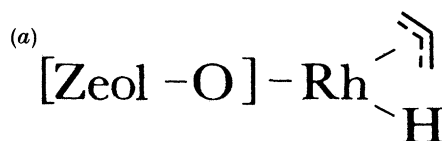


Figure 31. (a) Schematic illustration of a zeolite-bound rhodium hydride (cf. Huang & Schwartz 1982). (b) Illustration of an anchored organometallic catalytic centre anchored on the inner wall of a large cavity of a microporous crystal (rhodium atoms in purple, carbons green, oxygens red and hydrogens white) (see text).

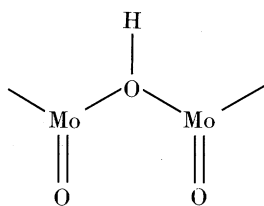
substitution, may be made to these multiply-charged ion by, for example, replacing one or more of the Al atoms by Cr or V (D. E. W. Vaughan, personal communication; Romanski & Jablonski 1988). This extends the range of tuneability of catalytic performance of the pillared clay.

But apart from fabricating such catalysts from naturally-occurring clays, which, because of the presence of impurities, may lead to less than optimal solid acids, it is also possible to synthesize smectite clays, especially beidellite (Diddams *et al.* 1984), in highly purified form. And these, too, are readily pillared thereby yielding a superior-quality catalyst.

5.2. Heteropolyacid (Keggin ion) catalysts

The polyvalent, polynuclear aluminium oxy-hydroxy cation used for pillaring clays is a special example of the so-called Keggin ion (Keggin 1934) in which a central tetrahedrally coordinated aluminium (AlO_4) is surrounded by twelve AlO_6 octahedra. It is now recognized that the silicophosphates, silicomolybdates and other variants, some of which were known to Berzelius in 1826, are structurally very similar to $[\text{Al}_{13}\text{O}_4(\text{OH})_{24}(\text{H}_2\text{O})_{12}]$ (see figure 10, plate 2).

For some time it has been recognized that heteropolyacids derived from $\text{H}_3\text{PMo}_{12}\text{O}_{40}$ can be good acid catalysts as well as good selective oxidation catalysts (Black *et al.* 1987). Their performance as acid catalysts is enhanced by substitution of one of three Mo atoms by V. A useful method of producing high-area solid acids of this kind has been described recently by Bruckman *et al.* (1989) where the series $\text{H}_{3+n}\text{PV}_n\text{Mo}_{12-n}\text{O}_{40}$ ($n = 0-3$) is either used in the pure form as extremely thin layers, or laid down epitaxially on the salt $\text{K}_3\text{PMo}_{12}\text{O}_{40}$. In the conversion of methanol to formaldehyde it is the surface Brönsted acidity of a grouping such as that shown below proves crucial:



Mechanistic features of the dehydration of alkanols and many other organic reactions catalysed by solid heteropolyacid (Keggin ions) have been summarized by Misono (1987) and Ono (1990). Catalytic activities of the solid acids follow the order:



And it is worth recalling that concentrated HNO_3 is a very much weaker acid than $\text{H}_4\text{SiMo}_{12}\text{O}_{40}$.

5.3. Metal phosphonates

The idea of creating a desirable microenvironment conducive for interlamellar catalysis may be extended to other, non-clay-based sheet structures such as those that exist in the metal phosphonates. Dines and his co-workers and Cusumano have showed that numerous metal tetrahalides may readily be converted to sheet structures, composed of metal, phosphorus and oxygen, on to which a variety of organic pendant groups could be attached (see Di Giacomo & Dines 1982; Dines &

Phil. Trans. R. Soc. Lond. A (1990)

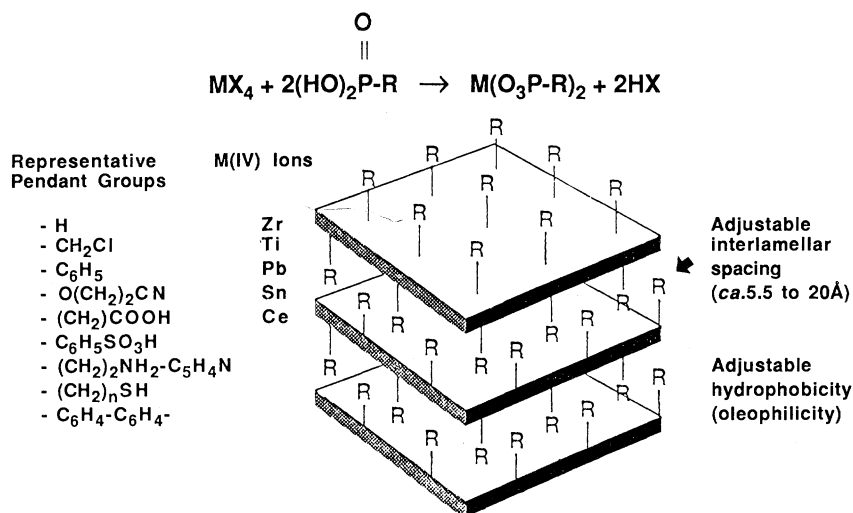


Figure 11. A wide variety of metal phosphonate acid catalysts may be engineered by adroit choice of the organic pendant group, R, and the tetravalent metal, M, that confers mechanical strength to the sheets (based on Cusumano 1990).

Griffith 1983; Cusumano 1990) (see figure 11). The merits of these molecular engineered solids as catalysts is that they: (a) have adjustable interlamellar spacings (thereby introducing an element of shape-selectivity to the ensuing reaction); (b) offer scope for fine-tuning the hydrophobicity of the interlamellar space (by appropriate choice of the organic moiety, R); (c) combine the advantages of mechanical strength, conferred by the inorganic component of the sheets, with the chemical selectivity conferred by the organic pendant group. The precise degree of acidity, as well as the concentration of acid sites is governed by the particular organic grouping that bears the sulphonic, carboxylic or phenolic OH, for instance.

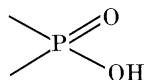
More will doubtless be heard of these so-called molecularly engineered layered structures (Cusumano 1990) in future since they are capable of serving as mechanically and chemically durable solid-acid catalysts for effecting many of the proton-catalysed reactions listed in table 5.

Sometimes 'monolayers' of oxide grafted on to the surface of another chemically different oxide possess a fair degree of acid catalytic activity (Bond 1989). It is clear from EXAFS (Kozłowski *et al.* 1983) and other techniques, that considerable scope exists for engineering novel forms of one (acidic) oxide catalyst as overlayers on another.

But as well as fashioning layered structures and their controllable Brønsted acidity to order, one may also, in principle, fashion accessible chains, along the backbone of which there are acidic groupings that may be harnessed for catalytic purposes. I am happy to report that, as a result of joint work carried out by Professor Ruren Xu and his team at Jilin University in China and by my own at the Davy Faraday Laboratory, we have discovered what promises to be a large family of inorganic linear structures capable of sustaining a recurrent array of acidic centres (see Jones *et al.* 1990).

What began as an extension of the practice first achieved by Professor Ruren Xu of producing novel, microporous aluminium phosphate (ALPO) structures (see below) from non-aqueous precursor environments, ended with the accidental synthesis of a

novel chain structure with the OH groups attached to phosphorus atoms recurrently along the chain (see figure 12, plate 2). The idealized formula of this chain is $\text{H}_2\text{AlP}_2\text{O}_8^-$. (Note that, in a sense, it is the analogue in AlPO_4 (compare SiO_2 with $2\text{Si}^{4+} \equiv 1\text{Al}^{3+} + 1\text{P}^{5+}$) of the chain silicate structures.) This novel structure is neither pyroxenic nor amphibolean but intermediate between them. The precise degree of acidity associated with the



groups is not yet known. Even if it transpires that it is low, there still exists the same scope as in the metal organophosphonates shown in figure 11 of attaching organic pendant groups, which themselves possess acid functionality. Another noteworthy possibility with this type of solid is that either the P^{5+} in the chain may be isomorphously replaced by Si^{4+} or the Al^{3+} by Mg^{2+} , or both. The resulting structure then has its anionic character boosted, just as in the case of the heteropolyacid catalysts $\text{H}_{3+n}\text{PV}_n\text{Mo}_{12-n}\text{O}_{40}$ ($n = 0-3$) described above. It remains to be seen, however, whether these silicon-substituted chain structures have the intrinsic thermal stability to function as viable acid catalysts.

5.4. Microporous, three-dimensionally uniform catalysts

An enormously large, and growing, family of microporous, microcrystalline catalysts is based on the naturally occurring zeolites, a group of aluminosilicate minerals with the general formula $\text{M}_{n/a}^{a+} \cdot \text{Si}_m\text{O}_{2m} \cdot \text{Al}_n\text{O}_{2n} \cdot x\text{H}_2\text{O}$. Here, M is an a -valent cation, and the macroanion has SiO_4^{4-} and AlO_4^{5-} tetrahedra corner-shared to form an open, microporous network within which zeolitic water (or other molecules) are housed. These crystalline solids, depending upon their precise structure, after their zeolitic water is removed, possess a porosity such that 30–50% of the solid is void space. Figure 13 illustrates the architectural principles upon which some of these structures are built.

An ion of Si^{4+} (or Al^{3+}) surrounded by a tetrahedral arrangement of oxygens may form in aqueous solution, or in a hydrothermal environment, the truncated octahedron known as the sodalite cage. (Very many different kinds of building units are also possible (see Barrer 1978).) When these polyhedra pack so as to share faces they produce the mineral sodalite. If, however, they pack by linking the sodalite cages via hexagonal prisms the resulting structure is that of the rare mineral faujasite (denoted FAU in figure 13). The sodalite cages in this structure are arranged like the carbon atoms in the diamond structure. When sodalite cages join up via cubes a new type of aluminosilicate, termed Linde type A (LTA), zeolite A, is formed. This does not occur naturally, and it was synthesized in the U.S.A. nearly forty years ago. The structure, labelled 6 in figure 11, was recently synthesized in a phase-pure state in France a few years ago. It is known (Audier *et al.* 1982; Treacy & Vaughan 1988) to intergrow with the faujasite structure, and the synthetic zeolites ZSM-20 and ZSM-3 consist of differing amounts of coherent intergrowths (RaO & Thomas 1985) of FAU and structure 6.

Until about a decade ago, it was thought that only Si, Al and a few other elements (apart from oxygen) were capable of being incorporated into the framework of these zeolites, which have apertures of molecular dimension typically ranging from 3–8 Å (Barrer 1978). By now it is known that some thirty elements (including transition

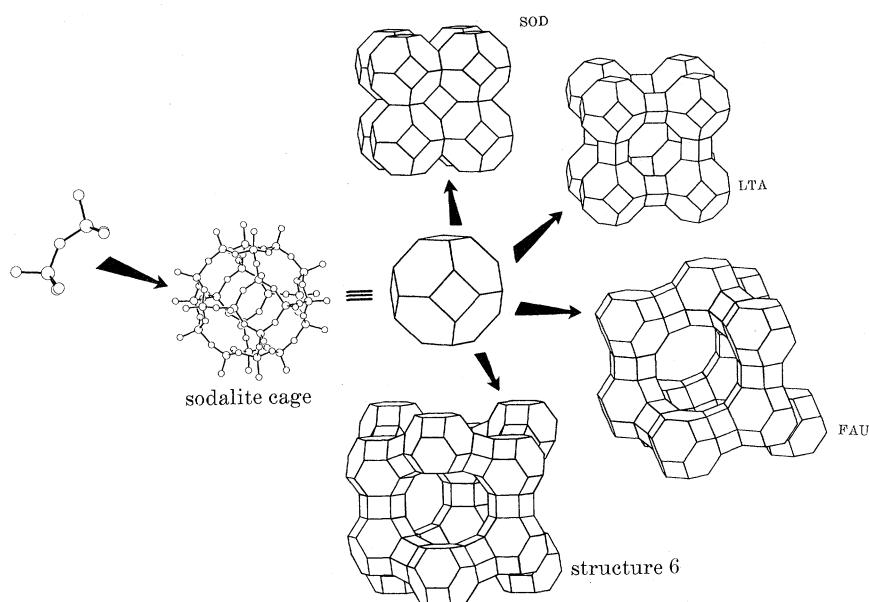


Figure 13. Schematic representation of the way in which various kinds of open structures of the macroanions of zeolites are formed. Each vertex is occupied by either a Si^{4+} or an Al^{3+} ion, tetrahedrally coordinated to oxygen atoms (not shown). The exchangeable cations have been omitted.

metal elements like Co, Ni, Fe and many main group elements like Mg, P, Ga, Li) can be tenants of these tetrahedral sites. And when one recalls the variety of exchangeable cation at our disposal (all the alkali metals, alkaline earths, rare earths, etc.), it means that the inorganic chemist and catalyst fabricator now have some 60% of all the elements in the periodic table to insert into a large set of zeolitic structures.

The aperture into the cages of faujasite – the synthetic variant is called zeolite Y, typical stoichiometry $\text{Na}_{58}\text{Al}_{58}\text{Si}_{134}\text{O}_{384} \cdot 240\text{H}_2\text{O}$ is used, in its acid form (see below) on the million tonne scale world wide to crack hydrocarbons catalytically – with its twelve oxygen rings are some 7.5 Å in diameter. The same is true of another comparable structure, that of zeolite L, the projection of the aperture of which is represented in figure 14, plate 3. Also shown in figure 14 is the 18-oxygen aperture, now some 12 Å in diameter, that is a feature of the recently synthesized so-called VPI-5 molecular sieve. Ignoring for the present the nature of the tetrahedrally bonded (T) tenants, be they Al, Si, P, etc., it is, in principle, possible to envisage an almost limitless range of new structures (Smith 1988). The relative sizes of the apertures in 12-, 18- or 24-oxygen rings are shown in figure 14, plate 3.

It is an exercise in tessellation and group theory to arrive at the various three-dimensional microporous structures possible in an infinite array of corner-sharing tetrahedra (Wells 1977). More sophisticated approaches, involving computations of the free energies of the various structures are required to evaluate their relative stabilities. From appropriate two-body, and three-body potentials – extracted from experimental data pertaining to the elasticity and phonon dispersions of zeolitic solids (see §8) – it is possible to arrive at these free energies (Catlow 1986; Catlow & Cormack 1987; Thomas & Catlow 1987).

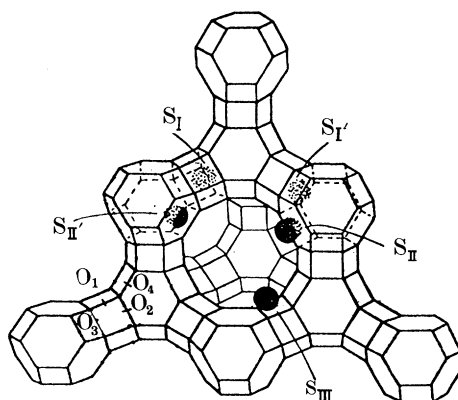
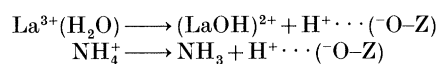


Figure 15. Exchangeable cations take up preferred high-symmetry sites in the cavities of faujasitic zeolites. Site S_I is situated at the centre of the hexagonal prism joining two sodalite cages. S_{II} lines the supercage and is situated just above the six-sided face of a sodalite cage, whereas S_{III} is just above the four-sided face. The S_I and S_{II} sites are mirror images of the parent sites and lie largely inside the sodalite cage. There are four distinct oxygen sites (O_1 to O_4) in the faujasite structure. The reactions that lead to the production of the acid form of zeolite Y catalysts are:



Extra framework (exchangeable) cations take up positions dictated principally by the electrostatics of the solid. Nowadays, as well as determining the cation positions (see figure 15) directly by crystallographic techniques, it is increasingly feasible to compute them using the procedures pioneered by Catlow. When the macroanion contains Si, Al and O this is, at present, easier than when Si, Al, P and O are present, solely because of an incomplete database of reliable potentials. The latter are required to achieve the same computational end points with the aluminium phosphates (ALPOS), with the silicon-aluminium phosphates (SAPOS) and with the metal (ME) analogues, MEASPOS, that are already attainable with aluminosilicates.

The key point to note so far as creating solid acid (molecular sieve) catalysts is concerned, is that, for every Al^{3+} ion in the framework of an aluminosilicate a proton becomes available; likewise, for the ALPO frameworks, for every P^{5+} replaced by a Si^{4+} and every Al^{3+} replaced by Mg^{2+} (or other divalent cation) a proton also becomes available.

The most convenient manner, in practice, of introducing high concentrations of quasi-free protons is either by heat-creating an NH_4^+ ion-exchanged molecular sieve, or by taking advantage of the cation hydrolysis associated with multiply charged ions such as La^{3+} – see equations given in figure 15. Although the resulting solids (e.g. H-Y zeolite) have an acidity that is greater by a millionfold than that of 100% H_2SO_4 – they are superacids in the sense conceived by J. B. Conant, the originator of the term – they are vulnerable to dissolution if treated directly with strong mineral acids.

5.4.1. Pinpointing the catalytic activity of solid, microporous, Brønsted acids

Now that we know how to prepare these powerful solid acid, microcrystalline catalysts, replete with their cages or channels which confer upon them the extra attribute of shape-selectivity, how do we set about characterizing their precise

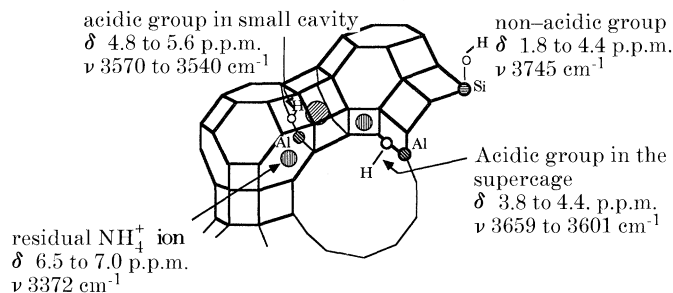


Figure 16. A combination of ^1H MASNMR and FTIR permits the precise identity of the acidic and non-acidic OH groups in a H-Y zeolitic catalyst to be identified. Hydrogen attached to oxygens bridging Si and Al in the framework is acidic (see text). (Based on Pfeiffer 1989.)

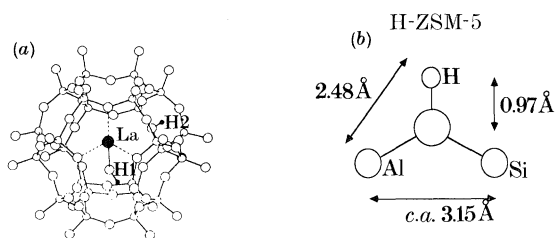


Figure 17. (a) The catalytically active site in La^{3+} -exchanged zeolite Y (solid acid) consists of a proton (H_2) which, although bound to the framework oxygen at low temperatures (*ca.* 10 K) is mobile at higher temperatures. (From neutron powder diffraction (Rietveld refinement).) (b) Projection drawings from solid state ^1H NMR of the active site in H-ZSM-5 (see text).

catalytic properties? Can we identify the active sites? Or are they delocalized in the sense that they are in the case of the clay catalysts?

All these questions, and others too, may be answered by using one or other or a combination of the following techniques enumerated in table 4.

Figure 16 shows the siting of three kinds of OH groups present in heat-treated NH_4^+ -exchanged zeolite Y. The resulting, so called H-Y catalyst has one acidic group pointing into the supercage, another with different NMR and infrared signatures, into the double-six (hexagonal prism) cavity. Residual NH_4^+ ions are sited at the inner wall of the supercage. It is the first of these three OH groups that predominates in the acid catalysis associated with H-Y zeolites. (The second has comparable acid strength and concentration, but is much less accessible than the first: so minute is the hexagonal prismatic cavity that only small bases, like NH_3 , can reach it.)

Figure 17 shows, in quantitative terms, the precise nature of the active site, from which the proton is donated to the reactant, in La^{3+} -exchanged zeolite Y and in H^+ -exchanged ZSM-5. Structural details of the former (see also figure 18, plate 4) were deduced from neutron diffraction studies by Cheetham *et al.* (1984), of the latter by measurement of ^1H NMR, second moments as outlined elsewhere (Thomas & Klinowski 1985; Hamden 1987).

The cardinal feature associated with these microporous, three-dimensionally uniform catalysts (and of comparable molecular sieve catalysts) is that their crystallography dictates in precise stoichiometric and stereochemical terms the concentration and accessibility of the active sites. We may therefore introduce Brønsted base reactants of requisite size into the micro-environment of the catalyst in a delicately controllable fashion.

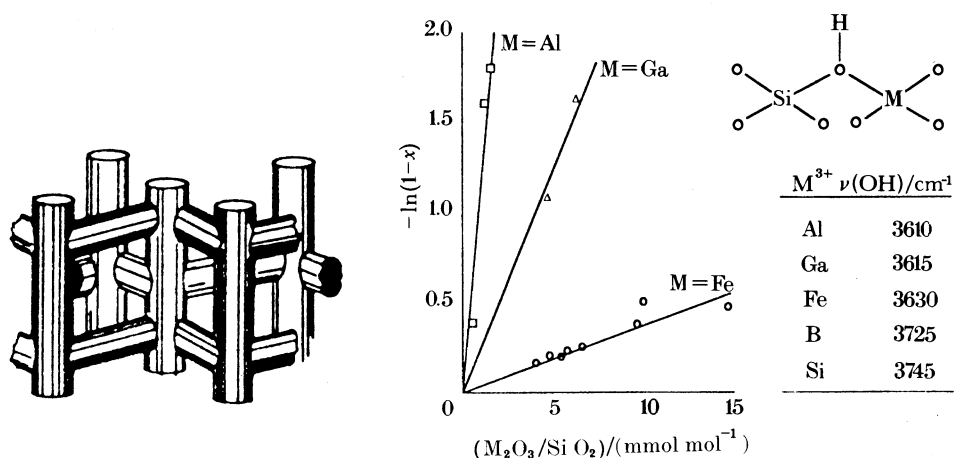


Figure 19. Many elements other than Si and Al may occupy the tetrahedral sites of H ZSM-5, the channel structure of which is schematized at the extreme left. The infrared frequency of the bridging OH group (see inset at right) is inversely proportional to the Brönsted acidity of the group. The catalytic acidity (for the cracking of *n*-hexane) of a series of isomorphously related (ZSM-5) solid acid scales with the infrared frequency (after Post *et al.* 1989).

5.4.2. Catalysis by H-ZSM-5 and its isomorphously substituted analogues

Crystals of ZSM-5, containing any desired H (acid site) concentration from *ca.* 1.0×10^{18} to $5 \times 10^{20} g^{-1}$, depending upon the magnitude of the Si/Al ratios and the crystallite size, may be readily prepared (Weisz 1980; Haag *et al.* 1984; Liu 1986; Makarova *et al.* 1990). They may also be prepared in a state of high phase-purity when elements such as Ga, B, Fe occupy the tetrahedral sites.

As the nature of the element occupying a T-site varies, so also does the intrinsic Brönsted acidity of the OH group in the bridging position between T and Si (see figure 19). The catalytic activity of isomorphously substituted ZSM-5 unsurprisingly scales with the infrared vibrational frequency: the lower the OH stretching frequency, the greater the aptitude to generate quasi-free protons and, hence, the greater the catalytic activity, as borne out (Post *et al.* 1989) in the thermal cracking of *n*-hexane.

Less demanding, in a catalytic sense, are the isomerization of xylenes and the alkylation of benzene. Both these reactions are widely used industrially. Available protons within the H-ZSM-5 uniform catalyst lead to the formation of a carbocation intermediate from *meta*-xylene (top right of figure 20, plate 5) which undergoes a methyl shift to generate a *para* isomer. The former is of minor importance commercially, the latter of great value as it is the precursor of terephthalic acid and hence the entry point into polyester fibres such as terylene.

(During the lecture, the results of a molecular dynamics calculation showing *m*-xylene and then *p*-xylene inside a silicalite I, the siliceous end-member of ZSM-5, at 350 K was shown at this juncture. The contrast in diffusivity of the *m*- and *p*-isomer was striking. Whereas the former remained more-or-less anchored to the intersection of the channels of the crystal, the former migrated rapidly along the [010] direction. This illustrates well the mode of action of the H-ZSM-5 as a zeolitic catalyst in the present example. The uniform catalyst provides the proton to the essentially static reactant which then rapidly undergoes isomerization, and the shape-selectivity of


ABW	REL	AFG	AFI	AFS	AFT	AFY	ANA	APC	APD	AST	
ATF	ATT	ATW	bea	beb	BIK	BOG	BPH	BRE	bsb	CAN	
CAS	CHA	-CHI	DAC	DOR	DOH	ERB	EDI	EPI	ERI	EUO	
FAU	FER	GIS	GME	GOD	HEU	KFI	LAU	LEU	LIO	LOS	
LOU	LTA	LTL	LTN	MAZ	MEL	MEP	MER	MFI	MFS	MOR	
MTN	MTT	MTW	NAT	NON	OFF	-PAR	PAU	PHI	RHO	-ROG	
SGT	SOD	STI	THO	TON	UFI	-WEN	YUG				

Figure 21. An alphabetized matrix of the three-letter codes designating all known (as of late 1989) naturally occurring and synthetic aluminosilicates that are zeolitic (Treacy & Newsam 1990).

the catalyst enables the *p*-isomer, as product, to migrate rapidly out of the crystal. It is a method of circumventing thermodynamic limitations by shape selectivity.)

The proton-catalysed addition of ethylene to benzene (bottom right, figure 20) yields ethyl benzene, a stepping stone to the production of styrene. This H-ZSM-5 catalysed alkylation is far more effective, cleaner in product range and type, and environmentally less harmful than the Friedel-Crafts methods of alkylation with its AlCl_3 catalyst that both corrodes containers and harms the environment.

6. Zeolites unlimited: new types of uniform heterogeneous catalyst

So far in this review only two types of zeolitic framework structures have been considered: faujasite, which is the parent type for zeolite Y, and ZSM-5, the most prominent member of the so-called pentasil family of highly siliceous zeolites. There are, however, well over sixty different kinds of zeolitic framework already characterized, and many more that have so far defied full structural analysis.

Several compilations of zeolite structures are available (see Barrer 1978; Olson & Meier 1987; Mortier & Schoonheydt 1985; Smith 1988). A recent set, prepared by M. M. J. Treacy and J. M. Newsam, shown in figure 21, is suitable for storage on a lap top computer. The three letter rotation is cryptic, but hallowed by extensive usage among zeolite scientists and technologists. Thus FAU, MOR, FER refer to the well-known faujasite, mordenite and ferrierite frameworks. STI stands for stilbite the first zeolite ever identified (by the Swedish nobleman Cronstedt in 1756). Close to it on the bottom line in the alphabetic sequence is one of the most recently characterized zeolites, theta-1, designated TON. Bearing in mind that over a quarter of the elements in the periodic table may be incorporated into many of these frameworks and that about half of the elements may serve as exchangeable ions, it is clear that several million different monophasic, spatially uniform zeolitic solids are, in principle, possible. Already tens of thousands have been prepared, characterized and tested as catalysts of one kind or another.

But if one recognizes that there are many new, tetrahedrally linked framework structures possible for the aluminium phosphates, silicon-aluminium phosphates and their metal-substituted analogues (Davis *et al.* 1988; Yan Xu *et al.* 1989, 1990; Flanigen 1986), the range of possible uniform crystalline catalysts is seen to expand further. Moreover, thanks to the elegant work of Ruren Xu *et al.* (1990), who has uncovered three new families of microporous crystals, of general formula MVO_4 , where the M atom is now often bonded to more than four O atoms, yet further

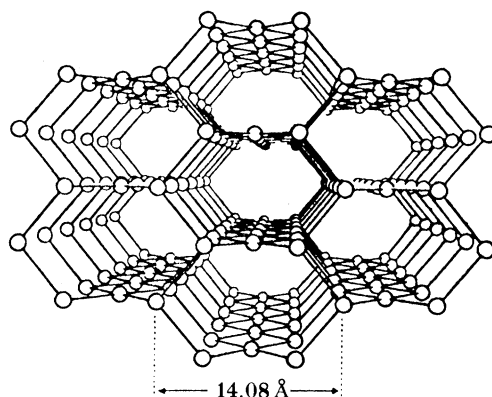


Figure 23. A recently discovered open structure exhibited by cadmium cyanide when crystallized in the presence of alcohol.

enlargements in the size of available new microcrystalline solids are already at hand. Ruren's work on gallium phosphates and arsenates and aluminium phosphates and arsenates, abbreviated GAPOS, ALASOS and GAASOS, are typified by the novel structure shown in figure 22, plate 5, a new microporous structure designated $\text{AlAsO}_4\text{-1}$. We (Jones *et al.* 1990) have recently found that crystals of aluminium phosphate harvested from a non-aqueous mother liquor are of two kinds. One crystallizes with this ($\text{AlAsO}_4\text{-1}$) structure, the other with that of the mineral berlinite.

It is known that some of these myriad new structures may be converted – by appropriate cation exchange, heat-treatment or isomorphous substitution as described above for conventional aluminosilicate zeolites – into solid acid catalysts. But solids exhibiting these structures, along with very many of the known solid structures of families of established zeolites, may also function as uniform heterogeneous catalysts for other (non acid–base) reactions. Transition-metal ion-exchanged zeolites, for example, are widely used as redox and comparable catalysts, especially for the conversions and synthesis of organic molecules (see Boreskov & Minachev 1979; Maxwell 1982, 1990; Hölderich *et al.* 1988; Kallo & Minachev 1988). With the renewed interest in designing new microcrystalline, microporous solids, it is likely that further expansion in range of uniform heterogeneous catalysts is imminent. The recent work of Robson, for example, on open cadmium cyanide structures, where certain kinships with and differences from zeolitic structures as potential new uniform catalysts are apparent (see figure 23), is relevant in this regard. Little wonder that the number of commercial patents, describing the use of microporous crystals as new catalysts, is now growing exponentially (Thomas & Vaughan 1989).

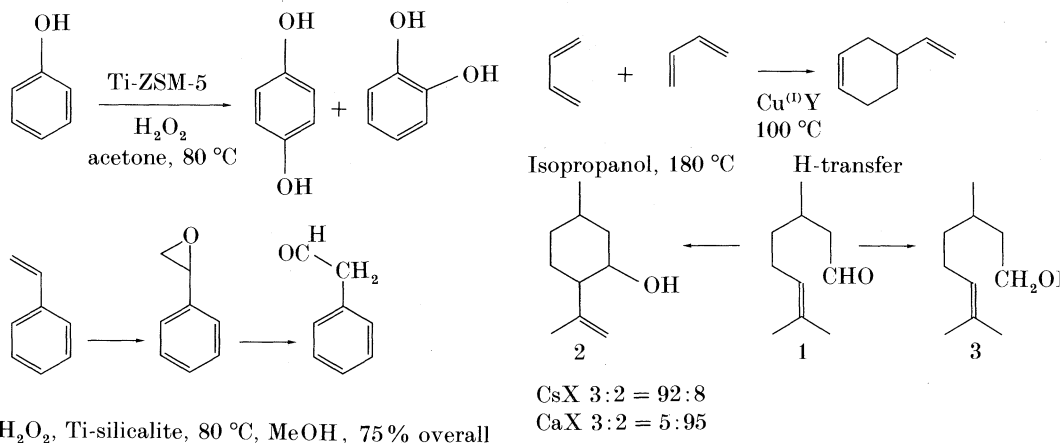
7. Metal-ion-exchanged zeolites as uniform heterogeneous catalysts

Scheme 1 illustrates a few of the useful organic reactions that may be smoothly catalysed by metal-containing (usually in extra-framework cationic form) zeolites. The compilations of Boreskov & Minachev (1979) and Kallo & Minachev (1988) as well as those of Maxwell (1982, 1990) and Hölderich *et al.* (1988) contain very many more. Almost all of the examples cited conform to the definition of uniform

Phil. Trans. R. Soc. Lond. A (1990)

194

J. M. Thomas



Scheme 1.

heterogeneous catalysis in the sense that the active sites are distributed in a spatially uniform fashion throughout the bulk, and they are all accessible to the reactant.

The nature of the active sites for these reactions is, however, less well understood than for the case of the uniform, solid-acid zeolitic catalysts. One of the reasons for this comparative state of ignorance is because the metal ions principally implicated in the active sites are relatively mobile; and there are strong indications (confirmed below) that these metal ions may migrate to locations within the zeolite quite remote from those associated with the as-prepared catalyst. With crystalline catalysts of this kind it is vitally important to determine the structure of the catalyst under operating conditions. A case study of just such a determination is therefore given in the next section.

7.1. Catalysis of the cyclotrimerization of acetylene by nickel-ion-exchange zeolite Y: an *in situ* study

Ni^{2+} ions embedded in certain environments catalytically convert acetylene to benzene. An as-prepared Ni^{2+} -exchanged zeolite Y is, however, inactive at first when exposed to acetylene at a progressively increasing temperature. In due course, with the changing environment of the Ni^{2+} ions (as evidenced by the changing diffractogram) the solid becomes an efficient catalyst (see figure 24 and Maddox *et al.* 1988). By conducting *in situ* studies, entailing parallel measurements of activity (by on-line chromatography) and detailed solid-state structure deduced from Rietveld refinement of powder diffractograms recorded with the aid of a rotating-anode facility), Couves *et al.* (1990) have charted the precise changes in the siting of Ni^{2+} ions before, during and after the cessation of catalytic action (see figure 25).

What, in essence, occurs, is that, during dehydration before the onset of catalytic action, the Ni^{2+} ions get buried into predominantly S_1 sites. Some, also, are entrapped inside sodalite cages, there being some residual water molecules bonded to the latter even in the nominally 'dehydrated' state. The process of activation of the catalyst evidently entails the migration of Ni^{2+} ions from the S_1 sites out into the supercage, this 'extraction' being induced by the reactant itself, acetylene. In due course, when the catalyst loses its activity, the Ni^{2+} ions still remain in the supercage. The poisoning of the catalysis is clearly not association with reburial of the Ni^{2+} ions. We are currently investigating whether the ion itself changes its electronic state and

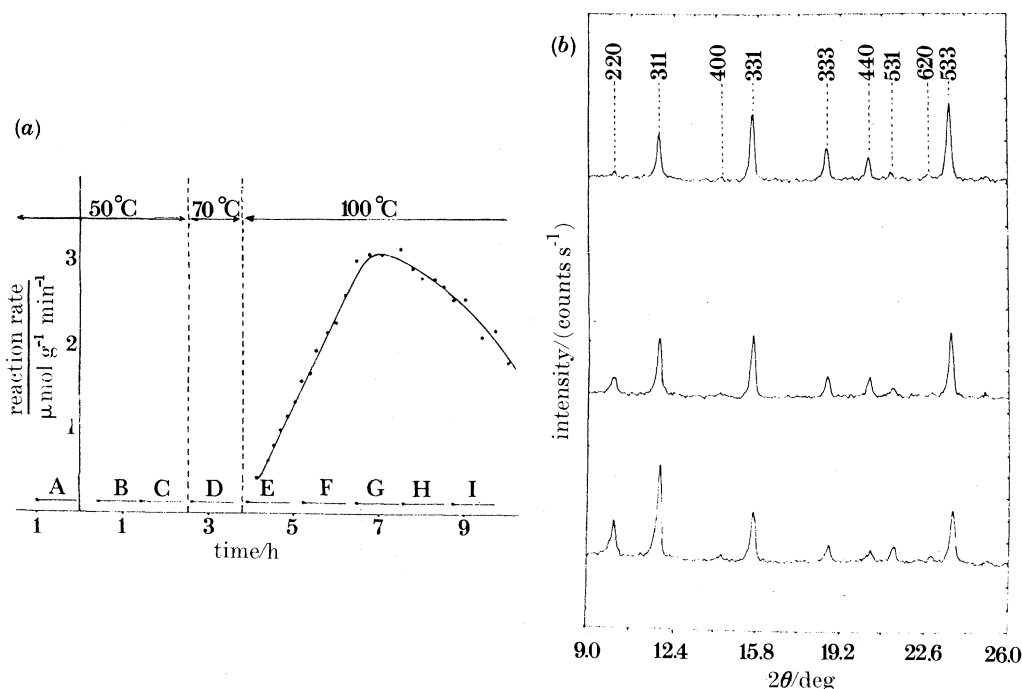


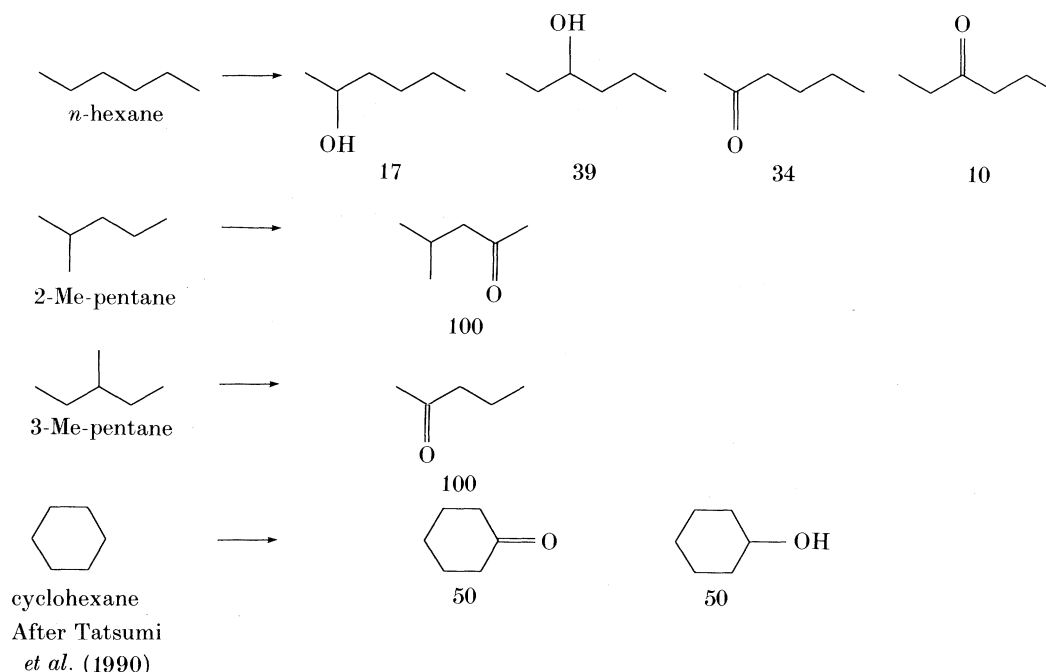
Figure 24. (a) Catalytic activity as a function of time and temperature. Acetylene introduced at time = 0. Horizontal lines indicate the time and duration of the collected diffraction patterns A to I. (b) Three of the diffractograms B, bottom; E, middle; and I top (Maddox *et al.* 1988).

or whether some carbonaceous or other reaction product is preferentially bound to the active sites. (For practical purposes it is more convenient to study $\text{Ni}^{2+}\text{Na}^{+}$ -exchanged Y or $\text{Ni}^{2+}\text{Li}^{+}$ -exchanged Y catalysts than the Ni^{2+} -Y analogue since the latter is very difficult to prepare. $\text{Ni}^{2+}\text{Li}^{+}$ -Y is the more convenient of the two to study as Li^{+} ions are less visible to X-rays than Na^{+} ions.)

There are very many redox (metal) catalysed reactions available for study involving uniform catalysts. These should, in due course, deepen our understanding of the mechanisms of catalysis. Apart from those uniform zeolitic catalysts where the active site (or cluster of ions constituting the active site) is in the extra framework cavities (as shown in figure 25, plate 6), there are other intriguing possibilities where the active site (or a component of it) is itself part of the framework (Young *et al.* 1989). It has been shown recently by Italian workers (Perego *et al.* 1986; Notari 1987) that titanasilicalite (that is the structure shown in figure 5 but with Ti ions tiling the channels, as symbolized in figure 26, plate 6) is an extremely good selective oxidation catalyst, see scheme 1, capable of converting propylene to propylene oxide and phenol to hydroquinone in the presence of H_2O_2 . (The last named reaction has already been brought to commercial fruition by the EniChem company in Italy.) Tatsumi *et al.* (1990) have recently shown that titanasilicalite at 50 °C is an effective selective oxidation catalyst for linear and branched alkanes (see scheme 2).

More is likely to be heard of this type of catalysis, which has kinship with certain features of biological oxidation process (see Herron *et al.* 1986; Herron & Tolman 1987), as and when greater precision is introduced to the preparation and characterization of modified zeolites. In a preliminary study of a zeolite Y catalyst

Phil. Trans. R. Soc. Lond. A (1990)



Scheme 2.

in which the Ni^{2+} ion is part of the framework (prepared by D. E. W. Vaughan, personal communication) we have found that there is little aptitude for this metal ion to catalyse acetylene to benzene, in contrast to the action of the same ion in the extra-framework position.

8. Catalysis by zeolites and the role of computational chemistry

With an embarrassment of choices already confronting us experimentally both with regard to structural type on the one hand and compositional variations within a given type on the other, and with an ever expanding family of zeolites at one's disposal as potentially viable catalysts, the question may rightly be asked if a more systematic strategy of selecting or tailoring new zeolitic catalysts may be evolved by harnessing the burgeoning power of the supercomputer. There are clear indications that computational chemical techniques are particularly apposite for probing the properties of uniform zeolitic catalysts. In less than a decade the penetrating power of the computational approach to the study of zeolitic catalysts has improved dramatically.

At first, using relatively primitive molecular mechanics procedures (Thomas & Ramdas 1985; Ramdas *et al.* 1984; Wright *et al.* 1985) it was possible first to quantify simple notions of shape selectivity, and then to estimate the magnitudes of activation energies of diffusion of rigid organic molecules within intrazeolitic cavities, and then to compute the siting and orientation of aromatic bases inside a zeolitic crystal (see figure 27, plate 7). Later, using Monte Carlo methods (Yashonath *et al.* 1988; Cheetham *et al.* 1989), the potential energy distribution functions of small hydrocarbons (such as CH_4) inside a subset of zeolite Y structures were evaluated, giving extra insight into the energetics of adsorption before the catalytic act. With

Phil. Trans. R. Soc. Lond. A (1990)

molecular dynamics (Cohen de Lara *et al.* 1989; Pickett *et al.* 1990; Pickett 1990) it has proved possible to compute, ahead of experiment, the magnitude of diffusion coefficients and their activation energies of sorbed molecules in various crystallographic directions within the zeolite. Figure 28, plate 8, taken from the work of Pickett *et al.* (1990) represents the results of trajectory calculations, using molecular dynamics, of Xe (comparable in size to CH₄) in the siliceous end-member of ZSM-5, silicalite. (Note that there is full accessibility of the interior surface of this (model) catalyst gained by the (model) reactant.)

Non-rigid molecules may now be routinely considered in molecular dynamics calculations; and the full flexibility of the catalyst framework itself – by taking into account three-body (bond bending) as well as two-body terms in the summation of the total interaction energy – has already been incorporated into calculations recently completed (B. Vessal & C. Freeman, personal communication).

(At this stage in the lecture, the results of a molecular dynamics computation with periodic boundary conditions carried out by Dr Vessal of Rutherford Appleton and the University of Keele covering a 12.5 ps run in a time-step of 1 fs for the silicalite structure at 300 K was shown in video form by my colleague Dr Freeman. This revealed the flexibility of the framework, and the reality of the dynamic nature of the variation in aperture dimensions of the model catalyst.)

Computational chemistry has several other contributions to make to our understanding of zeolitic catalysts. First, by combining molecular dynamic trajectory calculations with quantum mechanical ones, deeper insights into the nature of possible transitory intermediates and reaction pathways will be gained. A start has already been made on the initial stages of the catalysed dehydration of methanol to yield hydrocarbons. Such studies, like all experiments, require vindication by repetition. If, however, the preliminary results turn out to be valid it will have been demonstrated that intermediate states, quite unexpected on the basis of direct experimental study, will have been identified.

Secondly, computational methods have already (Deem & Newsam 1989) reached the stage whereby the structure of a zeolitic solid may be ‘extracted’ from a set of readily measurable properties, such as space group, framework density, the number of distinct crystallographic sites (which in turn is derivable from magic-angle-spinning NMR measurements (see Thomas *et al.* 1983)). Solution of crystal structures in this fashion, which owes much to Pauling’s stochastic approach in the mid-1930s (Pauling 1928, 1990), has for some years proved successful for organic molecular crystals (Ramdas *et al.* 1978) and for novel zeolites (see solution of structure of ZSM-23 by Wright *et al.* (1985)). Expansion in the power of supercomputers, be they mini or maxi versions, will inevitably accelerate the application of such techniques and related ones (Catlow 1986; Akporiaye *et al.* 1988) to the elucidation of the catalytic properties of new microcrystalline zeolitic solids.

Third, with full-blooded free-energy calculations based on a large enough and sufficiently reliable database of interatomic potentials, it ought to be feasible to predict which of the numerous (almost infinite) new structures permitted by group theoretical arguments (Wells 1977; Smith 1988) are, in practice, stable. This in turn will guide new preparative methods and the choice of yet newer catalysts.

Fourth, quantum mechanical studies of the intrinsic acidity of zeolitic catalysts are called for. Sauer (1989*a, b*) has recently shown how to extend formulations discussed earlier (Hehre *et al.* 1986 and Kazansky *et al.* 1983) so as to cope both with the *structure* of the various kinds of surface hydroxyls thought to function as *active*

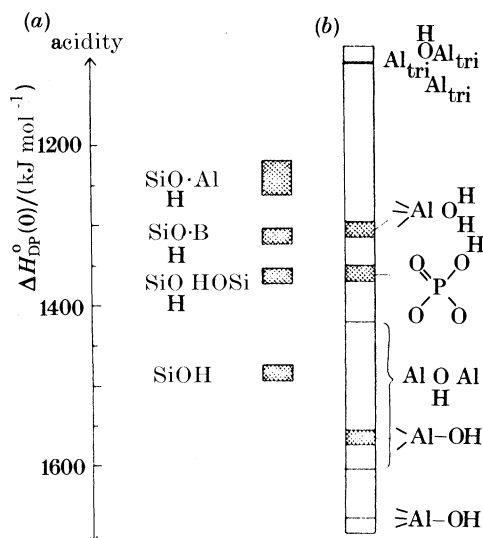


Figure 29. (a) An acidity scale (constructed by Sauer 1989*a*, *b*) for different kinds of hydroxyl groups associated with tetrahedrally bonded silicon in zeolitic catalysts. The standard enthalpy change for deprotonation, ΔH_{DP}° is also given. (b) The range of acidities (on the same scale) for hydroxyl groups associated with aluminium and (in one case) a tetrahedrally bonded phosphorus atom.

sites in zeolites and also the *energetics of proton transfer* from such sites to the reactant species (see figure 29). Key developments are expected on this front, especially when calculations are integrated with those pertaining to the first approach (above). Subtleties associated with the influence of internal electrostatic fields upon both structure and energetics should emerge from such work; and these will deepen our understanding of the dependence of catalytic performance upon structural type among the zeolites.

9. Solid oxides: pyrochlores and perovskites

Many ternary oxides that function as selective oxidation catalysts for the conversion of plentiful hydrocarbons such as CH_4 , butane and propene to more desirable products such as ethene, maleic anhydride and acrolein respectively entail sacrificial loss of oxygen which is removed from the solid oxides thereby converting them temporarily to non-stoichiometric materials. The gaseous oxygen present as one of the reactants is taken up by the catalyst thus making good the anion deficiency created by the sacrificial loss. The cycle is repeated for as long as the catalyst remains active. Typical examples of such catalysts, which have been the subject of much lively debate of late, are LiNiO_2 (a catalyst for converting CH_4 to ethene and ethane) and Bi_2MoO_6 (acrolein from propene). But it is already evident that there may well be very many more oxides that exhibit this kind of catalytic action. Furthermore, there are indications (Sleight & Linn 1976; Verhoeve 1977; Grasselli & Burrington 1981; Haber 1981; Buttrey *et al.* 1986; Thomas 1988) that some particular types of structure seem to favour sacrificial loss – to the appropriate hydrocarbon reactant – of constitutional oxygen and to sustain the requisite mobility of the corresponding anion, the rock-salt structure (of which NiO, CaO and MgO are

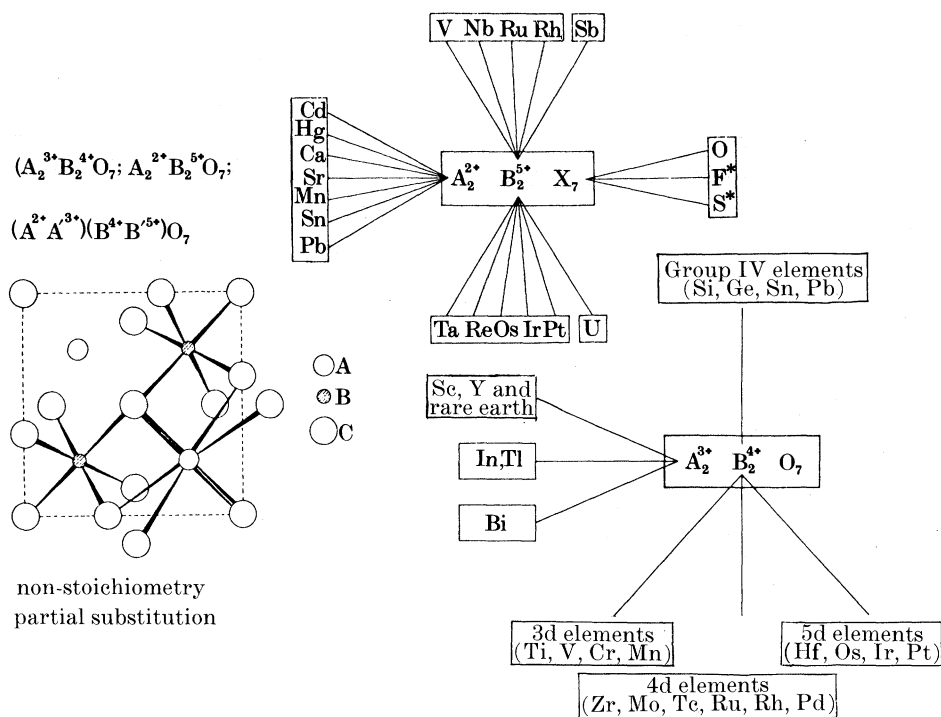


Figure 30. The pyrochlore structure, a section of which is given in projection at left, may accommodate 91 of the elements of the periodic table. Some of the possible permutations, and the various combinations of ions of variable valency, are indicated here.

catalytically demonstrated examples, see Campbell *et al.* 1989 and Pickering *et al.* 1989) is one prominent type. Perovskites, general formula ABO_3 (Reller *et al.* 1984), fluorites, general formula AO_2 (Buttrey *et al.* 1986), and pyrochlores, general formula $A_2B_2O_7$ (Ashcroft *et al.* 1989), are others. There is little doubt that certain individual members of these families of catalysts are endowed with a marked tendency to release oxygen from within their bulk, and that solid-state diffusion, permitting the flow of oxygen from the gas phase into and through the solid and on to another region of the surface, is facile (Catlow *et al.* 1990). Since any oxygen ion in the solid can, through migration, appear at the surface and be removed by a reactant, oxidizable hydrocarbon, these oxide catalysts may (like the zeolites and pillared clays discussed earlier see §4) also be legitimately termed uniform: within the solid there is a spatial uniformity in the arrangement of the species implicated in the catalysis.

Well over a hundred thousand different compositions crystallizing in one or other of the four oxide structures, rock-salt, fluorite, perovskite or pyrochlore, have recently been prepared. In the pyrochlore family alone, as may be seen from figure 30, several tens of thousands of distinct formulations are possible; many of these have indeed been recently prepared by G. V. Subba Rao (personal communication) and co-workers. Over 90% of the elements of the periodic table may be accommodated in the pyrochlore structure, which in addition, may assume variable valency ions in the A and B sublattices as well as non-stoichiometry through oxygen deficiency and incorporation of F^- or S^{2-} in place of O^{2-} ions. Scope for introducing

subtle changes in local atomic environment, in electronic and defect properties are legion; and very many of the resulting microcrystalline solids are catalytically active (Van Dijk *et al.* 1985; Korf *et al.* 1987).

Cheetham and Green and their co-workers (Ashcroft *et al.* 1990) have recently reported on the catalytic performance of a series of rare earth (RE) ruthenate pyrochlores which convert a 2:1 mixture of CH₄ and O₂ into a 1:2 so-called synthesis gas ('syngas') mixture:



The remarkable fact about these highly active catalysts is that, through their agency, this important reaction is effected at a temperature some four hundred degrees lower than that at which the process is otherwise operated (at about 1100 °C). It seems, however, that, under the rather severe conditions of operation, the original pyrochlore structure breaks down into a multicomponent, multiphase catalyst.

Perovskites are, if anything, even more extensive as a family, and more varied in their function as catalysts, than the pyrochlores. Ninety-one elements of the periodic table may be accommodated in the perovskite structure, which, like the pyrochlores, may assume variable valency in the A and B sublattices as well as gross anion deficiency. Perovskites possess the convenient property of remaining structurally intact, even when the oxygen content is progressively denuded during reaction (Reller *et al.* 1984). An octahedron becomes a square pyramid which, in turn, becomes a square and so on, the electroneutrality being conserved by concomitant changes in cation valency. In the multiple-layer perovskites, such as those that exhibit superconductivity at 'high' temperatures, variable valency, it seems, may occur within the oxygen sublattice.

Perovskite catalysts are capable, depending on their precise composition, degree of non-stoichiometry and structure, of functioning either as efficient total oxidation or as partial oxidation catalysts. The degree of product selectivity may also be influenced by the precise ratio of reactants. Considerable scope for fine-tuning exists, and some advantage of this fact has already been taken (Hansen *et al.* 1988; Misono & Koyama 1988; Pickering 1990). A 'total' oxidation catalyst, which ideally would convert CH₄ to CO₂ and H₂O yields better efficiency in power generation: the 'right' selective oxidation catalysts provides improved C₂, especially ethene, yields. Some carefully fabricated perovskite-based anode materials, such as La_{0.2}Sr_{0.2}FeO, are good electrocatalysts for the complete oxidation of CH₄ (Metcalf & Stule 1990). There will doubtless be increasing attention paid in future to such oxide catalysts bearing in mind the perceived need to develop fuel cells capable of running directly off CH₄.

In the study of uniform, solid-oxide catalysts, just as in the study of uniform zeolitic catalysts, it is desirable, and it has already proved feasible (Pickering *et al.* 1989; Pickering 1990), to chart the detailed structural changes that occur within the oxides under operating conditions. Rietveld analysis (Rietveld 1969) of *in situ* X-ray powder diffractograms, recorded using a rotating-anode laboratory source, makes this possible.

Crystalline oxides that function as good solid electrolytes are implicated in a new kind of catalytic system whereby the activity and selectivity of thin metallic films may be dramatically (and reversibly) enhanced by supplying or removing ions, such as O²⁻, to or from the catalyst surface via polarized metal–solid electrolyte interfaces. This effect, described recently by Vayenas (1990) produces increases in

steady-state catalytic rates of more than 10^5 times the rate of supply or removal of ions to or from the catalyst surface (typically microcrystalline silver in contact with yttrium-stabilized ZrO_2).

On the computational side, a great deal may be accomplished, thanks to the availability of supercomputers, using theoretical approaches such as density functional theory and pseudopotential methods, the most successful *ab initio* routes nowadays possible on the structure and energy of solids (Heine 1984; Srivastava & Weaire 1987; Kohn & Sham 1965; Gillan 1989). Recently, ideas have been proposed for improving the efficiency of *ab initio* calculations and extending their scope. They suggest ways of incorporating *ab initio* calculations in molecular dynamics simulation.

10. New vistas

All the reactions and all the catalysts that I have described so far have, without exception referred to processes that do not involve chiral recognition: I have made no reference to catalysts capable of recognizing the handedness of a reactant or of generating an enantiopreferred product. In the world of enzymes, as well as with the new breed of biological catalysts, be they abzymes (Schultz 1988), a term that refers to antibodies functioning as enzymes, or ribozymes (RNA functioning as enzymes, see Cech (1989)), or mutant enzymes, or even homogeneous transition-metal and organometallic complexes with chiral or prochiral ligands (see Noyori & Kitamura 1989; Davies *et al.* 1989; Brown & Davies 1990) so expertly used in recent years, chiral conversions are the rule rather than the exception. This is not so in the catalysis upon which I have focused above.

But why cannot things be different? Is it out of the question for the uniform, molecular sieve catalysts to be enantioselective? I believe that they can be, and for two reasons. First, it is in principle possible to design and synthesize an open network (microporous) crystal in which the cavities or channels are intrinsically chiral. One of the polymorphs of zeolite beta is, in fact, chiral; but it intergrows in coherent contact with another polymorph that is not, so that a chirally pure preparation of crystalline catalyst is difficult to fabricate (Newsam & Treacy 1988). But there are certainly real prospects to being able to produce a totally new type of molecular sieve catalyst which is intrinsically chiral. And when the inner walls of such microporous catalysts are tiled with appropriate metal-ions capable of behaving – as does Ti^{4+} in the titanosilicalite catalyst which converts alkenes to alkane oxides (see Scheme 1 above) – in a manner akin to oxidase enzymes, it will then be feasible to execute a number of subtle conversions that are now possible only with biological catalysts.

The second way of producing chiral molecular sieve catalysts is already demonstrably feasible, but not yet developed to its logical limit. This entails anchoring chirally discriminating organometallic or metal complexes inside the cavities and channels of the crystalline sieve. It may not even be necessary to anchor the agent at the inner walls of the cages: it may be adequate to permit the active agent to rattle around in its (molecular) container so long as it is accessible to the reactant and that it does not prevent the product being washed away so as to regenerate the original catalyst. There are great incentives to devise ‘tea-bag’ catalysts of this kind. Schwartz and co-workers (Ward & Schwartz 1981; Huang & Schwartz 1982; Schwartz 1985) have shown how triallylrhodium reacts with hydroxyl groups of silica to give stable, anchored $\text{Rh}(\text{allyl})_2$ pendant groups, and by appropriate use of faujasitic zeolites such entities, first treated with hydrogen, could

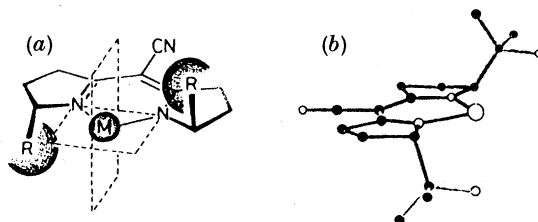


Figure 32. The C_2 -symmetry of a semicorrin ligand is illustrated in (a). The two substituents, R, at the stereogenic centres are held in close proximity to the coordination centre (metal M) by the rigid framework of the semicorrin ligand. (b) represents a molecular model when R is a $C(OH)(CH_3)_2$ group (after Pfaltz 1989).

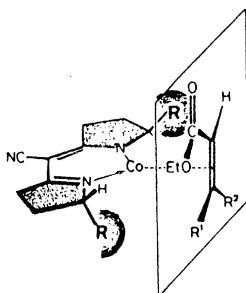


Figure 33. The transition state for the (semicorrinato) cobalt-catalysed reduction of α, β unsaturated carboxylic esters is thought to be as schematized here.

then function as shape-selective hydrogenation catalysts. With the H^+ form of zeolite Y containing the anchored $Rh(allyl)_2$ grouping (see schematic shown in figure 31, plate 8). Schwartz and co-workers have demonstrated that catalytic hydrogenation of olefinic reactants larger than cyclohexene were negligible, thereby demonstrating that the catalytically active centre is located within the intrazeolitic cavity. So also have Herrero *et al.* 1990. More recently, using a synthetic aluminium phosphate (VPI-5) of larger dimension, see figure 14, Davis *et al.* (1989) have shown that the size of the olefin that may be catalytically hydrogenated via the agency of anchored $Rh(allyl)$ groups is significantly larger than for faujasitic zeolites, in line with expectation.

This mononuclear organometallic complex of Rh is illustrative of what is achievable in the new vistas ahead in the field of fabricated catalysts. Other monometallic catalytic centres are, in principle, possible, though, because of size, it may be necessary to synthesize them *in situ* in the intrazeolitic cavities (see Bein *et al.* 1988). Some of these could be transition-metal semicorrins, schematized in figure 32. The C_2 -symmetry of these transition-metal complexes ($M = Co^{II}$, Ni^{II} or Cu^{II} as well as other ions) is readily apparent. The chirality elements are dictated by the size and nature of the R groups, which are in close proximity to the coordination centre.

With the aid of figures 33 and 34, we see how these semicorrin complexes, investigated by Pfaltz (1989), function as enantioselective catalysts. Assuming that the transition state of the enantioselectivity-determining step resembles the hypothetical π -complex depicted in figure 33, the observed selectivity may be rationalized in the following fashion. The ester group occupies a sterically unencumbered site of the coordination sphere, whereas the olefinic H-atom is placed

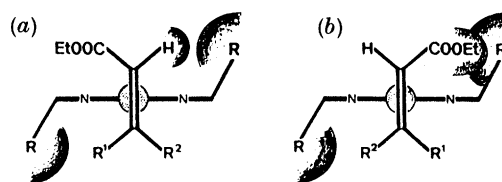


Figure 34. Illustration of the possible origin of enantioselection. For steric reasons, the transition state, represented in (b), is forbidden, and that shown in (a) is likewise preferred (Pfaltz 1989).

in a sterically more crowded environment (figure 34a). However, the transition structure leading to the opposite enantiomer (figure 34b) is expected to be considerably destabilized owing to steric repulsion between the ester group and the adjacent substituent of the semicorrin ligand. When such 'designed' homogeneous catalysts can be securely, or otherwise, tethered to the lining of cavities inside microporous crystalline catalysts, we shall be a step nearer to fabricating the 'tea-bag' catalyst alluded to earlier.

But organometallic clusters, of the type fashioned by Basset *et al.* (1990), Kuroda & Iwasawa (1990) and Shapley *et al.* (1990) can also be envisaged as the active, tethered agents in the 'tea-bag' catalysts which we endeavour to create. These agents can already be fastened in a catalytically useful manner to silica and silica-alumina surfaces: it is only a relatively small step to travel to the goal of securing the agent inside the inorganic 'tea-bag' environment.

Mr President, I have given you much fact. Many of the things that I have said have perhaps served more to edify than to educate. In tracing the trends in the theory and practice of heterogeneous catalysis, I have given you some pictures but many words; more words than equations, which was my deliberate choice. But, as the founding fathers of this Society insisted, *Nullius in Verba* – no man's word shall be final. I have certainly not uttered the last word on this topic. Thank you.

References

- Akporiaye, D. E., Pickett, S. D., Nowak, A. K., Thomas, J. M. & Cheetham, A. K. 1988 *Catal. Lett.* **1**, 133.
- Alstrup, I. & Anderson, N. T. 1987 *J. Catal.* **104**, 466.
- Ashcroft, A. T., Cheetham, A. K., Green, M. L. H., Grey, C. P. & Vernon, R. D. F. 1989 *J. chem. Soc. chem. Commun.* 1667.
- Ashcroft, A. T., Cheetham, A. K., Foord, J. S., Green, M. L. H., Grey, C. P., Murrell, A. J. & Vernon, P. D. F. 1990 *Nature, Lond.* **344**, 319.
- Audier, M., Thomas, J. M., Bursill, L. A., Ramdas, S. & Klinowski, J. 1982 *J. phys. Chem.* **86**, 581.
- Ballantine, J. A., Purnell, J. H. & Thomas, J. M. 1984 *J. molec. Catal.* **27**, 157.
- Ballantine, J. A. 1986 In *Chemical reactions in organic and inorganic constrained systems* (ed. R. Setton), p. 197. Dordrecht: Reidel.
- Barrer, R. M. 1978 *Zeolites and clay minerals*. London: Academic Press.
- Bassett, J. M., Candy, J. P., Chopin, A., Didillon, B., Augard, F. & Theolier, A. 1990 In *New perspectives in catalysis* (ed. J. M. Thomas & K. I. Zamaraev). Oxford: IUPAC-Blackwell. (In the press.)
- Bein, T., Mehain, S. J., Corbin, D. R., Farlee, R. D., Moller, K., Stucky, G. D., Wooleny, G. & Sayers, D. 1988 *J. Am. chem. Soc.* **110**, 1801.
- Black, J. B., Clayden, N., Gai, P. L., Scott, J. D. & Goodenough, J. B. 1987 *J. Catal.* **106**, 1. *Phil. Trans. R. Soc. Lond. A* (1990)

- Boreskov, G. K. & Minachev, K. M. (eds) 1979 *Applications of zeolites in catalysts*. Budapest: Akademiai Kiado.
- Boudart, M. & Djega-Mariadassou, G. 1984 *Kinetics of heterogeneous catalytic reactions*. Princeton University Press.
- Brown, J. M. & Davies, S. G. 1990 *Nature, Lond.* **342**, 631.
- Brown, R. S., Hengerty, B. E., Dewan, J. C. & Klug, A. 1983 *Nature, Lond.* **303**, 543.
- Bruckman, K., Haber, J. & Serwicka, E. M. 1989 *Faraday Discuss. chem. Soc.* **87**, 173.
- Buttrey, D. J., Jefferson, D. A. & Thomas, J. M. 1986 *Phil. Mag.* **53**, 897.
- Campbell, K. D., Zhang, H. & Lunsford, J. H. 1989 *J. phys. Chem.* **92**, 750.
- Catlow, C. R. A. 1986 *A. Rev. Mater. Sci.* **16**, 517.
- Catlow, C. R. A. & Cormack, A. N. 1987 *Int. Rev. phys. Chem.* **6**, 227.
- Catlow, C. R. A., Thomas, J. M. & Jackson, R. A. 1990 *J. phys. Chem.* (In the press.)
- Cech, T. R. 1989 *Nature, Lond.* **339**, 507.
- Cheetham, A. K., Eddy, M. M. & Thomas, J. M. 1984 *J. chem. Soc. chem. Commun.* 1337.
- Cheetham, A. K., Gale, J. D., Nowak, A. K., Peterson, B. K., Pickett, S. D. & Thomas, J. M. 1989 *Faraday Discuss. chem. Soc.* **87**, 79.
- Cohen de Lara, E., Kahn, R., Goulay, A. M. & Lebars, M. 1989 In *Zeolites: facts, figures, future* (ed. R. A. van Santen & P. A. Jacobs), p. 753. Amsterdam: Elsevier.
- Couves, J. W., Thomas, J. M., Greaves, G. N., Catlow, C. R. A. & Dent, E. 1990*a*. (In preparation.)
- Couves, J. W., Jones, R. H., Thomas, J. M. & Smith, B. J. 1990*b* *Adv. Mater.* **2**, 181.
- Cusumano, J. A. 1990 In *New perspectives in catalysis* (ed. J. M. Thomas & K. I. Zamarayev). Oxford: IUPAC-Blackwell. (In the press.)
- Davies, S. G., Brown, J. M., Pratt, A. J. & Heet, G. W. 1989 *Chem. Br.* **25**, 259.
- Davis, M. E., Montes, C., Hathaway, P. E., Arhauet, J. P., Hasha, D. L. & Gavces, J. M. 1989 *J. Am. chem. Soc.* **111**, 3919.
- Davis, M. E., Saldorheiga, C., Montes, C., Garca, J. & Crowder, C. 1988 *Nature, Lond.* **331**, 698.
- Deem, M. W. & Newsam, J. M. 1989 *Nature, Lond.* **342**, 260.
- Diddams, P. A., Thomas, J. M., Jones, W., Ballantine, J. A. & Purnell, J. H. 1984 *J. chem. Soc. chem. Commun.* 1340.
- Di Giacomo, P. M. & Dines, M. B. 1982 *Polyhedron* **1**, 61.
- Dines, M. B. & Griffith, P. C. 1983 *Polyhedron* **2**, 607.
- Dooryhee, E., Catlow, C. R. A., Thomas, J. M., Greaves, G. N., Steel, A. T. & Townsend, R. P. 1989 In *Int. Zeolite Association Conf. Report (Amsterdam, July 1989)*. Specialist Research.
- Dooryhee, E., Steel, A. T., Thomas, J. M., Catlow, C. R. A., Greaves, G. N., Townsend, R. P. & Carr, S. W. 1990 *Faraday Discuss. chem. Soc.* **89**, Paper 13.
- Eigen, M. 1964 *Angew. Chem. Int. Edn. Engl.* **3**, 1.
- Figueras, F. 1988 *Cat. Rev. Sci. Engng.* **30**, 457.
- Fitch, A. R. 1981 *J. chem. Soc. chem. Commun.* 784.
- Flanigen, E. M., Lok, B. M., Patton, R. L. & Wilson, S. T. 1986 In *New developments in zeolite science and technology* (ed. Y. Murakami, A. Iijina & J. W. Ward), p. 103. Amsterdam: Elsevier.
- Gillan, M. J. 1989 *J. chem. Soc. Faraday Trans.* **85**, 521.
- Grasselli, R. K. & Burrington, J. D. 1981 *Adv. Catal.* **30**, 133.
- Haag, W., Lago, R. M. & Weisz, P. B. 1984 *Nature, Lond.* **309**, 589.
- Haber, J. 1981 *Catal. Sci. Technol.* **2**, 13.
- Hamden, H. 1987 Ph.D. thesis, University of Cambridge, U.K.
- Hansen, S., Otamairi, J., Bovin, J. O. & Anderson, A. 1988 *Nature, Lond.* **334**, 143.
- Heine, V. 1984 In *NATO ASI electronic structure of complex systems* (Ghent, 1982; ed. P. Phoriseau and W. T. Tennakoon). New York: Panum Press.
- Herhe, W. J., Radom, L., Schleyer, P. V. R. & Pople, J. 1986 *Ab initio molecular orbital theory*, p. 10. New York: Wiley.

- Herrero, J., Blanco, C., Estervelas, M. A. & Oro, L. A. 1990 *Appl. Organometallic Chem.* (In the press.)
- Herron, N. & Tolman, C. A. 1987 *J. Am. chem. Soc.* **109**, 2837.
- Herron, N., Tolman, C. A. & Stucky, G. D. 1986 *J. chem. Soc. chem. Commun.* 1521.
- Hölderich, W., Hesse, M. & Naumann, F. 1988 *Angew. Chem. Int. Edn. Engl.* **27**, 226.
- Huang, T. N. & Schwartz, J. 1982 *J. Am. Chem. Soc.* **104**, 5244.
- Jones, R. H., Thomas, J. M., Xu, R., Xu, Y., Qisheng, H. & Cheetham, A. K. 1990 *J. chem. Soc. chem. Commun.* (In the press.)
- Joyner, R. W. 1990 *J. chem. Soc. Faraday Trans.* (In the press.)
- Kallo, D. & Minachev, K. M. (eds) 1988 *Catalysis on zeolites*. Budapest: Akademiai Kiado.
- Kazansky, V. B., Kustov, L. M. & Borskov, V. Yu. 1983 *Zeolites* **3**, 77.
- Keggin, J. F. 1934 *Proc. R. Soc. Lond. A* **144**, 75–100.
- Koga, N. & Morakuma, K. 1989 In *The challenge of d and f electrons: theory and computation* (ed. D. R. Salahub & M. C. Zerner), p. 79. A.C.S. Symp. Series, No. 394.
- Kohn, W. & Sham, L. J. 1965 *Phys. Rev.* **140**, 1133.
- Korf, S. J., Koopmans, H. J. A., Lippens, B. C. & Burggrof, A. J. 1987 *J. chem. Soc. Faraday Trans.* **83**, 1485.
- Kozlowski, R., Pettifer, R. F. & Thomas, J. M. 1983 *J. phys. Chem.* **87**, 5172 and 5176.
- Kuroda, H. & Iwasawa, Y. 1990 *Int. Rev. phys. Chem.* **8**, 207.
- Liu, X. 1986 Ph.D. thesis, University of Cambridge, U.K.
- Maddox, P. J., Stachurski, J. & Thomas, J. M. 1988 *Catal. Lett.* **1**, 191.
- Makarova, M. A., Williams, C., Rommannikov, V. N., Thomas, J. M. & Zamaraev, K. I. 1990 *J. chem. Soc. Faraday Trans.* **86**, 581.
- Maxwell, I. E. 1982 *Adv. Catal.* **31**, 1.
- Maxwell, I. E. 1990 In *New perspectives in catalysis* (ed. J. M. Thomas & K. I. Zamaraev). Oxford: IUPAC-Blackwell.
- Metcalfe, I. S. & Stule, B. C. H. 1990 In *Abstracts of Rideal conference on chemisorption and catalysis*, Cambridge, April 1990.
- Misono, M. 1987 *Cat. Rev. Sci. Engng* **29**, 269.
- Misono, M. & Koyama, T. 1988 *J. chem. Soc. chem. Commun.* 299.
- Mortier, W. J. & Schoolheydt, R. A. 1985 *Prog. Solid State Chem.* **16**, 1.
- Newsam, J. M. & Treacy, M. M. J. 1988 *Nature, Lond.* **332**, 249.
- Notari, B. 1987 In *Innovation in zeolite materials science* (ed. P. J. Grobet, J. A. Marteus & P. A. Jacobs), p. 143. Amsterdam: Elsevier.
- Noyori, R. & Kritamura, M. 1989 In *Medium synthetic methods 1989* (ed. R. Scheffold), vol. 5, p. 115. Heidelberg: Springer-Verlag.
- Olson, D. H. & Meier, W. M. 1987 *Atlas of zeolite structure types*, 2nd edn. London: Butterworths.
- Ono, Y. 1990 In *New perspectives in catalysis* (ed. J. M. Thomas & K. I. Zamaraev). Oxford: IUPAC-Blackwell. (In the press.)
- Pauling, L. 1928 *Proc. natn. Acad. Sci. U.S.A.* **14**, 603.
- Pauling, L. 1990 *Proc. natn. Acad. Sci. U.S.A.* **87**, 244.
- Perego, G., Bellusi, G., Corno, C., Jaramasso, M., Buomomo, F. & Esposito, H. 1986 In *New developments in zeolite science and technology* (ed. Y. Murokami, A. Zijuma & J. W. Ward), p. 129. Amsterdam: Elsevier.
- Pfaltz, A. 1989 In *Modern synthetic methods 1989* (ed. R. Scheffold), vol. 5, p. 199. Heidelberg: Springer-Verlag.
- Pfeifer, H. 1989 *Colloids surfaces* **36**, 169.
- Phillips, D. C. 1967 *Proc. natn. Acad. Sci. U.S.A.* **57**, 484.
- Pickering, I. J. 1990 Ph.D. thesis, University of London, U.K.
- Pickering, I. J., Maddox, P. J. & Thomas, J. M. 1989 *Angew. Chem. Adv. Mater.* **101**, 828.

- Pickett, S. D. 1990 Ph.D. thesis, University of London, U.K.
- Pickett, S. D., Nowak, A. K., Cheetham, A. K., Post, M. F. M., Den Ouden, J., Smit, B., Peterson, B. K. & Thomas, J. M. 1990 *J. phys. Chem.* **94**, 1233.
- Post, M. F. M., Huishigia, T., Emeis, G. A., Name, J. M. & Stork, W. H. T. 1989 *Stud. Surf. Sci. Catal.* **49** A, 237.
- Purnell, J. H. 1990 *Catal. Lett.* (In the press.)
- Ramdas, S., Thomas, J. M. & Jones, W. 1978 *Chem. Phys. Lett.* **54**, 490.
- Ramdas, S., Thomas, J. M., Bettridge, P. W., Cheetham, A. K. & Davies, E. K. 1984 *Angew. Chem. Int. Edn. Engl.* **23**, 671.
- RaO, C. N. R. & Thomas, J. M. 1985 *Acct. chem. Res.* **18**, 113.
- Reller, A., Thomas, J. M. & Uppal, M. K. 1984 *Proc. R. Soc. Lond. A* **344**, 223.
- Rietveld, H. M. 1969 *J. appl. Crystallogr.* **2**, 65.
- Romanski, W. & Jablonski, J. M. 1988 In *Catalysis on zeolites* (ed. D. Kallo & K. M. Minackev), p. 277. Budapest: Akademiai Kiado.
- Sachlter, W. H. M. 1981 *Faraday Discuss. chem. Soc.* **72**, 7.
- Sauer, J. 1989a *Chem. Rev.* **89**, 199.
- Sauer, J. 1989b *Stud. Surf. Catalysis* **52**, 73.
- Schultz, P. G. 1988 *Angew. Chem. Int. Edn. Engl.* **27**, 1172.
- Schwartz, J. 1985 *Acct. chem. Res.* **18**, 302.
- Shapley, J. R., Uchiyama, W. S. & Scott, R. A. 1990 *J. phys. Chem.* **94**, 1190.
- Sinfelt, J. H. 1983 *Bimetallic catalysts*. New York: Wiley.
- Sleight, A. W. & Linn, W. J. 1976 *J. Catal.* **41**, 134.
- Smith, J. V. 1988 *Chem. Rev.* **88**, 149.
- Somorjai, G. A. 1990 In *New perspectives in catalysis* (ed. J. M. Thomas & K. I. Zamaraev). Oxford: IUPAC-Blackwell. (In the press.)
- Srivastava, G. P. & Weaire, D. 1987 *Adv. Phys.* **36**, 463.
- Tatsumi, T., Nakamura, M., Negishi, S. & Tonuniaga, H. 1990 *J. chem. Soc. chem. Commun.* 476.
- Tennakoon, D. T. B., Thomas, J. M. & Jones, W. 1986 *J. chem. Soc. Faraday Trans.* **82**, 3081.
- Terasaki, O., Thomas, J. M., Millward, G. R. & Watanabe, D. 1989 *Chem. Mater.* **1**, 158.
- Thomas, J. M. 1974 *Phil. Trans. R. Soc. Lond. A* **277**, 251.
- Thomas, J. M. 1982a In *Intercalation chemistry* (ed. A. J. Jacobson & S. Whittingham), p. 56. New York: Academic Press.
- Thomas, J. M. 1982b *Ultramicroscopy* **8**, 13.
- Thomas, J. M. 1984 *Phil. Trans. R. Soc. Lond. A* **251**, 311, 271.
- Thomas, J. M. 1988 *Angew. Chem. Int. Edn. Engl.* **27**, 1673.
- Thomas, J. M. 1989a In *Zeolites: facts, figures, future* (ed. P. A. Jacobs & R. A. van Santen), p. 3. Amsterdam: Elsevier.
- Thomas, J. M. 1989b *Angew. Chem. Adv. Mater.* **101**, 1105.
- Thomas, J. M. & Catlow, C. R. A. 1987 *Progr. inorg. Chem.* **35**, 1.
- Thomas, J. M. & Klinowski, J. 1985 *Adv. Catalysis* **33**, 191.
- Thomas, J. M. & Ramdas, S. 1985 *Chem. Br.* **21**, 49.
- Thomas, J. M. & Theocharis, C. R. 1989 In *Modern synthetic methods* (ed. R. Scheffold), **5**, p. 249. Heidelberg: Springer-Verlag.
- Thomas, J. M. & Vaughan, D. E. W. 1989 *J. Phys. Chem. Solids* **50**, 449.
- Thomas, J. M., Tennakoon, D. T. B., Adams, J. M. & Graham, S. H. 1976 *A.C.S. Symp.* **163**, 248.
- Thomas, J. M., Ramdas, S., Klinowski, J., Fyfe, C. A. & Gobbi, G. 1982 *J. phys. Chem.* **86**, 124.
- Thomas, J. M., Ramdas, S., Klinowski, J., Hunter, B. K. & Tennakoon, D. T. B. 1983 *Chem. Phys. Lett.* **102**, 158.
- Treacy, M. M. J. & Newsam, J. M. 1990 *Zeofile*. (In the press.)

- Treacy, M. M. J. & Vaughan, D. E. W. 1988 In *Microstructure and prospective of catalysis* (ed. M. M. J. Treacy, J. M. Thomas & J. M. White). Symposium Proceedings 111, Mater. Res. Soc. Pittsburgh.
- Van Bekkum, H., Van der Gaag, F. J., Adriaansers, R. J. O. & Van Green, P. L. 1989 *Stud. Surf. Sci.* **52**, 283.
- Van Dijk, M. P., Burggraf, A. J., Cormack, A. N. & Catlow, C. R. A. 1985 *Solid St. Ionics* **17**, 159.
- Vaughan, D. E. W. & Lusier, R. J. 1980 In *Proc. 5th Int. Conf. Zeolites, Naples 1980* (ed. L. V. C. Rees), p. 94. London: Heyden.
- Vayenas, C. G. 1990 *Nature, Lond.* **343**, 297.
- Vayenas, C. G. & Bebelis, S. 1989 *J. Catal.* **118**, 125.
- Verhoeve, R. J. H. 1977 In *Advanced materials on catalysis* (ed. J. J. Burton & R. L. Garten), p. 129. New York: Academic Press.
- Ward, M. D. & Schwartz, J. 1981 *J. molec. Catal.* **11**, 397.
- Weisz, P. B. 1980 *Proc. 7th Int. Congr. Catalysis*, Tokyo.
- Wells, A. F. 1977 *Three dimensional nets and polyhedra*. New York: Wiley.
- Williams, C., Makarova, M. A., Thomas, J. M. & Zamaraev, K. I. 1990 *J. chem. Soc. Faraday Trans.* (In the press.)
- Williams, R. J. P. 1982 *Pure appl. Chem.* **54**, 1889.
- Wright, C. J., Thomas, J. M., Vasudevan, S. & Sampson, C. 1982 *Bull. Soc. Chim. Belg.* **90**, 1215.
- Wright, P. A., Thomas, J. M., Millward, G. R. J. & Barrie, S. A. I. 1985 *J. chem. Soc. chem. Commun.* 1117.
- Xu, R., Chen, J. & Feng, S. 1990 In *Int. Symp. on chemistry of microporous crystals*, Tokyo, June 1990.
- Xu, Y., Maddox, P. J. & Couves, J. W. 1990 *J. chem. Soc. Faraday Trans.* **86**, 425.
- Xu, Y., Maddox, P. J. & Thomas, J. M. 1989 *Polyhedron* **8**, 819.
- Yashonath, S., Thomas, J. M., Nowak, A. K. & Cheetham, A. K. 1988 *Nature, Lond.* **331**, 601.
- Young, D. A., Vaughan, D. E. W., Pruett, R. I. & Tunison, M. E. 1989 *U.S. Patent* 4, 855, 528.
- Zamaraev, K. I., Balshininbaev, B. S. M., Ivanov, A. A., Lapina, O. B. & Mastikihin, V. M. 1989 *Faraday Discuss. chem. Soc.* **87**, 133.

Lecture delivered 15 February 1990; typescript received 30 April 1990

Colour plates printed in Great Britain by George Over Ltd, Rugby, U.K.

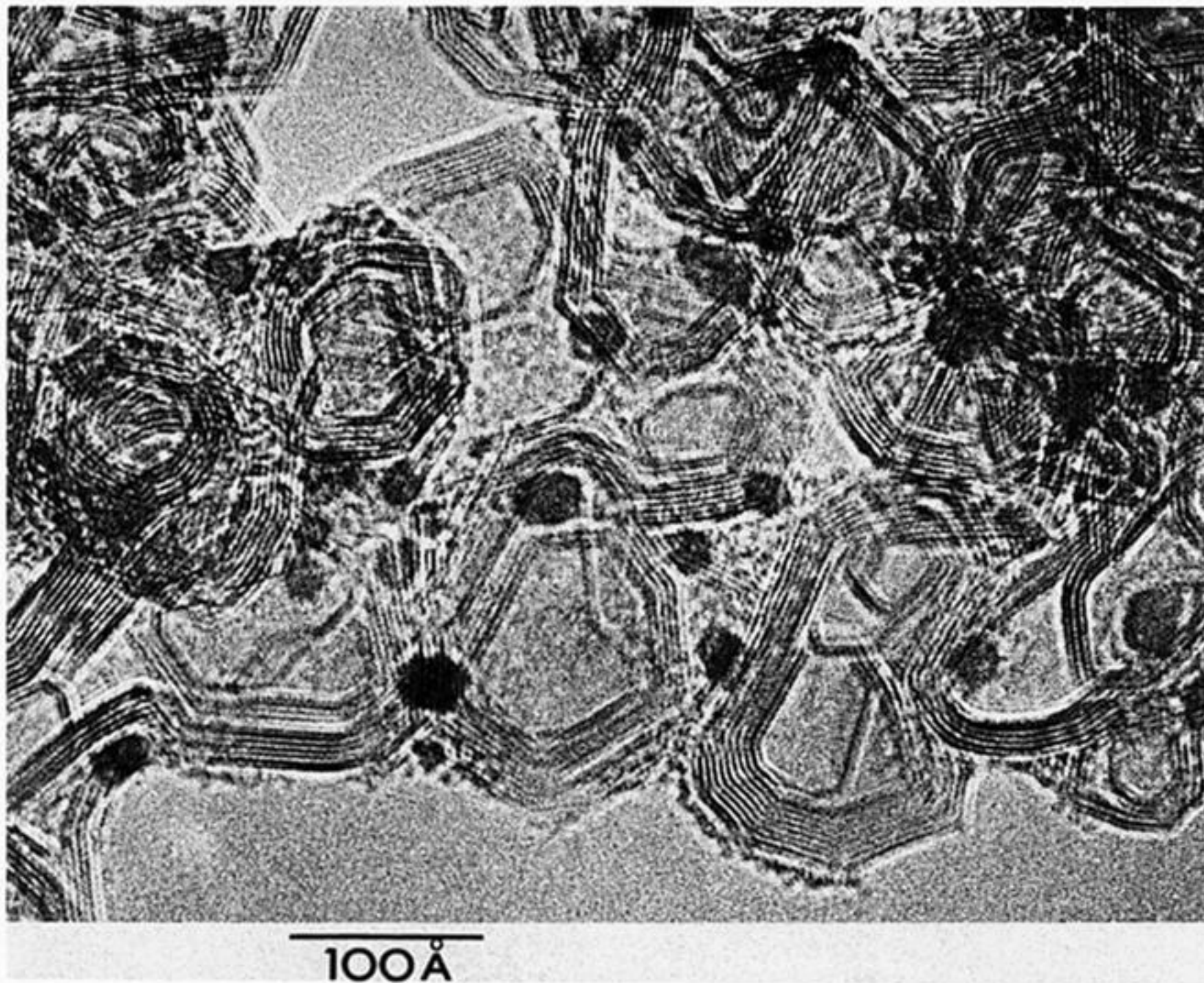


Figure 4. Electron micrograph showing the multiphase, multicomponent nature of a powerful new catalyst for the synthesis of NH_3 . The small black patches are microcrystallites of Ru distributed on a graphitic carbon (interplanar spacings *ca.* 0.34 nm) support. A veneer of a calcium-rich phase (*ca.* 0.1 nm thick) covers the catalyst.

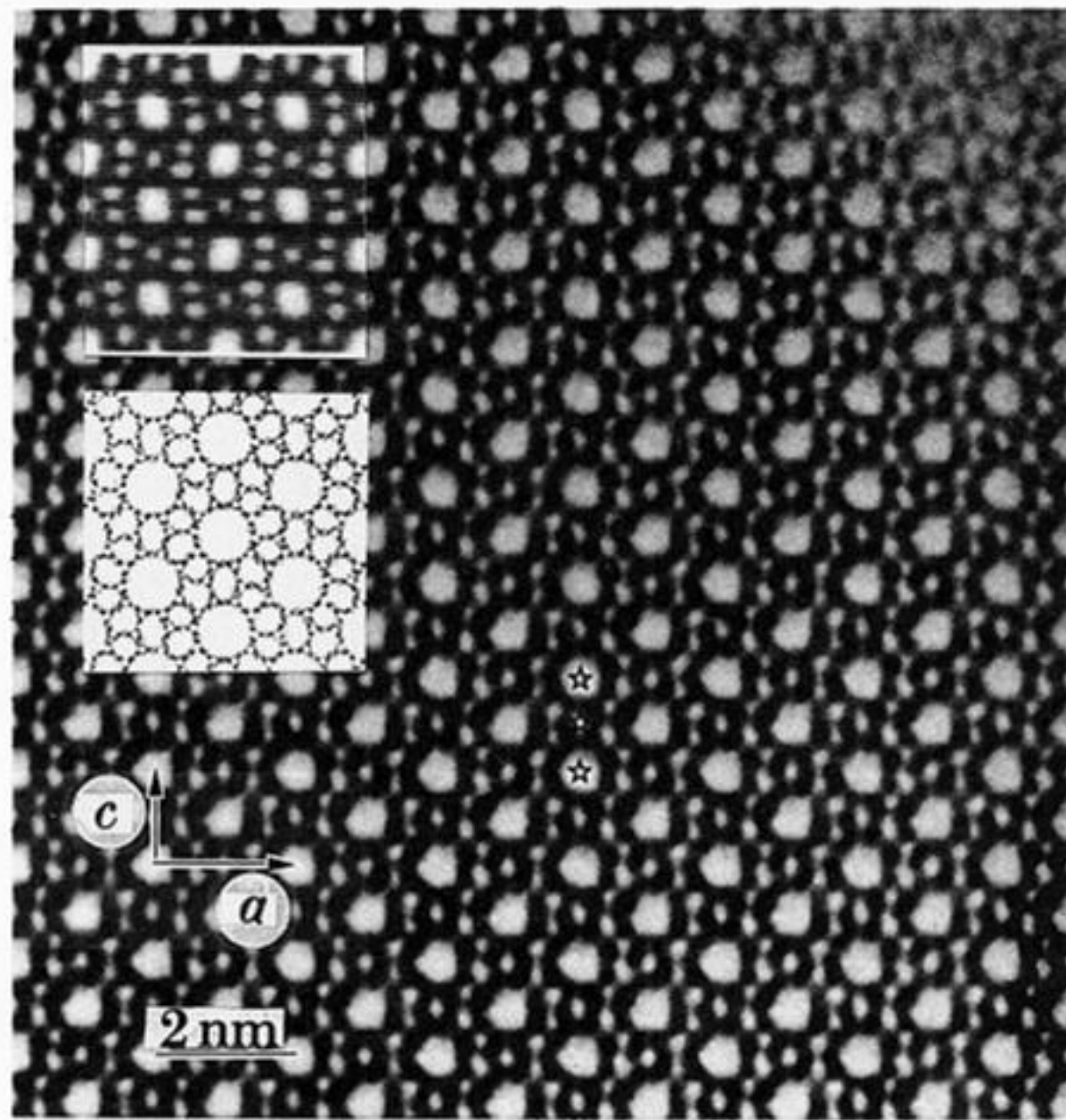


Figure 5. High-resolution electron micrograph of a ZSM-5 (molecular sieve) uniform heterogeneous catalyst. The regular white patches denote apertures of 5.5 Å diameter. (At the top left (inset) is shown the computed electron-optical image and, centre left, a projection drawing of the structure. The asterisks denote local centres of symmetry.)

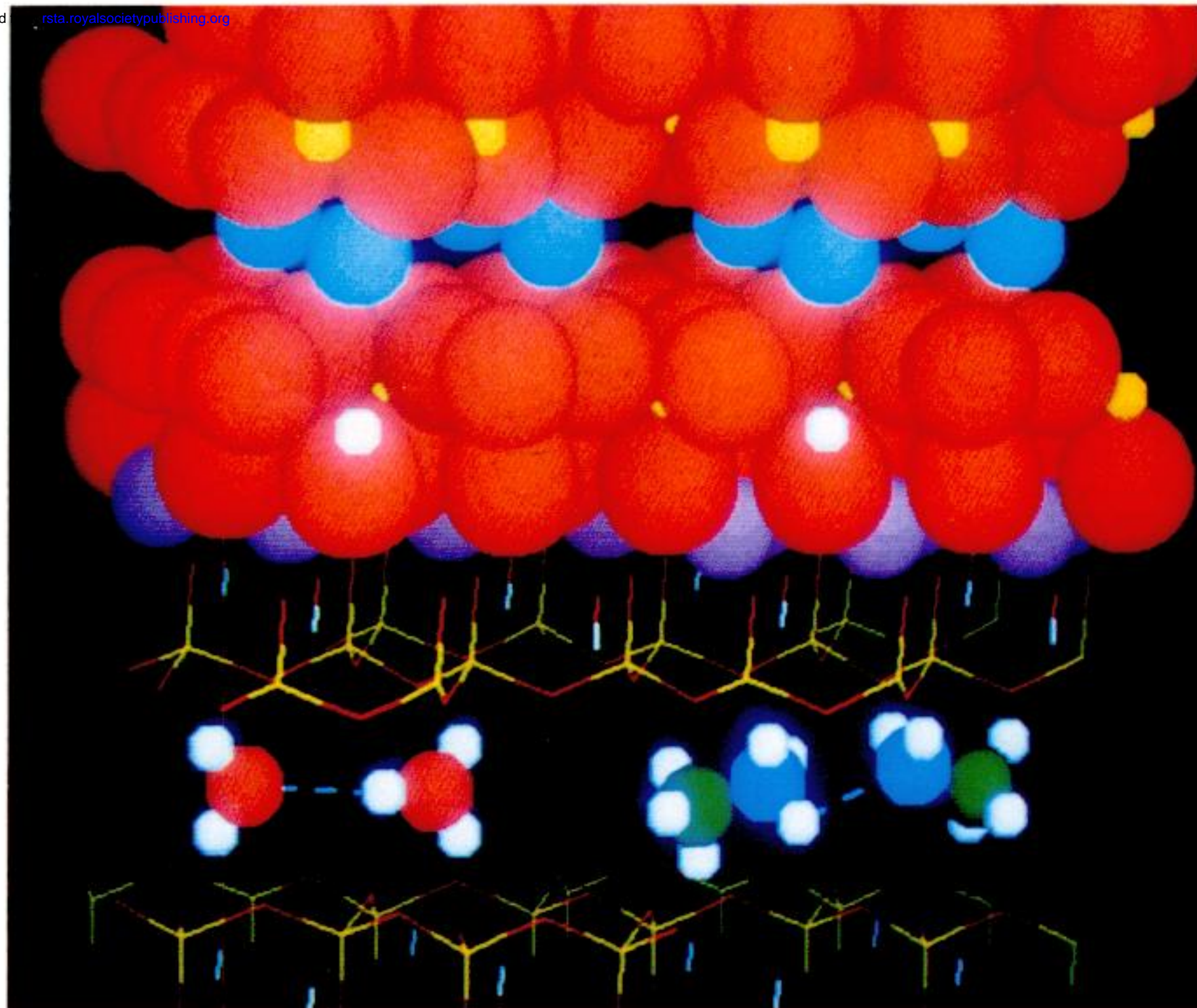


Figure 8. The top half, with ions approximately to scale, shows a Na^+ -exchanged vermiculite; the lower half is a skeletal representation of a vermiculite in which the Brønsted acid sites of the interlamellar region is represented by the 'free' hydronium ions (H_3O^+) and by a protonated amine. Vermiculite itself has the idealized formula $\text{Mg}_3(\text{Si}_3\text{Al})\text{O}_{10}(\text{OH})_2 \cdot \text{Mg}_{0.5}(\text{H}_2\text{O})_4$. The interlamellar $\text{Mg}_{0.5}(\text{H}_2\text{O})_4$ may be readily replaced by other ions or ions and organic reactants taken up by intercalation. Colour code: oxygen ions, red; Na^+ , light blue; Al^{3+} and Si^{4+} , yellow; hydrogen, white; nitrogen, dark blue.

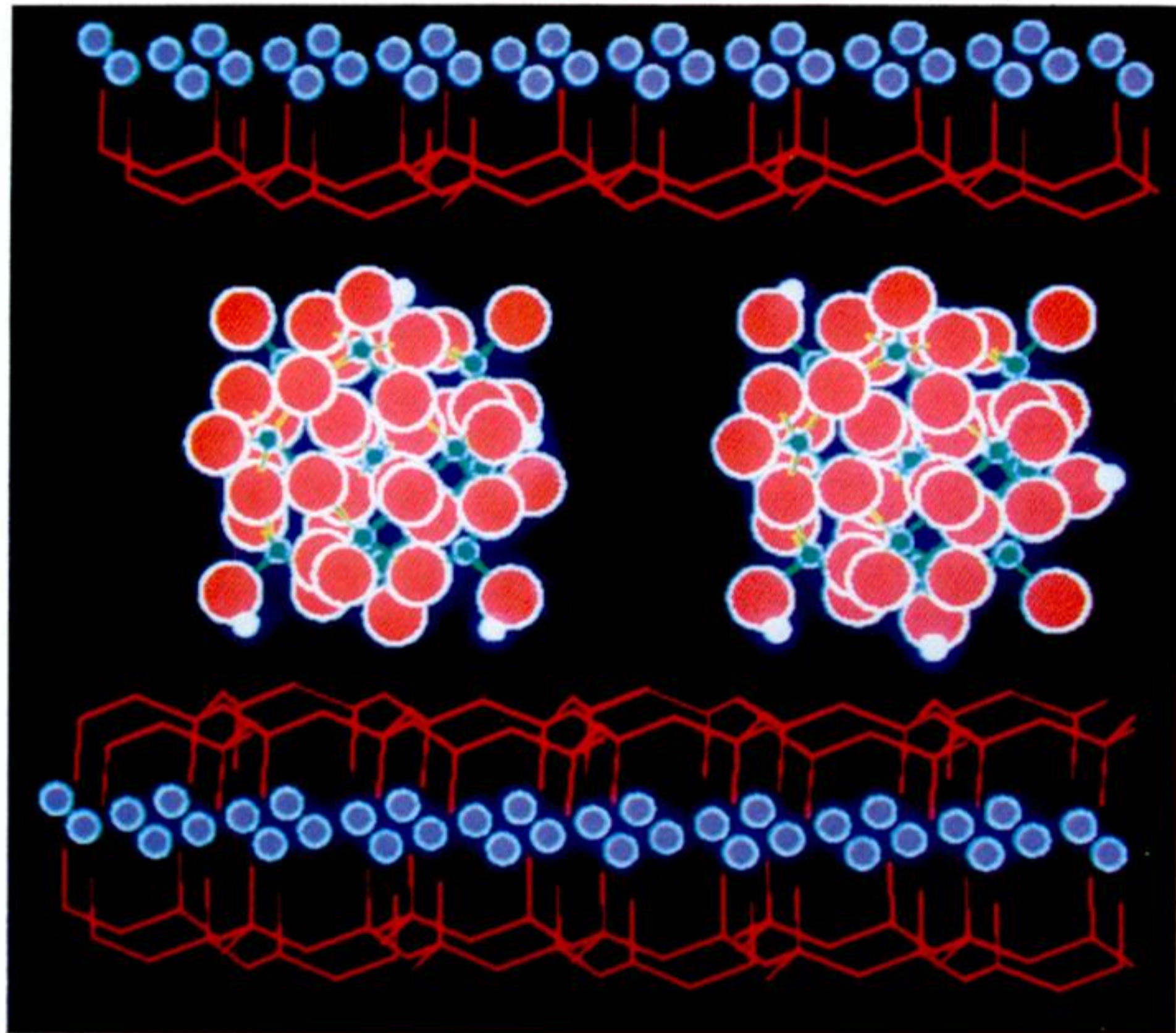


Figure 9. View of clay catalyst in which the interlamellar spaces contain Keggin ions such as $[\text{Al}_{13}\text{O}_4(\text{OH})_{24}(\text{H}_2\text{O})_{12}]^{7+}$ (see figure 10). Each polynuclear cation has a central tetrahedrally coordinated Al, surrounded by twelve octahedrally coordinated ones (Al, O and H atoms shown in green, red and white respectively, and the aluminosilicate sheets are represented skeletally)

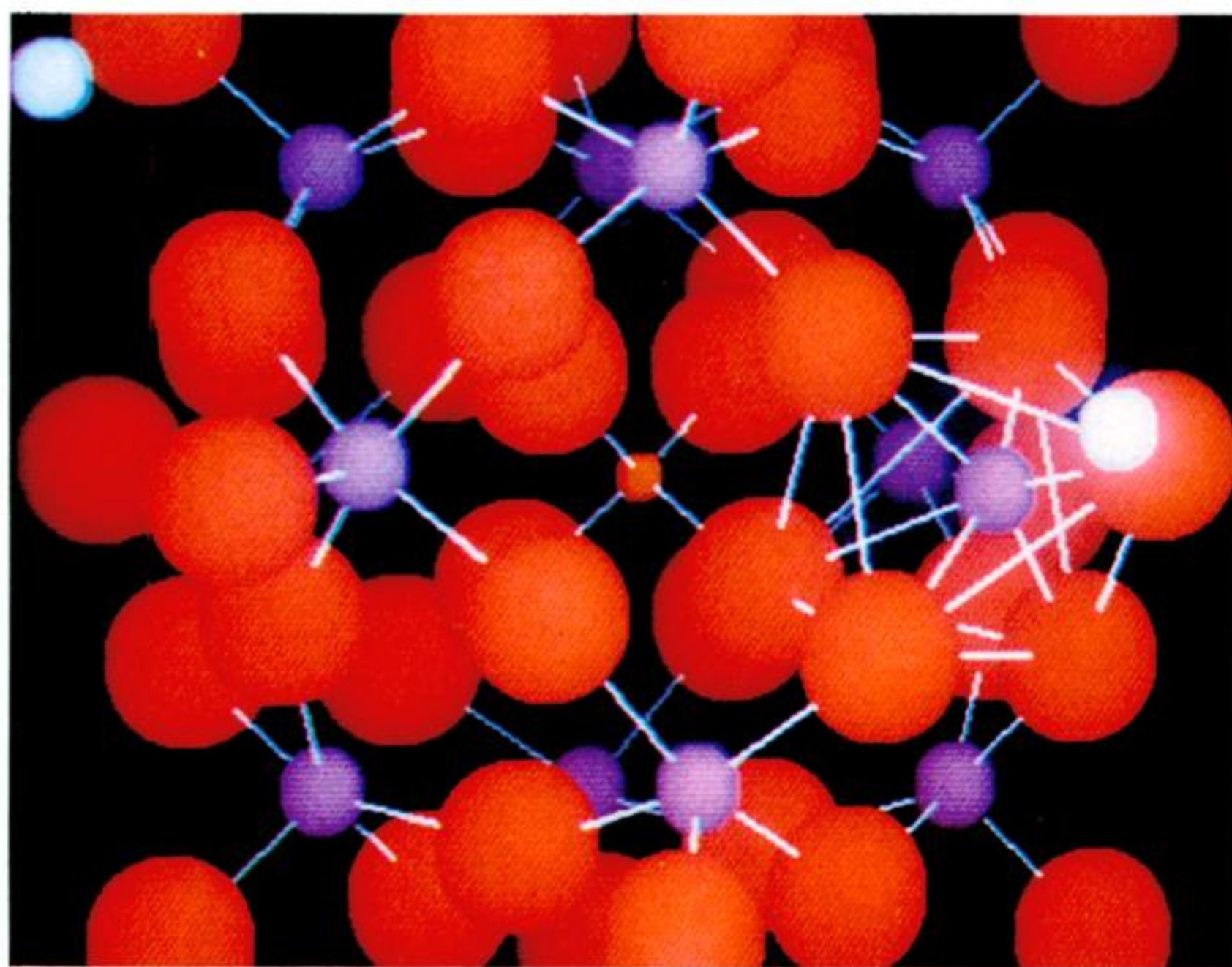


Figure 10. The Keggin anion may have P, As, Si, Ge or B in the central, tetrahedrally coordinated atom (small red atom), whereas the twelve surrounding, octahedrally coordinated ones (larger purple atoms) may be W, Mo, V, Cr, etc. Phosphomolybdic acid is $\text{H}_3\text{PMo}_{12}\text{O}_{40}$. (Small white atoms note detachable hydrogens.)

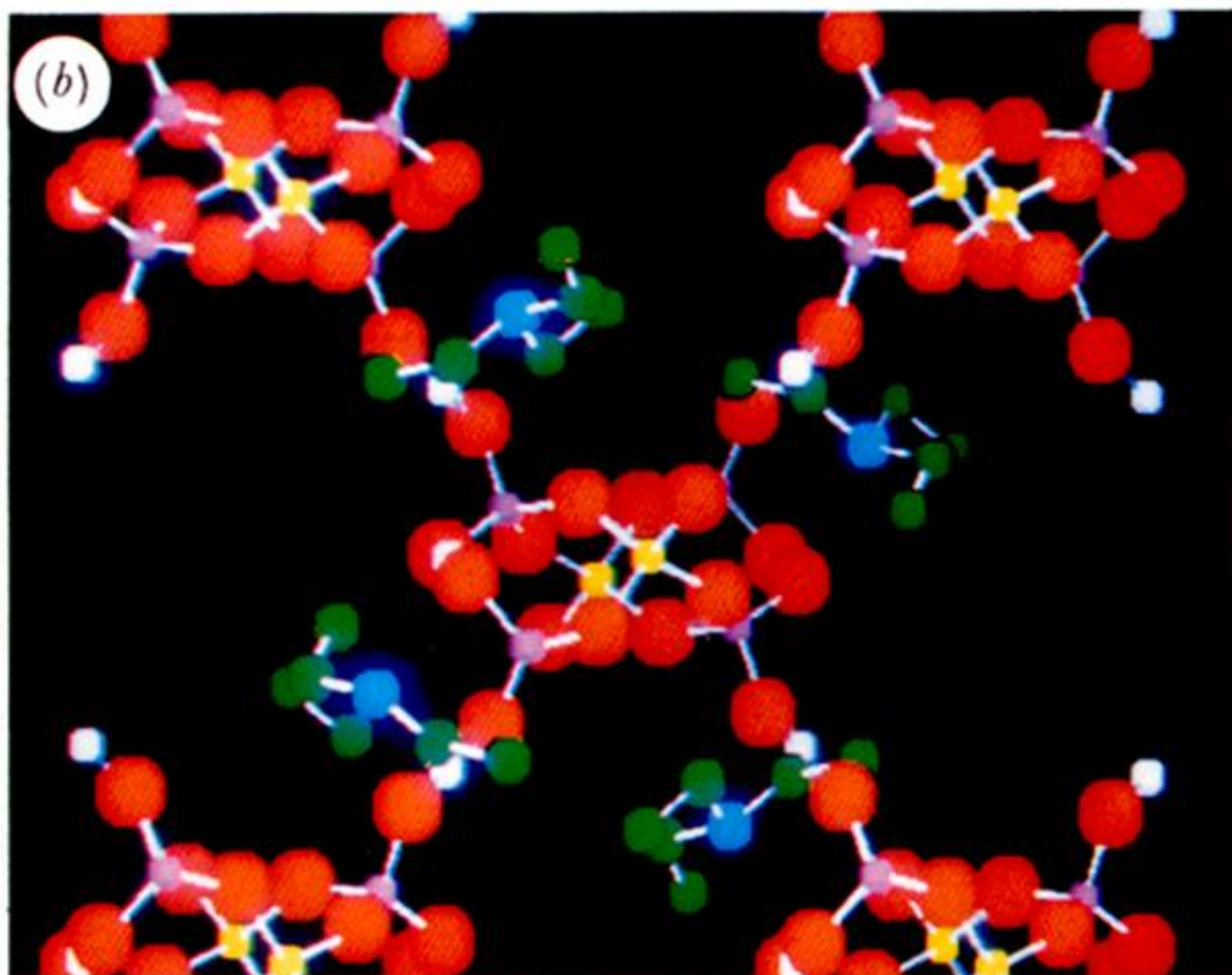
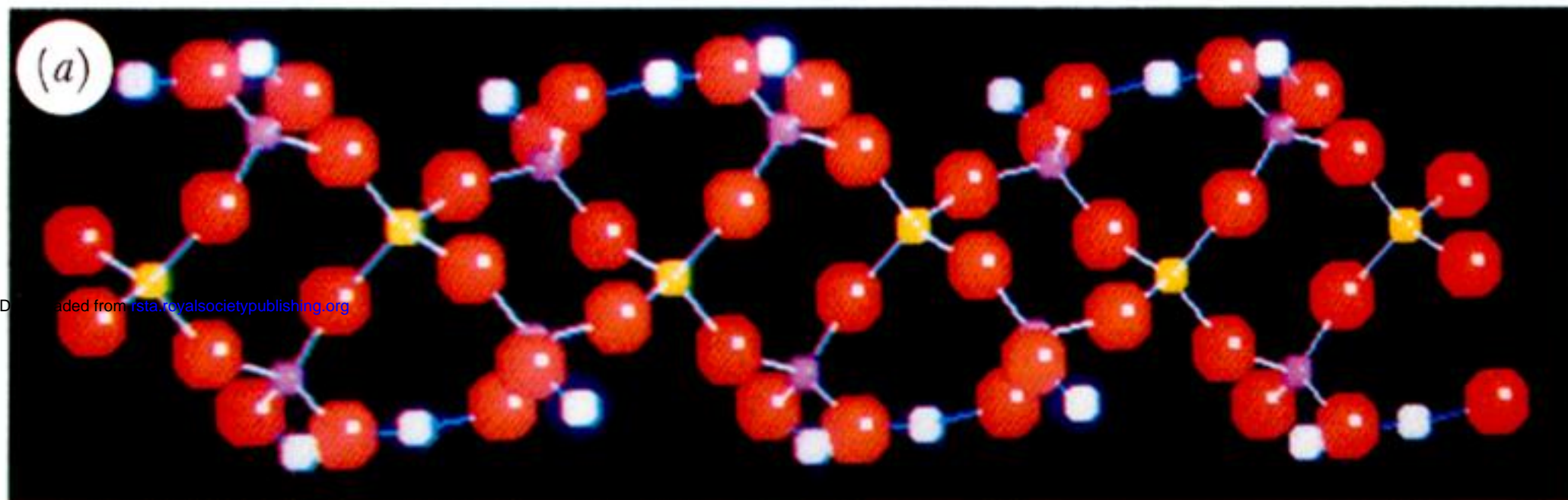


Figure 12. A newly discovered chain structure $(\text{AlH}_2\text{P}_2\text{O}_8)^-$ along the back-bone of which there occurs a recurrence of OH groups attached to phosphorous (after Jones *et al.* 1990). (a) Shows the view perpendicular to the chain axis. The sites of the protonated triethylamine are shown in (b), the view along the chains $(\text{C}_2\text{H}_5)_3\text{NH}^+(\text{AlH}_2\text{P}_2\text{O}_8)$. Aluminium atoms are yellow and phosphorous are purple.

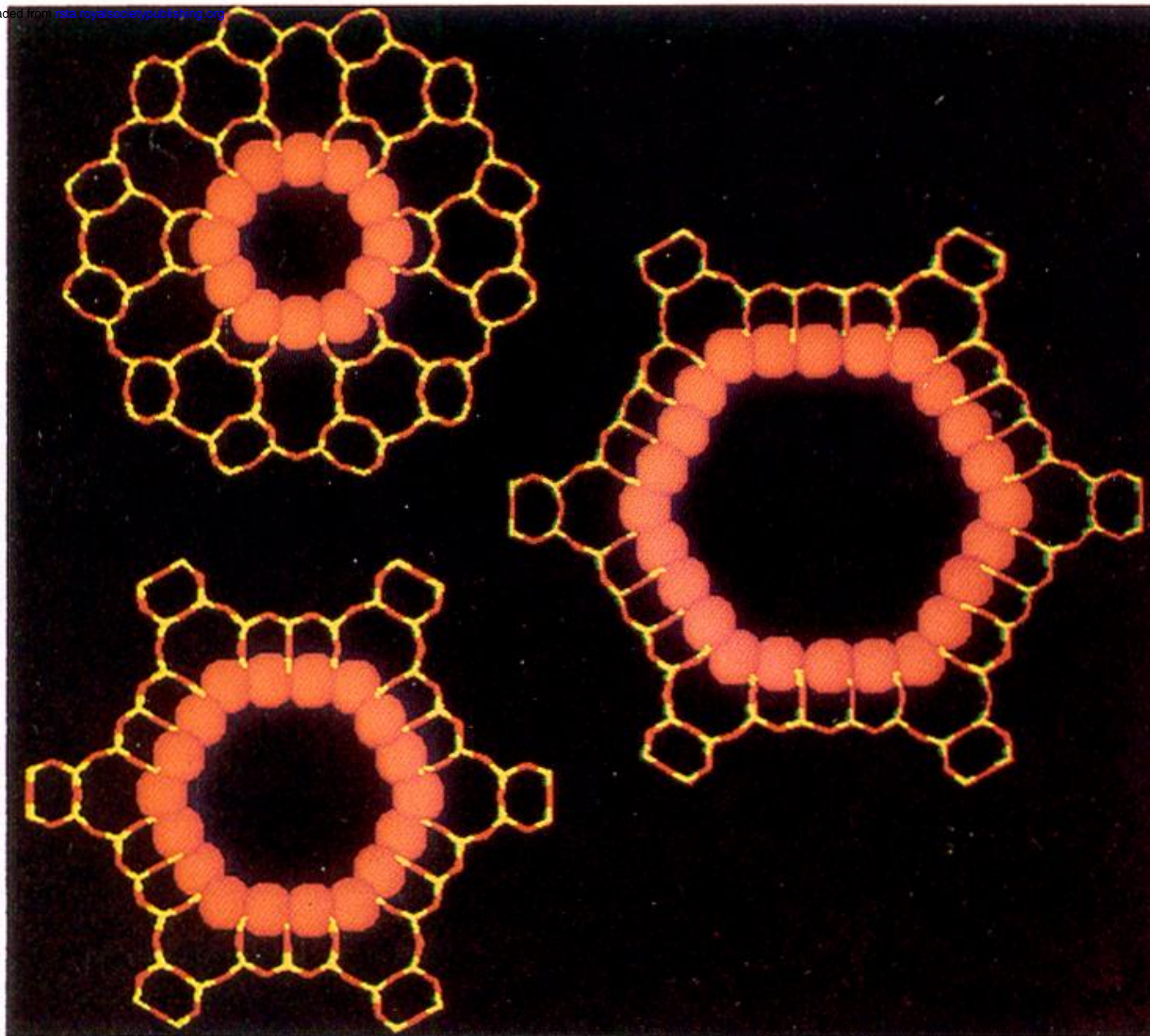


Figure 14. Representations (to scale) of the apertures in zeolite L (top left), where the diameter of the 12-ring of oxygen atoms is *ca.* 7.4 Å, in VPI-5 (bottom left) which has 18-ring openings (*ca.* 12.0 Å), and in the hypothetical (right) 24-ring opening (*ca.* 18 Å) (see text).

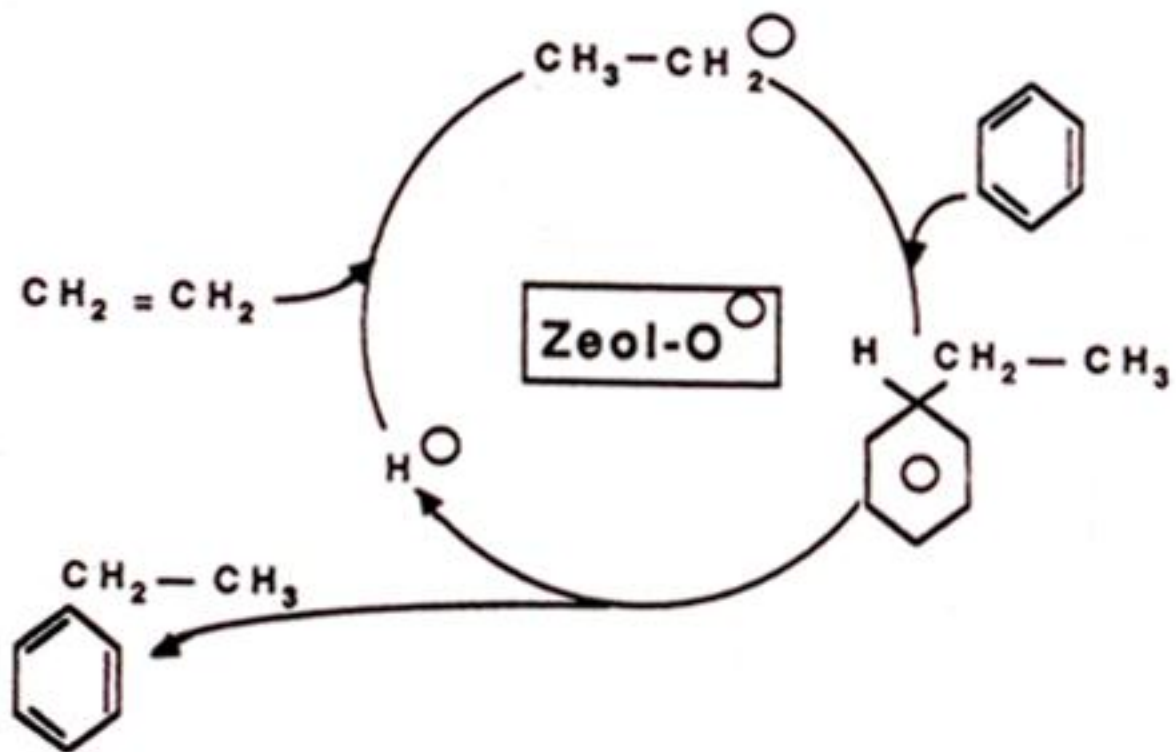
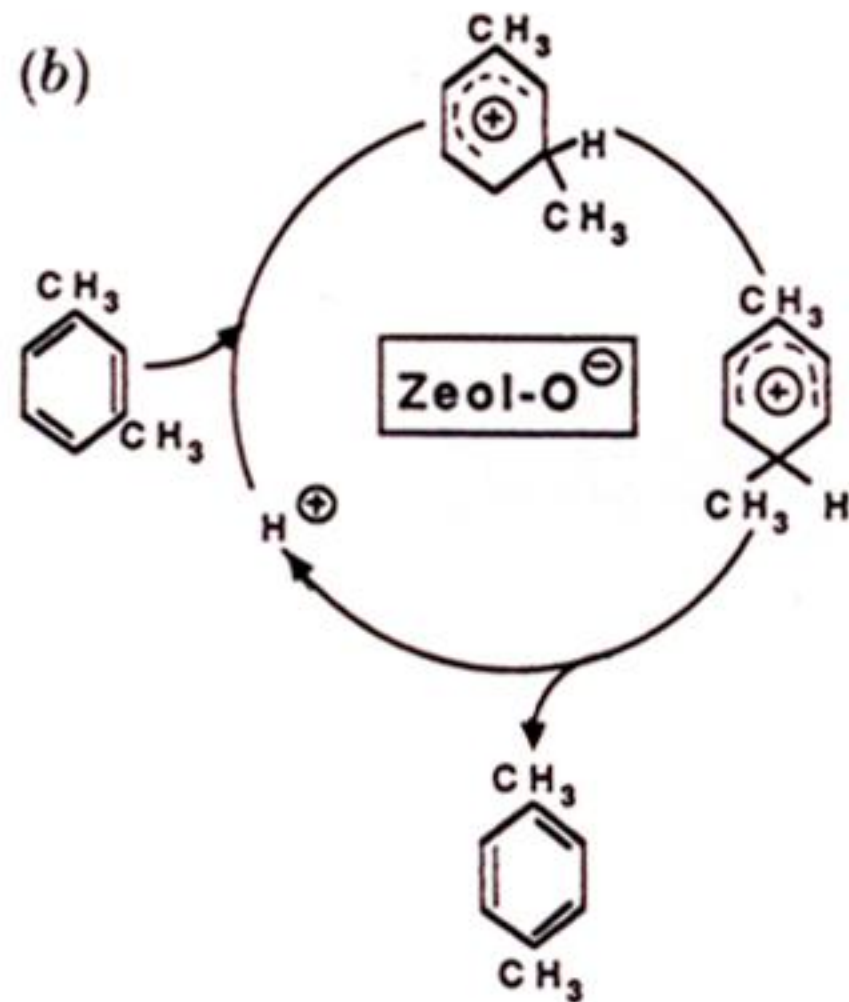
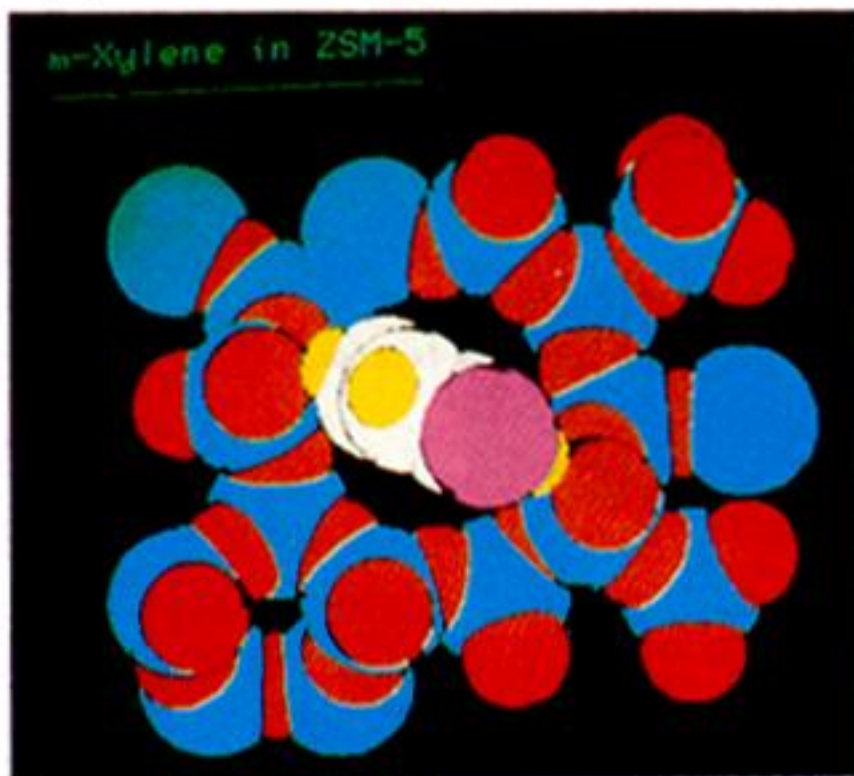


Figure 20. (a) It is easier (bottom) for *para*-xylene, more difficult for *meta*-xylene (top), because of their shape, to diffuse through a H-ZSM-5 catalyst. (b) Examples of proton-catalyzed reactions of hydrocarbons: the isomerization of *meta*- to *para*-xylene (top) and the alkylation of benzene by ethene to yield ethylbenzene (bottom).

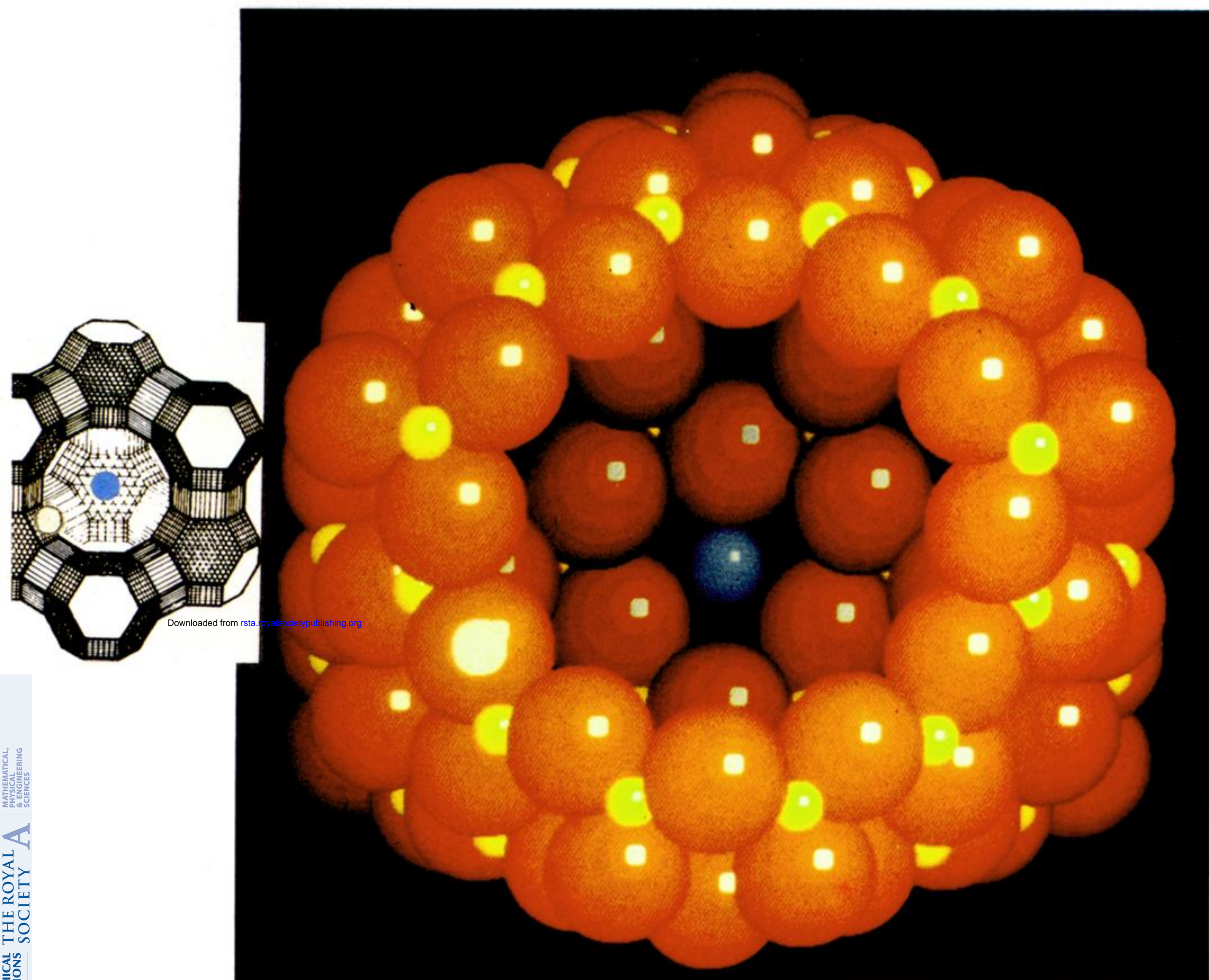


Figure 18. The white spot in the drawing on the left, and the white spot on one of the (red) oxygen atoms in the aperture of La^{3+} -exchanged zeolite Y denote the position of the detachable proton in the catalytically active site. There are six crystallographically equivalent sites for the proton around the periphery of the cage (after Cheetham *et al.* 1983).

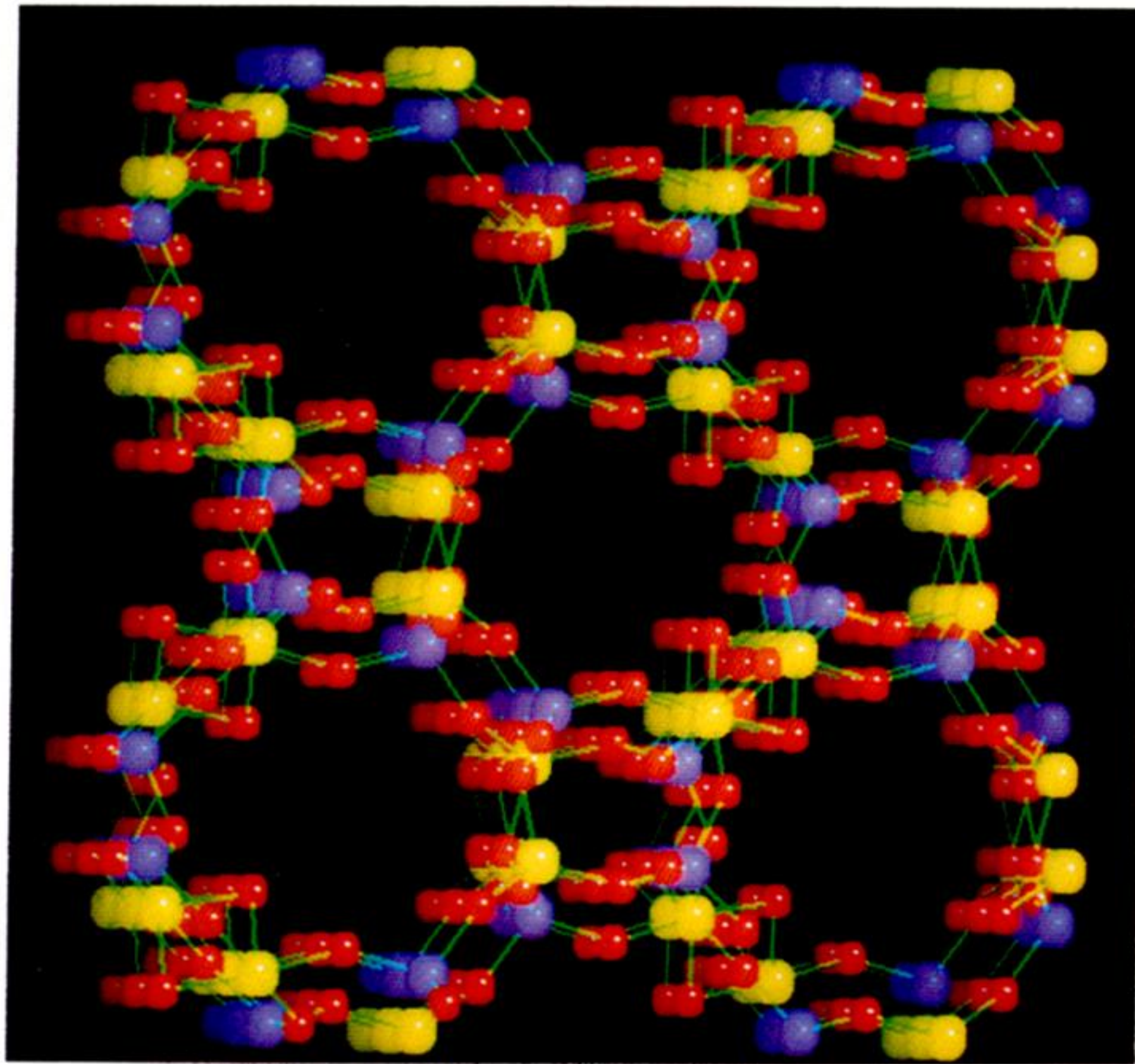


Figure 22. Segment of the structure of a new zeolitic solid discovered by R. Xu and co-workers and designated AlAsO₄-1.

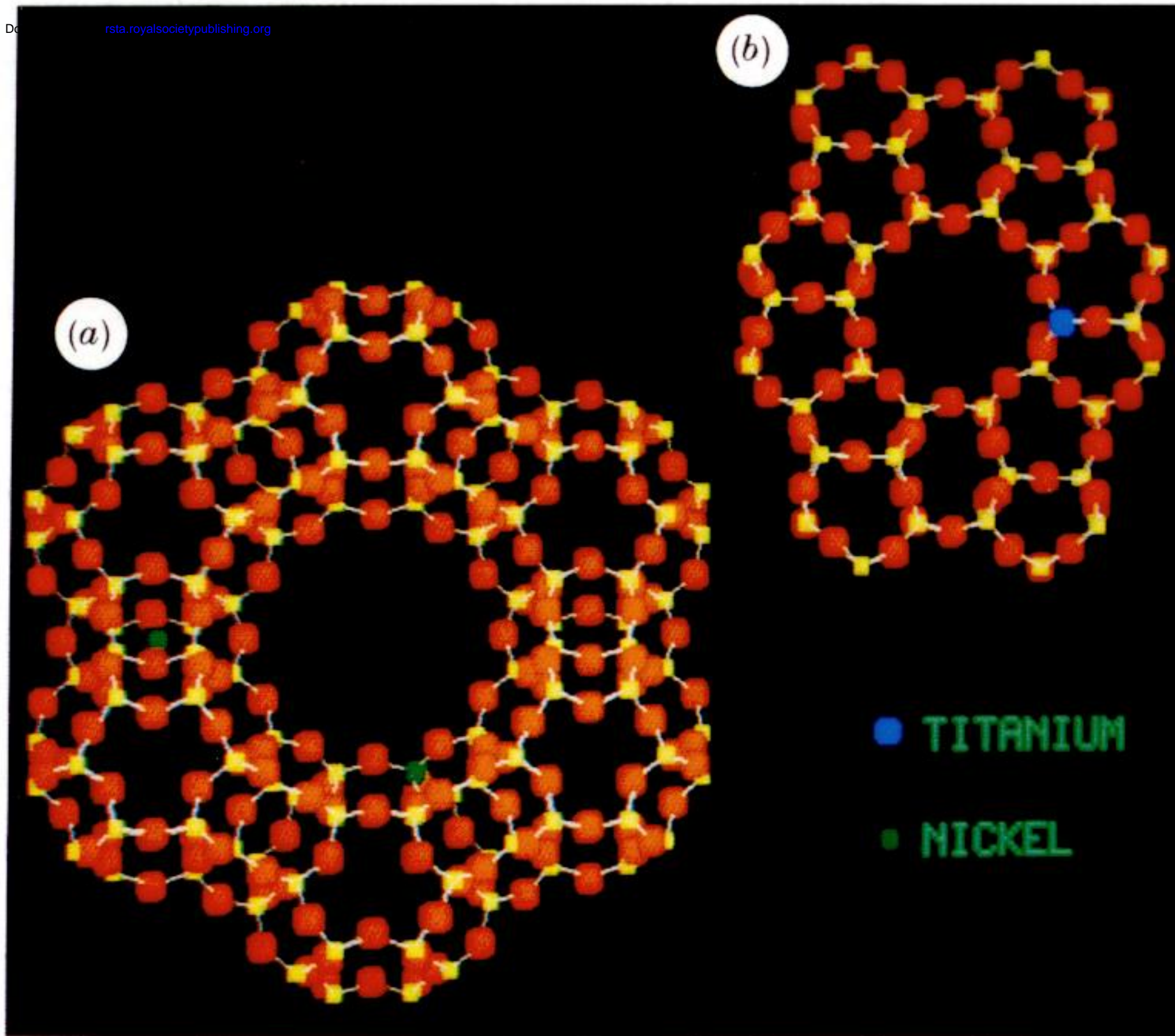


figure 26. (a) Ni^{2+} ions may occupy extraframework sites (like the S_1 shown here) or framework tetrahedral sites. (b) In titanosilicalite the Ti^{4+} ions are part of the framework lining. Some doubt exists as to whether they occur singly or in associated pairs (see Young *et al.* 1989) (see text).

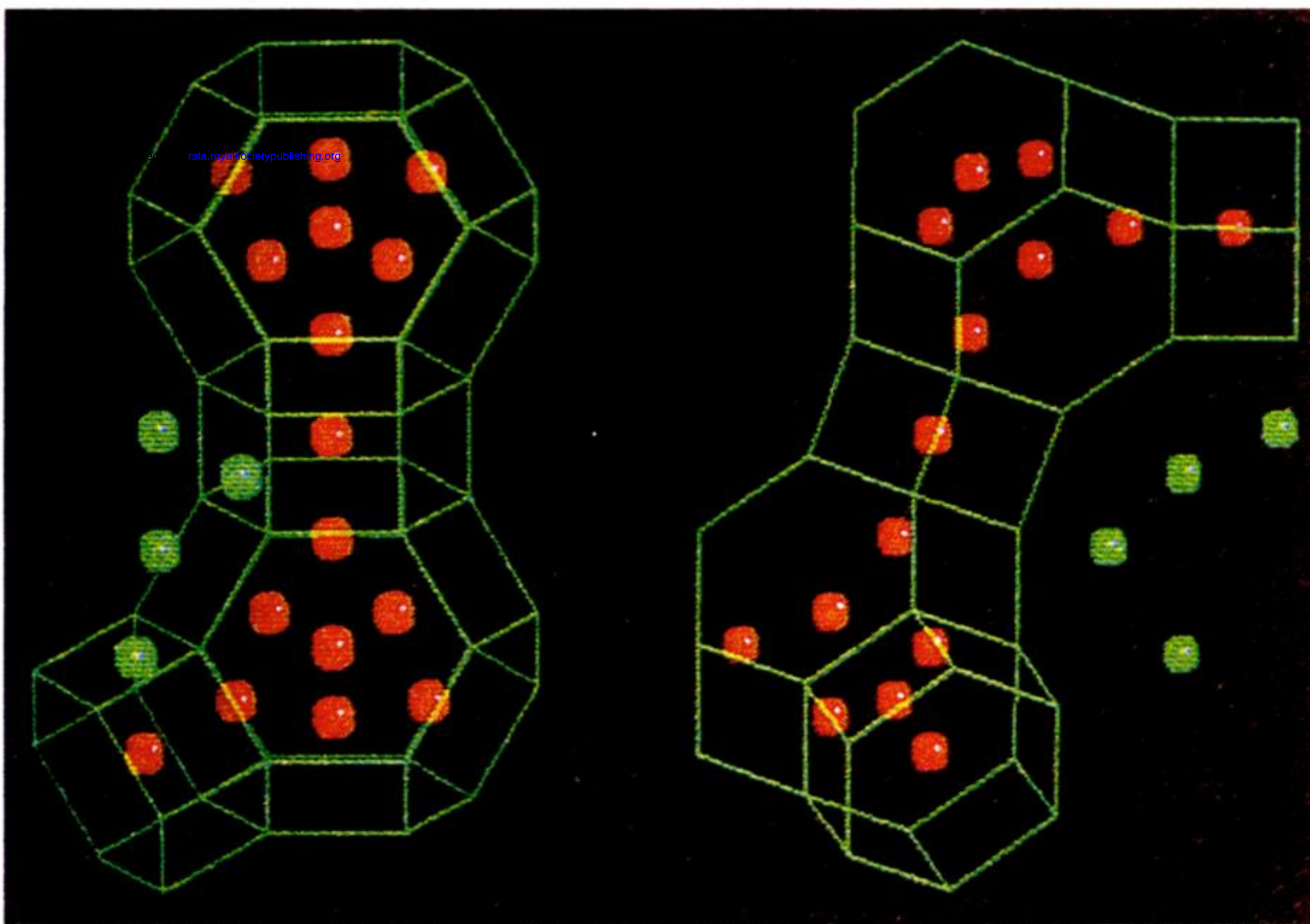
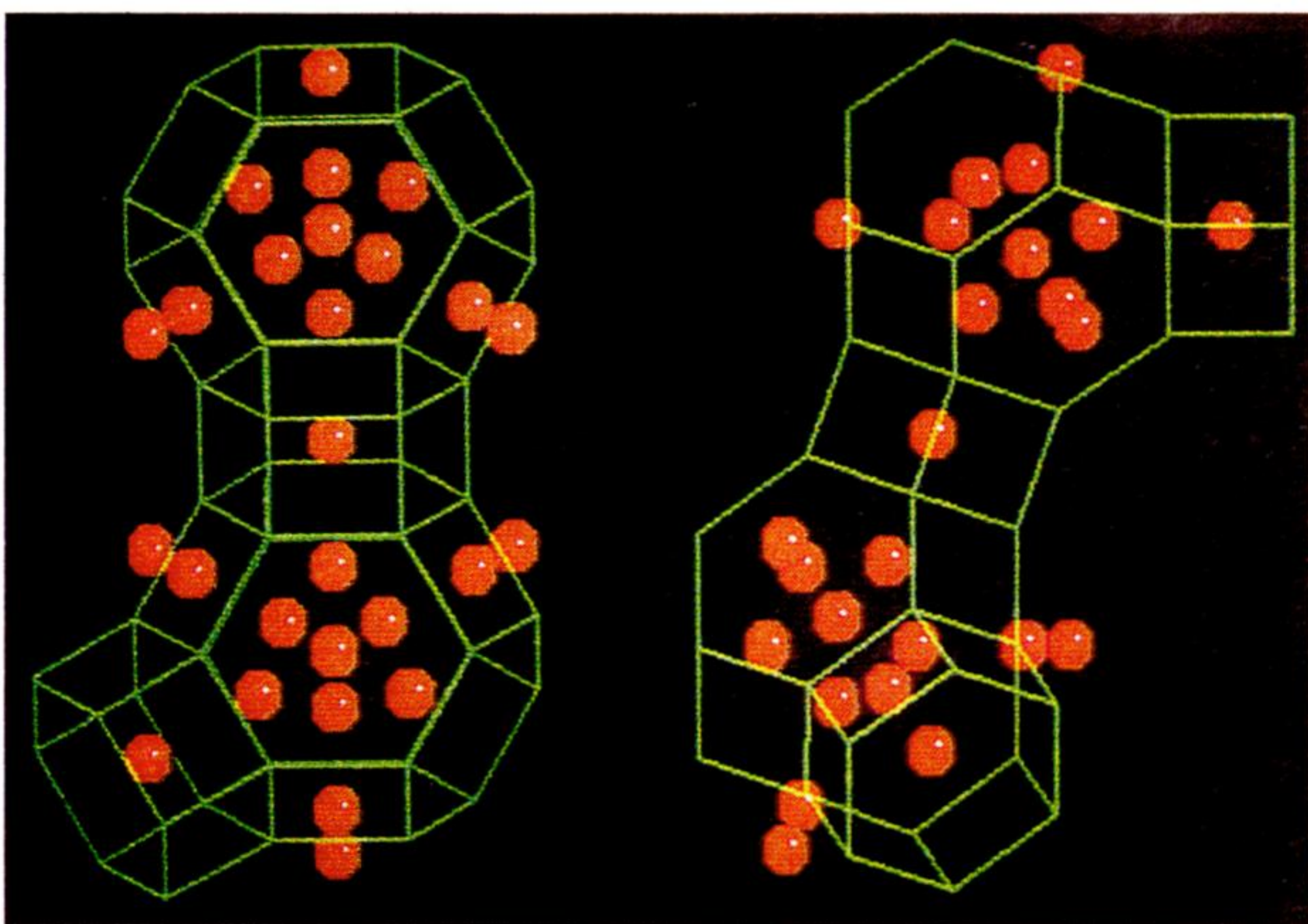


Figure 25. Computer graphic representation showing the marked difference in location of the Ni^{2+} and Na^+ ions in the dehydrated zeolite before (upper) and after (lower) the onset of catalysis. All the extra framework cations (Ni^{2+} and Na^+) are shown in the same colour in the 'before' state, whereas in the catalytic state those Ni^{2+} that have migrated out of the supercage are shown in green. (Note that the S_1 site is situated in the centre of the double six prisms joining the adjacent sodalite cage.) The framework structure, consisting of corner shared tetrahedra TO_4 ($\text{T} = \text{Si}, \text{Al}$) is also shown in green. The two adjacent views in each representation show the pair of sodalite cages rotated by 90° with respect to one another (Couves *et al.* 1990a).

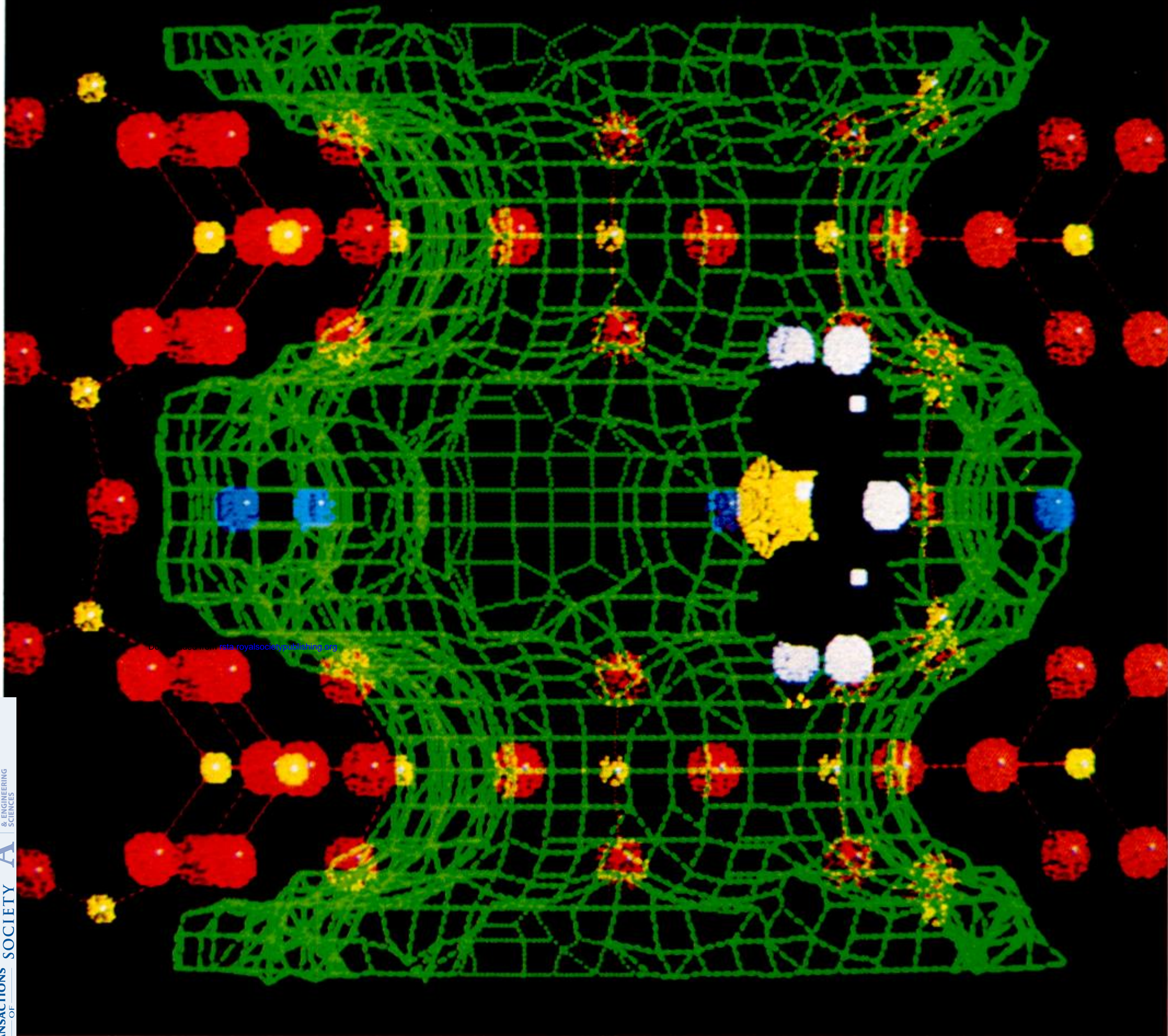


Figure 27. Elevation view of the location of a single deuteropyridine molecule in the channel of zeolite L. The green lines represent the van der Waals limits of the framework atoms shown in small yellow and red spheres. Blue spheres are K; white, H; black, C; large yellow, N. The siting was determined from a Rietveld analysis of the neutron powder diffraction profile (Wright *et al.* 1985).

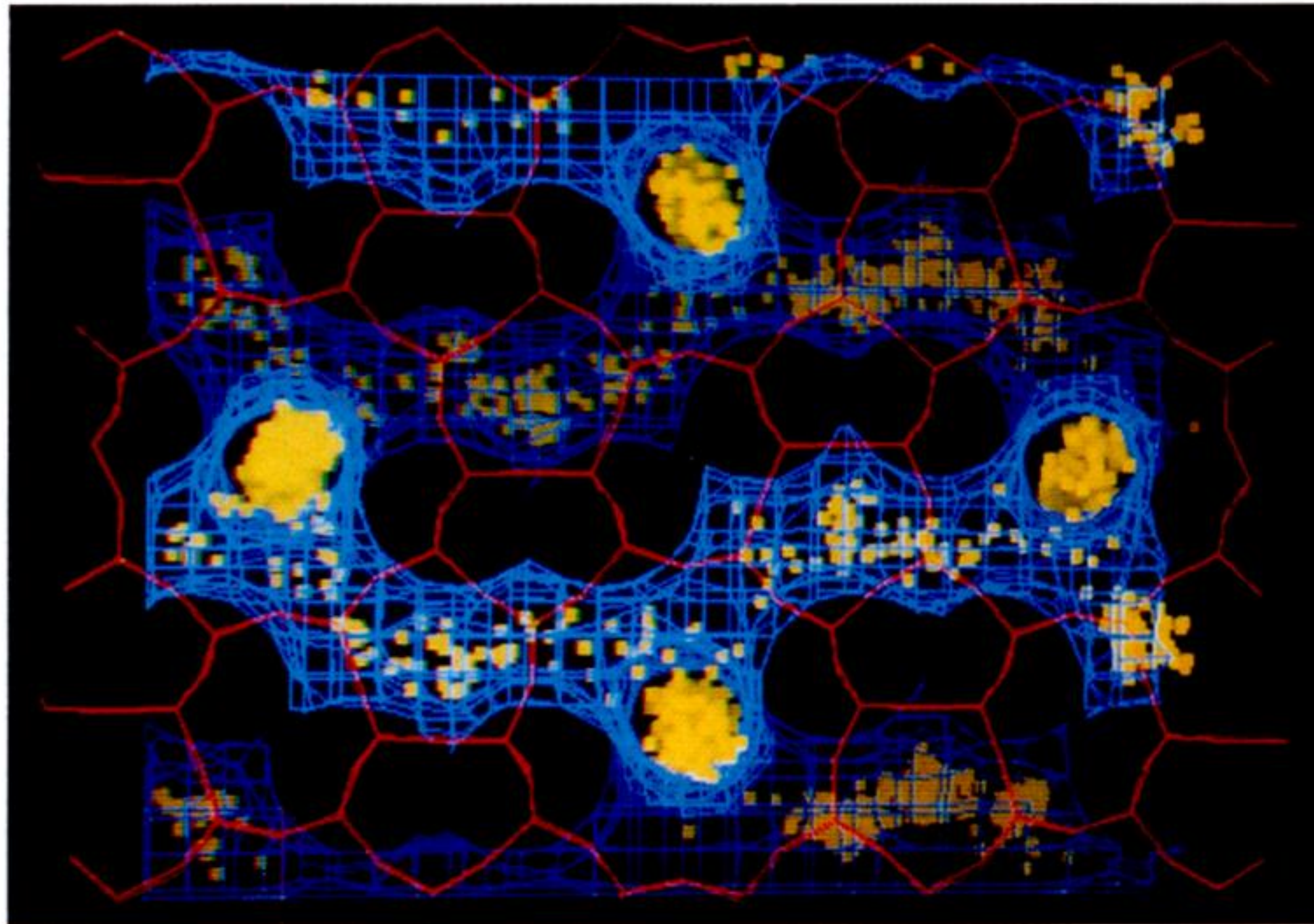
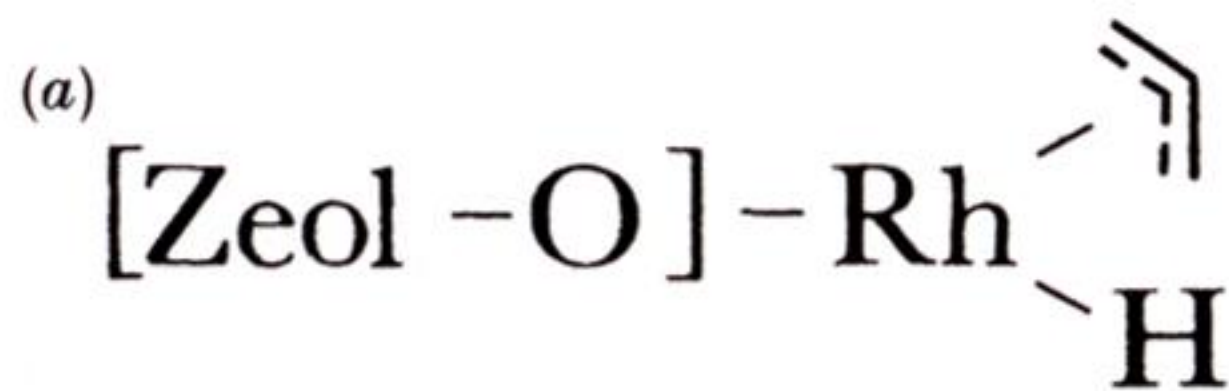


Figure 28. Trajectories of Xe at 298K in the straight and the sinusoidal channels of silicalite, the liceous end-form of ZSM-5. Xe centre-of-mass positions are shown in yellow, Si-O bonds in red and the internal zeolitic surface is represented by the blue net (Pickett *et al.* 1990).



Downloaded from rsta.royalsocietypublishing.org

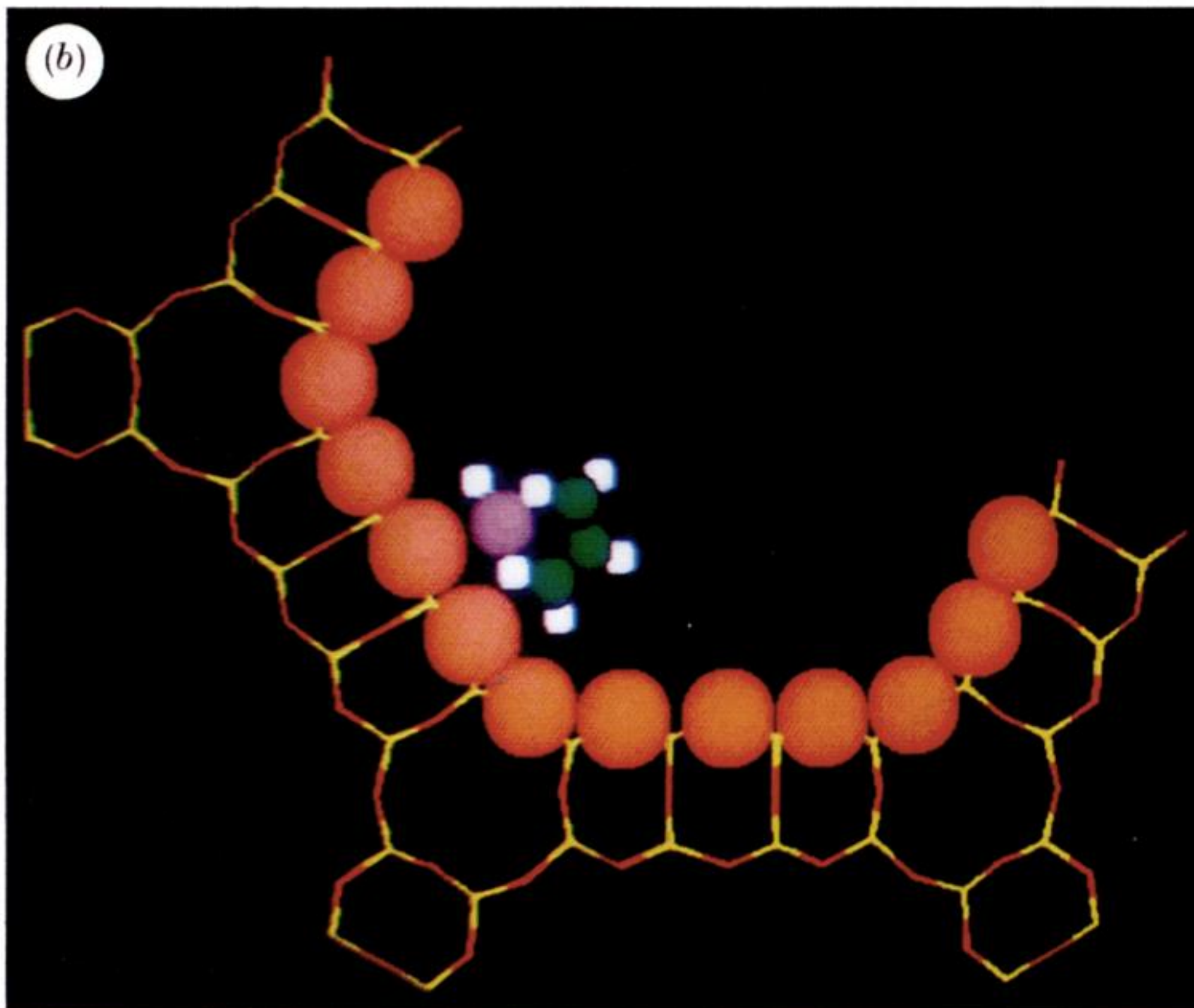


Figure 31. (a) Schematic illustration of a zeolite-bound rhodium hydride (cf. Huang & Schwartz 1982). (b) Illustration of an anchored organometallic catalytic centre anchored on the inner wall of a large cavity of a microporous crystal (rhodium atoms in purple, carbons green, oxygens red and hydrogens white) (see text).